1-1-2016

Engineered Cartilage on Chitosan Calcium Phosphate Scaffolds for Osteochondral Defects

Anuhya Gottipati

Engineered cartilage on chitosan calcium phosphate scaffolds for osteochondral defects

By

Anuhya Gottipati

A Dissertation
Submitted to the Faculty of
Mississippi State University
in Partial Fulfillment of the Requirements
for the Degree of Doctor of Philosophy
in Biomedical Engineering
in the Department of Agricultural and Biological Engineering

Mississippi State, Mississippi

May 2016

Engineered cartilage on chitosan calcium phosphate scaffolds for osteochondral defects

By

Anuhya Gottipati

Approved:

_____

Steven H. Elder
(Major Professor/ Graduate Coordinator)

_____

James Ryan Butler
(Committee Member)

_____

Jun Liao
(Committee Member)

_____

Lakiesha N. Williams
(Committee Member)

_____

Chartrisa LaShan Simpson
(Committee Member)

_____

Jason M. Keith
Dean
Bagley College of Engineering

Name: Anuhya Gottipati

Date of Degree: May 6, 2016

Institution: Mississippi State University

Major Field: Biomedical Engineering

Major Professor: Steven H. Elder

Title of Study: Engineered cartilage on chitosan calcium phosphate scaffolds for osteochondral defects

Pages in 136

Candidate for Degree of Doctor of Philosophy

Articular cartilage provides an almost frictionless surface for the articulating ends of the bone. Cartilage functions to lubricate and transmit compressive forces resulting from joint loading and impact. If the cartilage is damaged, through traumatic injury or disease, it lacks the ability of self-repairing as the tissue lacks vascular system. If the injuries to articular cartilage are left untreated, they may progress to Osteoarthritis. Osteoarthritis, a degenerative disease, is one of the leading disabilities in the United States. Tissue engineering has the potential to regenerate healthy hyaline cartilage, which can alleviate pain and restore the functions of normal tissue.

This study explores the production of engineered cartilage on top of composite calcium phosphate scaffold. The current research is related to a biphasic approach to cartilage tissue engineering — in which one layer supports to form subchondral bone (osteogenesis) and another supports cartilage formation (chondrogenesis). Chondrocyte and bone marrow-derived stem cell attachment to chitosan will be investigated for producing a bilayered construct for osteochondral repair. The main objectives of my research include the following: attachment and proliferation of human mesenchymal stem

cells on chitosan calcium phosphate scaffolds, techniques to create a biphasic construct, the effect of coating chitosan calcium phosphate scaffolds with type I collagen and determining the ideal bead size for making chitosan calcium phosphate scaffolds.

Keywords: cartilage, chitosan, osteochondral defects, tissue engineering

DEDICATION

I want to express my sincere gratitude and appreciation to my family and friends for assisting me throughout this long journey. I would like dedicate my work and this dissertation to my parents Prasad Gottipati and Pankeruham Gottipati for their love, encouragement and providing unending support. I would also like to dedicate my dissertation to my loving husband Nikhil for bringing so much joy and happiness to my life.

ACKNOWLEDGEMENTS

I would like to acknowledge and thank each and every one who has been involved with my research and studies these past four years. First, I would like to express my sincere gratitude to my major advisor Dr. Steve Elder, for his continuous support, patience, motivation, and immense knowledge. His guidance helped me a lot in my research. I could not have imagined having a better advisor and mentor for my Ph.D. Besides my advisor, I would like to thank the rest of my dissertation committee members: Dr. Ryan Butler, Dr. Jun Liao, Dr. Lakiesha Williams, and Dr. LaShan Simpson, for their time, insightful comments, and encouragement. My sincere thanks also go to Ms. Amanda Lawrence, Dr. Raj Prabhu, and Dr. Andrew Oppedal, who helped me in learning various new techniques. Without all your support it would not be possible to complete my research.

TABLE OF CONTENTS

DEDICATION ii

ACKNOWLEDGEMENTS iii

LIST OF TABLES vii

LIST OF FIGURES viii

LIST OF ACRONYMS xii

CHAPTER

I. INTRODUCTION 1

1.1 Articular Cartilage 2
1.1.1 Composition 3
1.1.2 Structure 7
1.1.3 Functions 9
1.2 Articular cartilage damage 12
1.3 Current treatment options for cartilage defects 15
1.3.1 Microfracture 17
1.3.2 Chondroplasty 18
1.3.3 Mosaicplasty 18
1.3.4 Autologous Chondrocyte Implantation 19
1.3.5 Osteochondral grafts (allografts) 20
1.3.6 Total knee replacement 21
1.4 Tissue Engineering 22
1.5 Motivation and Specific aims 25
1.6 References 29

II. ATTACHMENT AND PROLIFERATION OF HUMAN MESENCHYMAL STEM CELLS ON CHITOSAN CALCIUM PHOSPHATE SCAFFOLDS 33

2.1 Introduction 33
2.2 Methods 36
2.2.1 Scaffold fabrication 36
2.2.2 Scaffold mechanical testing 40
2.2.3 Cell source 41

2.2.4 Biphasic constructs 42
2.2.5 DNA and GAG quantification 43
2.2.6 SEM sample preparation 44
2.3 Results 44
2.3.1 Scaffold mechanical testing 44
2.3.2 Cell attachment and proliferation 47
2.4 Discussion 49
2.5 References 52

III. TWO DIFFERENT APPROACHES FOR MAKING BIPHASIC CONSTRUCTS 54

3.1 Introduction 54
3.2 Methods 55
3.2.1 Scaffold fabrication 55
3.2.2 Scaffold characterization 56
3.2.3 Cell source 56
3.2.4 Biphasic constructs 57
3.2.4.1 Approach # 1 57
3.2.4.2 Approach # 2 58
3.2.5 SEM sample preparation 59
3.2.6 DNA and GAG quantification 60
3.2.7 Histology and Immunohistochemistry 60
3.2.8 Degradation 61
3.2.9 Statistics 62
3.3 Results 62
3.3.1 Scaffold characterization 62
3.3.2 Biphasic constructs 63
3.3.3 Degradation 69
3.4 Discussion 70
3.5 References 73

IV. MESENCHYMAL STEM CELL MEDIATED CHONDROGENESIS ON CHITOSAN - CALCIUM PHOSPHATE SCAFFOLDS: EFFECT OF COLLAGEN COATING 76

4.1 Introduction 76
4.2 Methods 78
4.2.1 Fabrication of composite chitosan calcium phosphate scaffolds 78
4.2.2 Scanning Electron Microscopy 79
4.2.3 Porosity and Swelling ratio 79
4.2.4 Contact angle 80
4.2.5 Human mesenchymal stem cell culture 80
4.2.6 Cell attachment and proliferation 81

4.2.7 Creation and Evaluation of Biphasic Osteochondral Constructs 82
4.2.8 Statistics 84
4.3 Results 84
4.3.1 Scaffold Characterization 84
4.3.2 Cell attachment and proliferation 87
4.3.3 Biphasic constructs- DNA quantification 88
4.3.4 Chondrogenesis 88
4.3.5 Histology 89
4.4 Discussion 91
4.5 References 97

V. EFFECT OF BEAD SIZE ON SCAFFOLD CHARACTERISTICS 100

5.1 Introduction 100
5.2 Methods 102
5.2.1 Scaffold fabrication 102
5.2.2 Porosity and swelling ratio 102
5.2.3 Mechanical testing 103
5.2.4 Degradation 103
5.2.5 Mouse Osteosarcoma cell line 104
5.2.6 Porcine chondrocytes 104
5.2.7 Biphasic constructs 105
5.2.8 SEM sample preparation 106
5.2.9 Statistics 107
5.3 Results 107
5.3.1 Scaffold characteristics 107
5.3.2 Mechanical testing 113
5.3.3 Degradation 114
5.3.4 Biphasic constructs 117
5.4 Discussion 124
5.5 References 129

VI. SUMMARY 133

6.1 Summary 133
6.2 References 136

LIST OF TABLES

1.1 Advantages and Disadvantages of various cell types for cartilage tissue engineering [27] 23

3.1 Physical characteristics. 62

3.2 DNA and GAG content after 28 d culture of porcine bone marrow MSCs on freeze-dried CHI-CaP scaffolds. 68

4.1 Physical characteristics of collagen coated and uncoated scaffolds. 86

5.1 Physical characteristics of CHI-CaP scaffolds formed using three different bead sizes. 112

LIST OF FIGURES

1.1 Diagram showing a healthy knee joint....3

1.2 Articular cartilage tissue showing chondrocyte, collagen, GAG, and water molecules. 4

1.3 Molecular organization of a proteoglycan aggregate molecule....6

1.4 Macro to nano scale organization of an articular cartilage tissue [4] 7

1.5 Structure of articular cartilage 8

1.6 Diagram shows the different forms of lubrication when load is applied to the articular cartilage tissue. [7]....11

1.7 Effects on chondrocyte functions upon loading [9]....12

1.8 Schematic representation of Osteochondral (or full- thickness) and Chondral (or partial thickness) defects [11]....13

1.9 Diagram showing healthy and osteoarthritis knee joint....15

1.10 Current treatment paradigms for articular cartilage degeneration 16

1.11 Schematic representation of microfracture process 17

1.12 Diagram showing the process of Mosaicplatsy where autologous osteochondral grafts were implanted in defect site.....19

1.13 Schematic representation of Autologous Chondrocyte Implantation (ACI) [11] 20

1.14 Diagram showing a healthy knee joint and a total knee replacement....21

1.15 Overview of engineered cartilage on CHI-CaP scaffolds for osteochondral defects approach. 24

2.1 Extraction of chitosan from Shellfish wastes from food processing [7].....34

2.2 Chemical Structure of chitosan [7]. 35

2.3 Chitosan calcium phosphate solution dripping drop wise into a magnetically stirring precipitate bath at a rate of 15ml per hour. 38

2.4 CHI-CaP beads separated individually into a dish and air dried overnight at room temperature. 39

2.5 Two separate plates – one having cylindrical shape holes for scaffold fabrication to be place on top of the other flat plate. 40

2.6 CHI-CaP beads filled into cylindrical shape molds and fused together using 2% acetic acid. 41

2.7 Freeze dried cylindrical shaped scaffold of approximately 6 mm in diameter and 7 mm in height. 45

2.8 Young's modulus of scaffolds in unconfined compression 46

2.9 Scaffolds after mechanical testing 47

2.10 Scanning electron micrographs of human MSCs on top of a bead made up of CHI-CaP after 24 h of cell seeding (200X). 48

2.11 Scanning electron micrographs of human MSCs in the pore between the beads made up of CHI-CaP after 24 h of cell seeding. 49

3.1 Schematic representation of crating biphasic constructs created using two different approaches. 59

3.2 micro CT image of CHI-CaP beads fused into a cylindrical shaped scaffold showing interconnected pores. 63

3.3 Scanning electron micrographs showing the presence of thin sheet of porcine bone marrow mesenchymal stem cells on top of CHI-CaP beads created using approach # 1 (85X). 64

3.4 Scanning electron micrographs showing the presence of more chondrocyte like cells in the deep crevices between the beads of composite CHI-CaP scaffolds formed using approach # 1. 65

3.5 Neo cartilage like tissue formed on composite CHI-CaP scaffolds 66

3.6 Toluidine blue stained section of cartilage like tissue formed on composite CHI-CaP 67

3.7 Cartilage like tissue intensively stained for collagen type II, formed on composite CHI-CaP scaffolds 68

3.8 Results from CHI-CaP bead degradation using lysozyme. 69

3.9 Dried biphasic constructs created using approach # 1, showing the presence of tissue covered 72

4.1 Scanning Electron micrograph of freeze dried collagen coated and uncoated composite CHI-CaP scaffold showing a slightly bumpy surface at 15000X magnification. 85

4.2 Contact angle measurement on colalgen coated and uncoated CHI-CaP discs....86

4.3 The bar graph shows the amount of DNA on collagen coated and uncoated scaffolds at 1 hour and 7 day time interval....87

4.4 Live dead staining of hbMSCs on CHI-CaP discs....88

4.5 Area of neocartilage formed on collagen coated and uncoated composite CHI-CaP scaffolds. 89

4.6 Toluidine blue and collagen type II staining on the neocartilage formed on collagen coated and uncoated CHI-CaP scaffolds. 90

4.7 Picosirius red stained neocartilage on collagen coated scaffolds. 91

5.1 Schematic representation of the formation of biphasic constructs using collagen coated CHI-CaP scaffolds. 106

5.2 Scanning electron micrograph of a porous CHI-CaP scaffold formed by fusing medium size beads using acetic acid. 108

5.3 Scanning electron micrograph showing the junction between two medium size beads fused together. 109

5.4 Micro computed tomography images of freeze dried CHI-CaP scaffolds formed using three different bead sizes. 110

5.5 Micro computed tomography images of freeze dried and hydrated CHI-CaP scaffold formed using medium size beads. 111

5.6 Histograms showing the pore size range in dry and hydrated CHI-CaP scaffolds of different bead sizes....113

5.7 Compressive modulus of different bead size CHI-CaP scaffolds after rehydrating in culture media for 24 h, 2 weeks or 4 weeks. 114

5.8 Total amount of calcium released after 3 d, 6 d, and 9 d of incubation in lysozyme solution. 115

5.9 Average absolute weight loss with respect to initial weight after 3 d, 6 d, and 9 d of incubation in lysozyme solution. 116

5.10 SEM images showing fibroblast like cell coverage on big bead size CHI-CaP scaffolds after incubating scaffolds in osteosarcoma cell suspension for 3 weeks. 118

5.11 SEM images showing increased mineral deposition on big bead size CHI-CaP scaffolds after incubating scaffolds in osteosarcoma cell suspension for 6 weeks. 119

5.12 SEM image of a native clean bone. 120

5.13 Side and top view of the medium bead size biphasic construct showing the mineral deposition and neocartilage formation when dried using hexamethyldisilazane for SEM. 121

5.14 Scanning electron micrographs of different bead size collagen coated CHI-CaP scaffolds showing the neotissue formed using porcine chondrocytes and the remnants after scrapping the tissue. 122

5.15 microCT images of medium size biphasic constructs....123

5.16 Top view microCT images of the bipahsic constructs formed using CHI-CaP scaffolds and osteosarcoma and chondrocytes....124

5.17 Side and top view of the microCT images of medium bead size biphasic constructs, ...124

LIST OF ACRONYMS

OA = Ostoarthritis

ECM = Extracellular Matrix

GAG = Glycosaminoglycans

DNA = Deoxyribonucleic acid

ACI = Autologous Chondrocyte Implantation

TKA = Total Knee Arthroplasty

PBS = Phosphate Buffer Saline

FBS = Fetal Bovine Serum

DMEM = Dulbecco's Modified Eagle Medium

DCM = Defined Chondrogenic Medium

TGF-β = Transforming Growth Factor – Beta

CHI-CaP = Chitosan Calcium Phosphate

SEM = Scanning Electron Microscopy

TEM = Transmission Electron Microscopy

DDA = Degree of Deacetylation

MSC = Mesenchymal Stem Cells

hbMSC = Human Bone Marrow Derived Mesenchymal Stem Cells

CHAPTER I

INTRODUCTION

Treatment of articular cartilage injuries is challenging because the tissue has limited capacity of intrinsic healing due to lack of blood vessels. This study explored one approach to cartilage tissue engineering, whereby cartilage forms *in vitro* on top of biodegradable composite chitosan-calcium phosphate (CHI-CaP) scaffolds. CHI-CaP microbeads were fused to make cylindrical scaffolds of approximately 35% porosity. The scaffold supports bone ingrowth and provides a platform for cartilage formation. Stem cells or chondrocytes were seeded onto the scaffolds at such high densities that they produce a layer of cartilage through self-assembly. These experiments have demonstrated the efficiency of cell adhesion, rate of proliferation, the influence of cell seeding technique, the effects of coating scaffolds with type I collagen, and also the effects of bead size. Coating the scaffolds with collagen made them more hydrophilic and increased cell attachment and chondrogenesis. It also facilitated formation of a continuous layer of hyaline-like cartilage over the area of cell seeding. CHI-CaP scaffolds also showed biocompatability and mineral deposition when seeded with osteosarcoma cells. These studies indicate the potential for creating a bilayered construct consisting of an osteoconductive CHI-CaP phase and a tissue-engineered cartilage phase.

1.1 Articular Cartilage

Articular cartilage, also known as hyaline cartilage, is one of the three types of cartilage found in the human body. It is the smooth, white tissue that covers the articular surface of bones in synovial joint. It decreases friction, absorbs shock, distributes load and provides a smooth lubricating surface for easy joint movements. This cartilage tissue is susceptible to injury through a number of mechanisms, including trauma (e.g., patellar dislocation or hyperflexion) and congential anatomical abnormality. Articular cartilage is devoid of blood vessels, lymphatics and nerves. The normal wound healing process is not provoked by blood cells and the tissue has a limited capacity of intrinsic healing due to the absence of vascular system [1]. Therefore, if the injuries to articular cartilage are left untreated, it would advance to osteochondral defects and lead to osteoarthritis. Osteoarthritis (OA) is one of the leading disabilities in United States. A long standing therapy for treating OA is not yet available. The treatment and repair of articular cartilage is quite challenging due to its complex architecture. The emerging field of cartilage tissue engineering shows promising results in regenerating healthy hyaline cartilage, which can alleviate pain and restore the functions of normal tissue. Basic composition, structure, and functions of the articular cartilage need to be studied to regenerate healthy tissue.

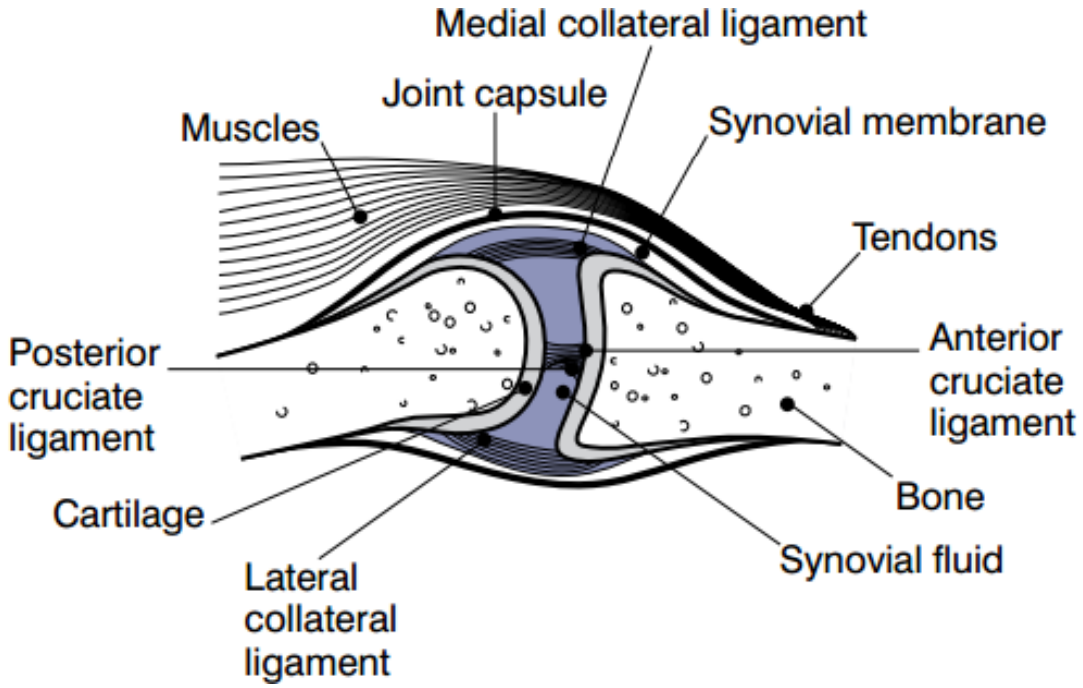

Figure 1.1 Diagram showing a healthy knee joint

(Courtesy - http://www.niams.nih.gov/Health_Info/Osteoarthritis/)

1.1.1 Composition

Articular cartilage is mainly composed of water, collagen and proteoglycans and its composition varies with depth, which influences the mechanical behavior of the tissue [1,2]. Articular cartilage also has cells known as chondrocytes, which are surrounded by an extracellular matrix (ECM). Chondrocytes are spherical shaped cells and do not exhibit any cell-to-cell contact (Figure 1.2) [3]. The material parts other than chondrocytes in a cartilage tissue constitute ECM. The structure and composition of ECM dictates tissue mechanics and also influences cell differentiation, migration, and cellular synthesis. The ECM of articular cartilage is primarily proteoglycan and collagen. The high concentration of proteoglycan creates osmotic pressure and chemical expansion stress (due to high negative fixed charge density), which contributes to the tissue's

compressive resistance and maintains water content of approximately 80% of the total wet weight of the tissue. In cartilage tissue type II collagen accounts for 90% to 95% of the total collagen content. Collagen is a structural protein and it helps in providing tensile strength to cartilage.

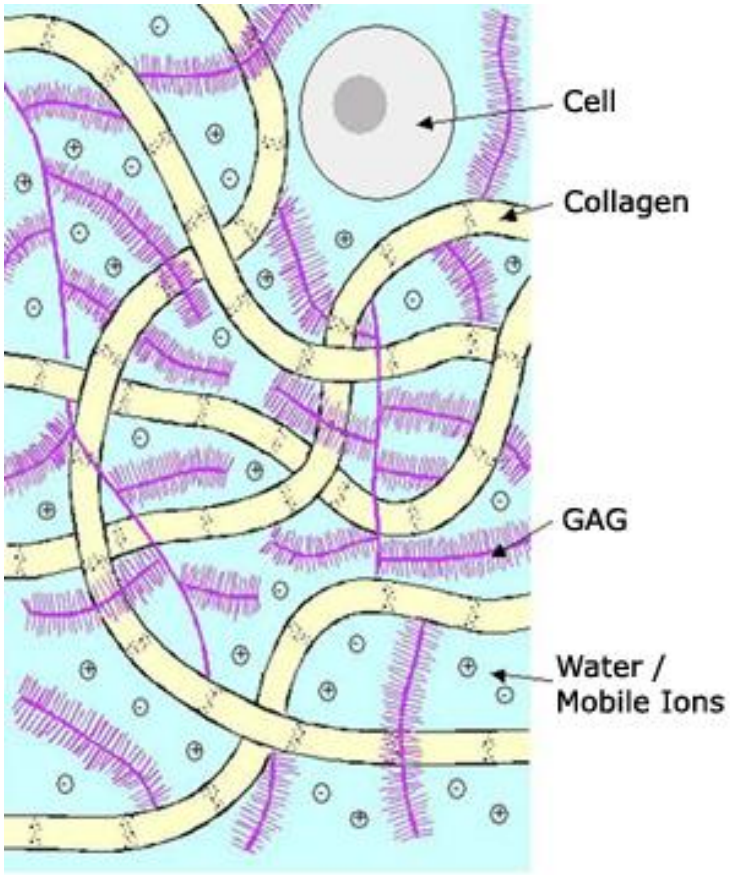

Figure 1.2 Articular cartilage tissue showing chondrocyte, collagen, GAG, and water molecules.

(Courtesy - www.bidmc.org/Research/Departments/Radiology/Laboratories/Cartilage.aspx)

Chondrocytes are the sparsely spread cells found in cartilage. They are about 1% in volume in adult human articular cartilage [2]. Chondrocytes play an important role in

the production and maintenance of extracellular matrix in cartilage tissue. They are derived from mesenchymal stem cells (MSC) from matured bone marrow. MSCs differentiate into chondrocytes during embryogenesis and develop extracellular matrix [3]. Although chondrocytes vary in size, shape, and metabolic activity in various zones of cartilage, cells contain organelles necessary for synthesizing extracellular matrix. Spheroidal shaped mature chondrocytes also synthesis type II collagen, large aggregating proteoglycans, and specific noncollagenous proteins. As the cartilage tissue lacks vascular system, it relies on chondrocytes for the exchange of nutrients and waste material.

Proteoglycans are macromolecules found in the extracellular matrix of the cartilage tissue. Proteoglycans contribute to 25%-35% of the total dry weight of the articular cartilage tissue. Proteoglycans consists of a core protein covalently attached to one or more polysaccharides called glycosaminoglycans (GAG) (Figure 1.3). Chondritin sulfate and keratin sulfate are the two main types of GAGs present in cartilage extracellular matrix. Functions of the proteoglycans include but are not limited to lubricants that absorb water, shock absorbers that resist compression, and also regulate diffusion and flow of both water and macromolecules.

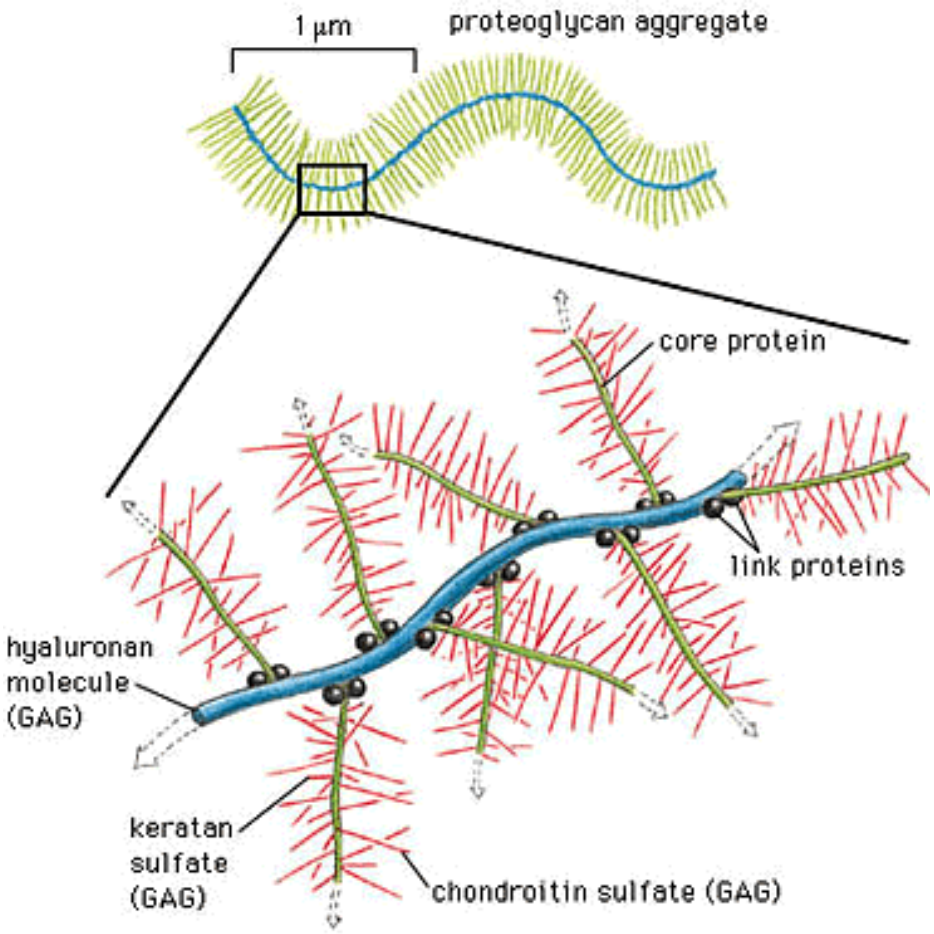

Figure 1.3 Molecular organization of a proteoglycan aggregate molecule (Courtesy - www.marvistavet.com/html/normal_joint_structure.html)

Collagen, a structural protein, accounts for 60% of the dry weight of the cartilage [2]. Collagen is made up of repeating chains of amino acids which form a triple helical structure. Cartilage has an abundance of type II collagen and other types are present in much smaller amounts. The structure of the cartilage is due to the collagen fibrillar mesh work present in the extracellular matrix. Collagen provides mechanical strength, carries tension, provides a platform for bone mineralization, and supports attachment for numerous cells.

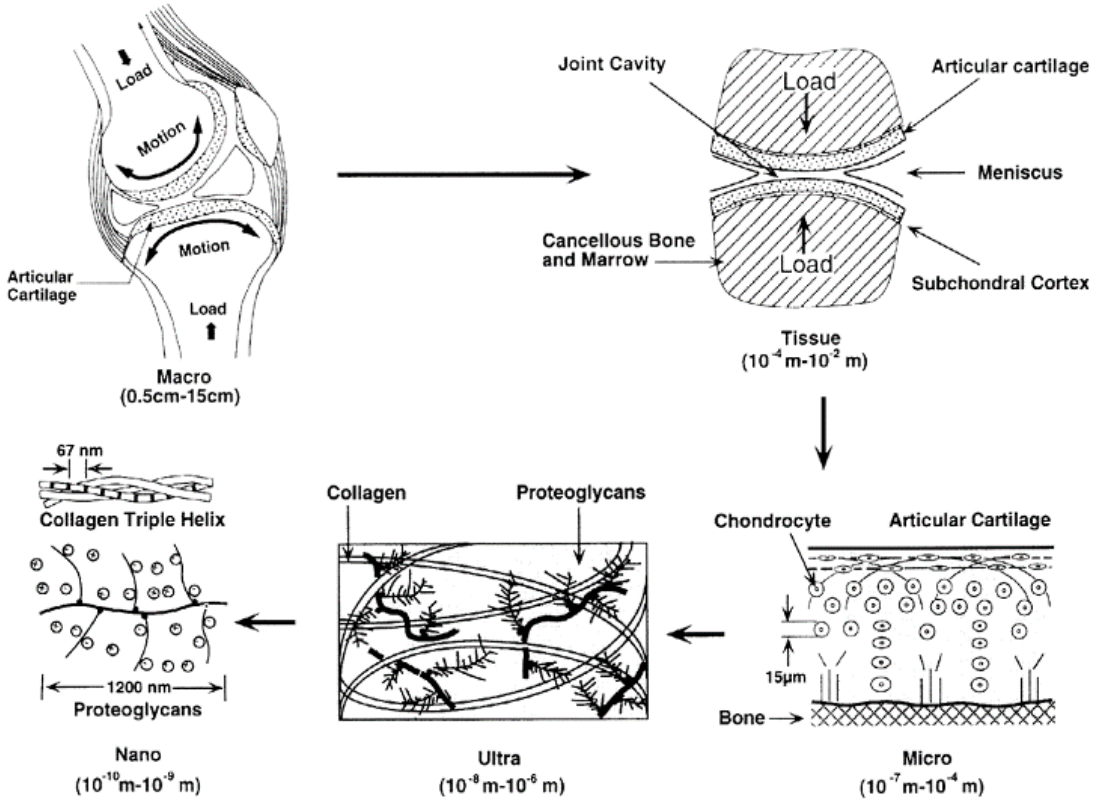

Figure 1.4 Macro to nano scale organization of an articular cartilage tissue [4]

1.1.2 Structure

Chondrocytes regulate the arrangement of collagen, proteoglycan, and all other proteins into a unique and systemized order to form an articular cartilage [2]. The arrangement, configuration, mechanical properties, and metabolic activity of the tissue vary with depth. The cartilage tissue region starting from the articular surface to the sub chondral region is divided into four zones. They are tangential (or superficial), transitional (or middle), radial (or deep), and calcified cartilage zones (Figure 1.5). These zones vary in the concentrations of water, proteoglycan, and collagen. Chondrocytes in

each zone vary in volume, architecture, and orientation with respect to the articular surface.

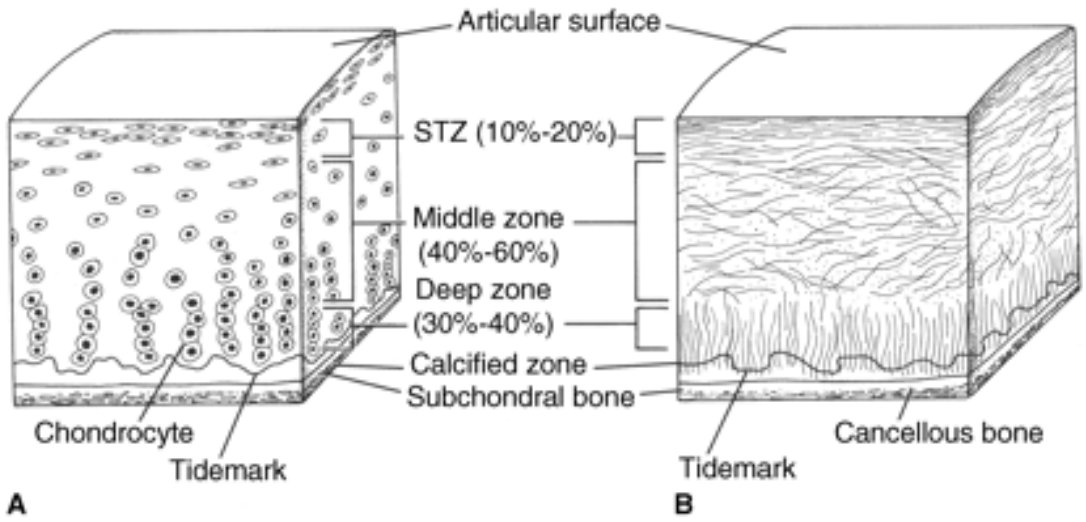

Figure 1.5 Structure of articular cartilage

A) chondrocyte organization in different zones of an articular cartilage B) Collagen fiber orientation [1]

The superficial, also known as tangential, zone is the outer covering layer of the cartilage that forms the articulating surface for joint movements. It is the thinnest of all the zones in articular cartilage. It has parallel arrangement of small diameter collagen fibers and elongated (or flattened) chondrocytes with respect to articular surface. These parallel collagen fibers provide tensile strength to the tissue to withstand joint forces. It also has condensed collagen fibers and sparsely arranged proteoglycans, which make it a highest water content zone. This is the only zone in which articular cartilage progenitor cells can be found. The cells in this region are covered with a layer of lubricin which helps in easy joint movements and helps to avoid wear and tear of the tissue due to frictional forces. Superficial zone is a crucial layer of cartilage, and its loss has shown to

increase ECM permeability and deformation, which is mostly seen in the early stages of osteoarthritis [5].

The middle, or transitional, zone is the thickest of all the four zones, constituting about 40%-60% of the total tissue thickness. Collagen fibrils having large diameter compared to those in superficial zones are oriented randomly in middle zones. Chondrocytes attain a more spherical shape and the ECM has abundant proteoglycans, limited collagen and water in this zone. Presence of more proteoglycan helps the middle zone to withstand compression.

The deep or the radial zone constitutes about 30% of the total tissue thickness. This layer contains large diameter collagen fibrils, highest proteoglycans, and the lowest water content. Chondrocytes in this zone are round in shape and are arranged in columns parallel to the collagen fibrils and perpendicular to the articular surface. This zone holds the largest collagen fibrils and the highest amount of proteoglycans of articular cartilage [6].

Calcified cartilage is the last zone of articular cartilage and sits on top of a subchondral bone. Tidemark, a borderline, separates the deep zone from the calcified zone. The cells in this zone are smaller, covered by ECM and have less metabolic activity. The large collagen fibers present in the deep zone penetrate into calcified zone and eventually ends in subchondral bone, providing a connection between cartilage and bone.

1.1.3 Functions

Articular cartilage surrounding the articular surfaces of a bone provides cushion like surface for easy, painless joint movements. The tissue has a unique composition and

characteristic: it attributes to the mechanical properties of articular cartilage, which makes it able to withstand weight without disrupting the cartilage. It also helps in shock absorption because of its flexible nature.

Nancy S et al. related the articular cartilage to the mixtures theory, as a mixture of four elements which can constitute into two phases – the fluid phase and the solid phase. The fluid phase is composed of all the interstitial fluid that is free to move and the solid phase is comprised of fibrous network of collagen, proteoglycan, and lipids. The interstitial fluid in the extracellular matrix is reorganized in the presence of mechanical loads, which results in viscoelastic behavior. Viscoelastic behavior of the articular cartilage is mainly due to the fluid flow through the pores and due to the rate of deformation of solid components (Figure 1.6) [7]. Joseph N Mansur proposed that articular cartilage is similar to a sponge, even though fluid does not pass through it freely. For modeling cartilage, the fluid phase is taken as an incompressible and inviscid, whereas the solid phase is taken as an elastic material [8].

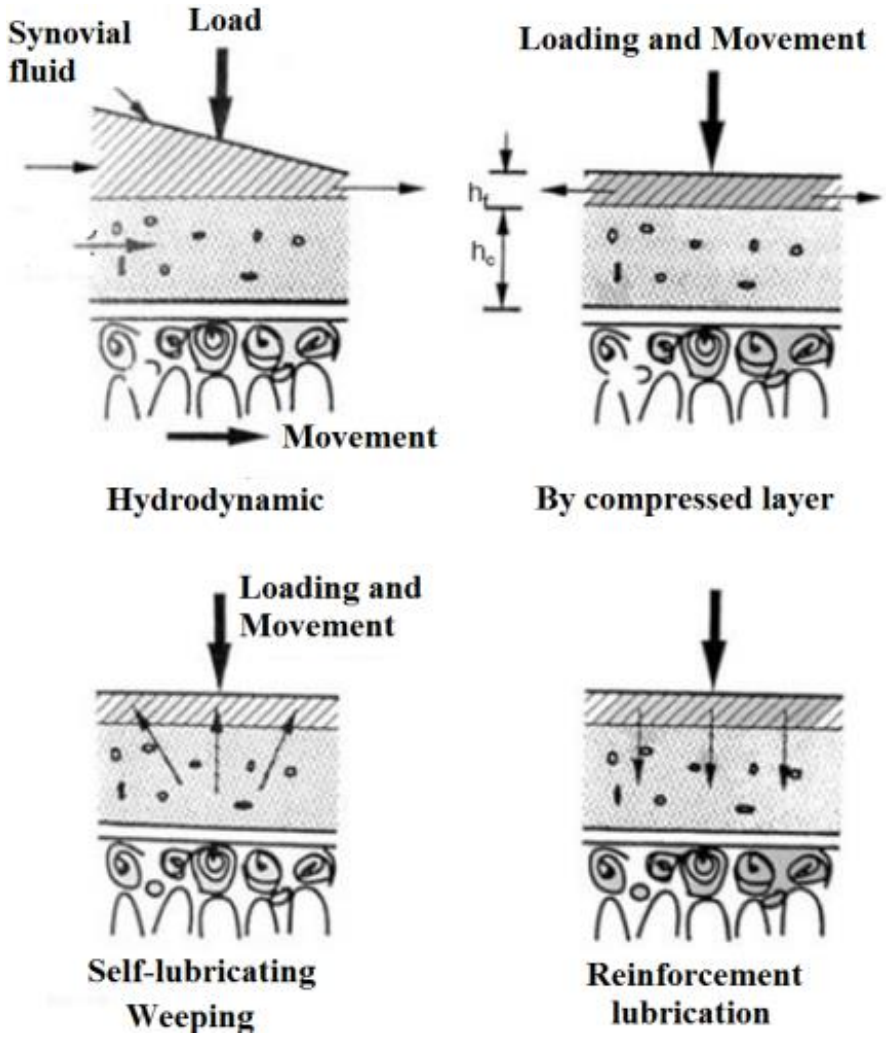

Figure 1.6 Diagram shows the different forms of lubrication when load is applied to the articular cartilage tissue. [7]

When a mechanical load is applied to the cartilage, chondrocytes respond to it and regulate several functions such as growth, cellular differentiation, and metabolism. Certain types of mechanical load also cause damage to the cartilage tissue (Figure 1.7). Chondrocyte apoptosis can also be seen when tissue is loaded under high levels of magnitude and strain.

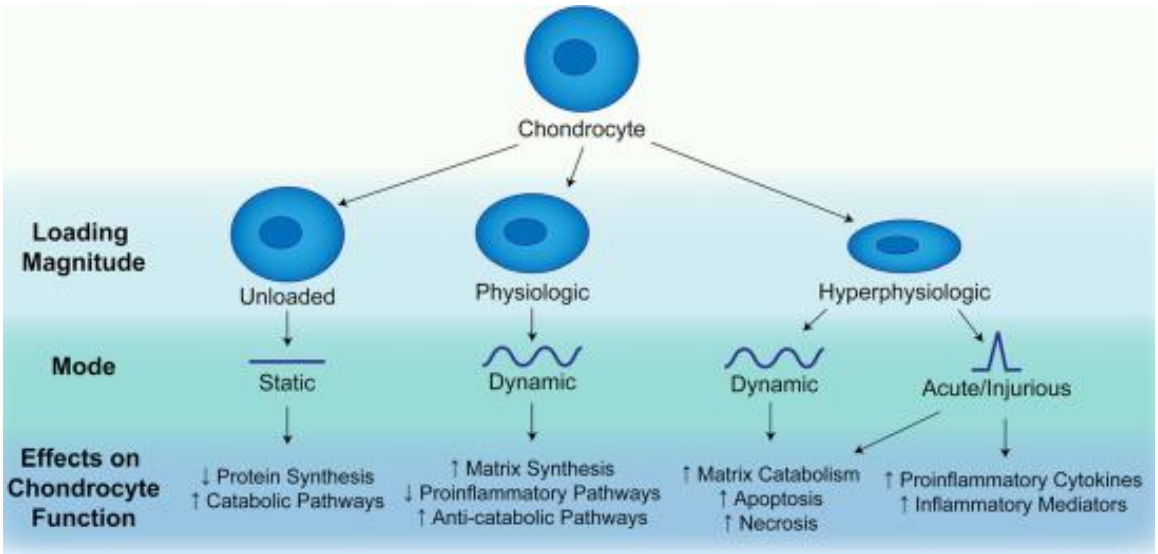

Figure 1.7 Effects on chondrocyte functions upon loading [9]

1.2 Articular cartilage damage

Traumatic or mechanical degeneration (wear and tear) of the joint can lead to articular cartilage injuries, which is the loss of cartilage tissue in the joint. Unfortunately, cartilage tissue is not capable of self-healing. If these cartilage defects are left untreated, they expand and damage the surrounding healthy hyaline cartilage. Articular cartilage defects are usually classified into two types – osteochondral or full thickness defect and chondral or partial thickness defect (Figure 1.8). The cartilage defects limited to the cartilage region are known as partial thickness defect or chondral defect, whereas the defects that penetrate the subchondral bone are known as full thickness defect or osteochondral defect. The defects confined to the cartilage region, chondral or partial thickness defects results in the disruption of collagen arrangement and GAG. As the cartilage tissue lacks blood vessels, the chondral defects cannot initiate self-repair process. In case of osteochondral or full thickness defects, as the defect reach the

subchondral bone, self-repair process is initiated as the blood cells and undifferentiated mesenchymal stem cells make their way to the defect. This leads to the formation of a scar or fibrous cartilage in the defect region [10]. Fibrous cartilage is the toughest among the three types of cartilages. This tissue cannot form a continuous cartilage and cannot perform all the functions of a native hyaline cartilage. Instead of alleviating pain, this formed fibrous cartilage increases pain and may advance to osteoarthritis.

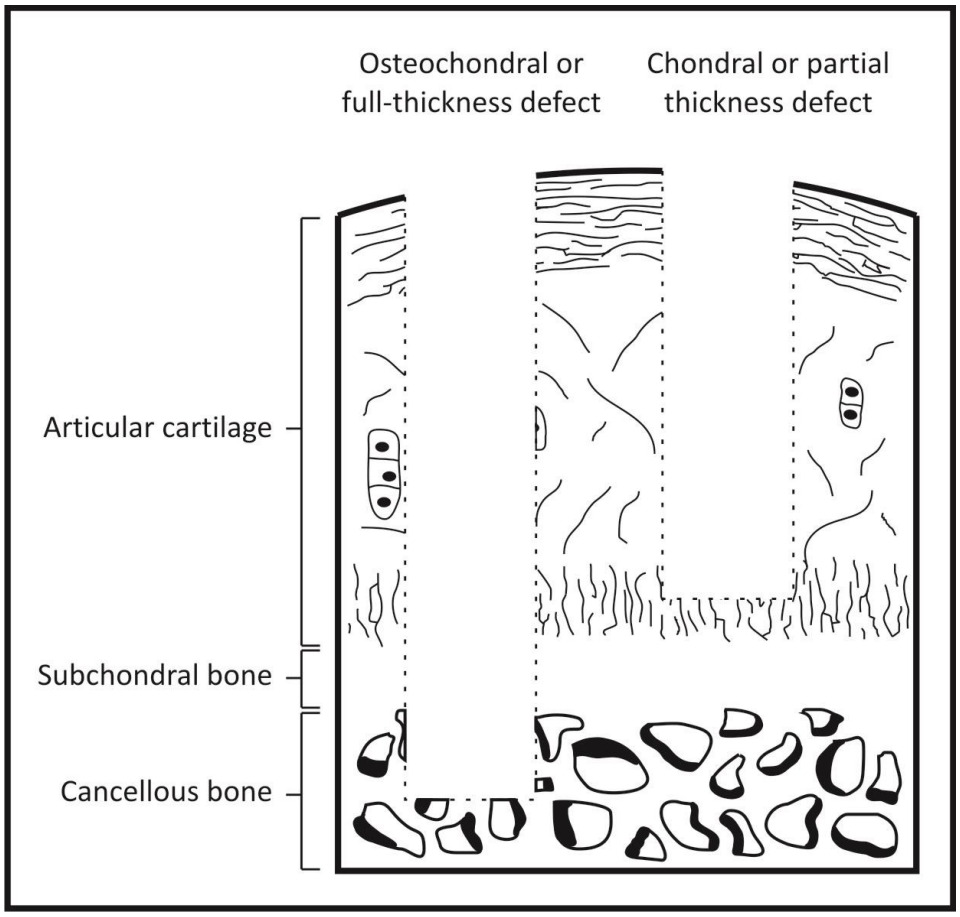

Figure 1.8 Schematic representation of Osteochondral (or full- thickness) and Chondral (or partial thickness) defects [11]

Osteochondral defect or full thickness defect is graded on a scale from stage 1 to 5 based on the stability and severity of the injury from MRI findings. Stage 1 is limited to articular cartilage injury, where a small rupture of cartilage is noticed. At stage 2, the injury spreads to the subchondral bone, but damaged cartilage is still intact to the subchondral bone. In the next stage, the cartilage defect gets separated from the bone. In the fourth stage, these damaged osteochondral fragments were dislocated in the joint causing severe pain. The last stage was evidenced by the formation of subchondral cysts in the joint. There is no study to date that showed the advancement of osteoarthritis from subchondral cysts but, these subchondral cysts were observed in osteoarthritis patients [12,13,14].

Osteoarthritis (OA) is a degenerative joint disease and mostly seen among older people (severity advances with age) or in athletes after injuries. 15% (40 million) of Americans had some form of arthritis in 1995 and it is estimated that 18.2% (59.4 million) of Americans will be diagnosed with arthritis by 2020 [4]. OA damages the exterior layer of cartilage, breaks and wears it away. Due to this, the bones lying below the cartilage defect rub together during joint movements. This rubbing together causes pain, swelling, and finally results in loss of joint movement. If these damages are not fixed, the joint may be deformed and also small deposits of bone called osteophytes (or bone spurs) grow in the joint causing more pain and damage (figure 1.9).

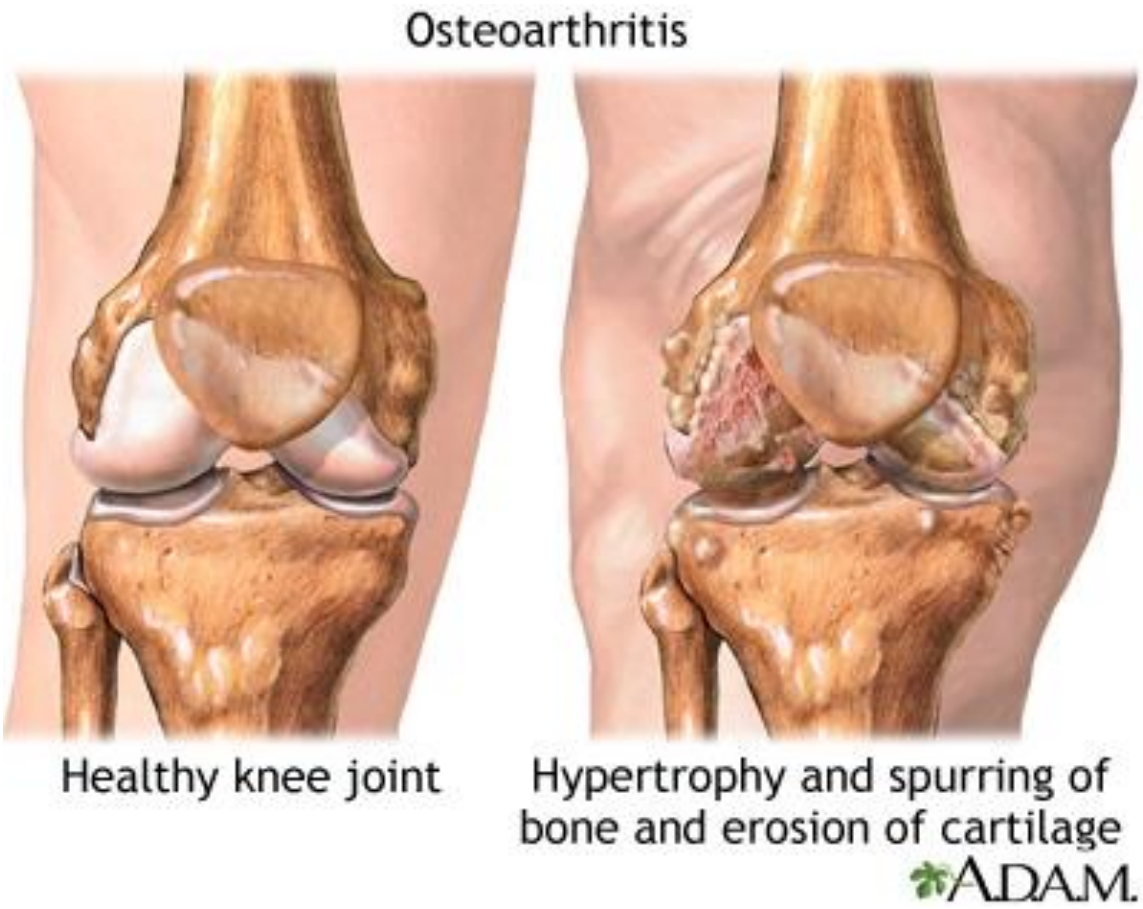

Figure 1.9 Diagram showing healthy and osteoarthritis knee joint

(Courtesy - https://www.nlm.nih.gov/medlineplus/ency/imagepages/17103.htm)

1.3 Current treatment options for cartilage defects

There is no permanent cure for osteochondral lesions to date and this treatment in young patients is more challenging as they engage in higher levels of physical activity. As the cartilage tissue is devoid of blood vessels, this tissue lacks the capacity of intrinsic healing. Various treatment options are now available for treating damaged cartilage. In most of the current therapies, either cells capable of chondrogenic differentiation are implanted in the defect site or blood supply is allowed from subchondral bone to the defect site to initiate healing process. In most of the cases, it results in the formation of

fibrous cartilage. This formed fibrous cartilage can alleviate joint pain but cannot perform all the functions of an articular cartilage. The present-day surgical treatment approaches to the damaged cartilage depends on the size and severity of the lesions [15] (Figure 1.10).

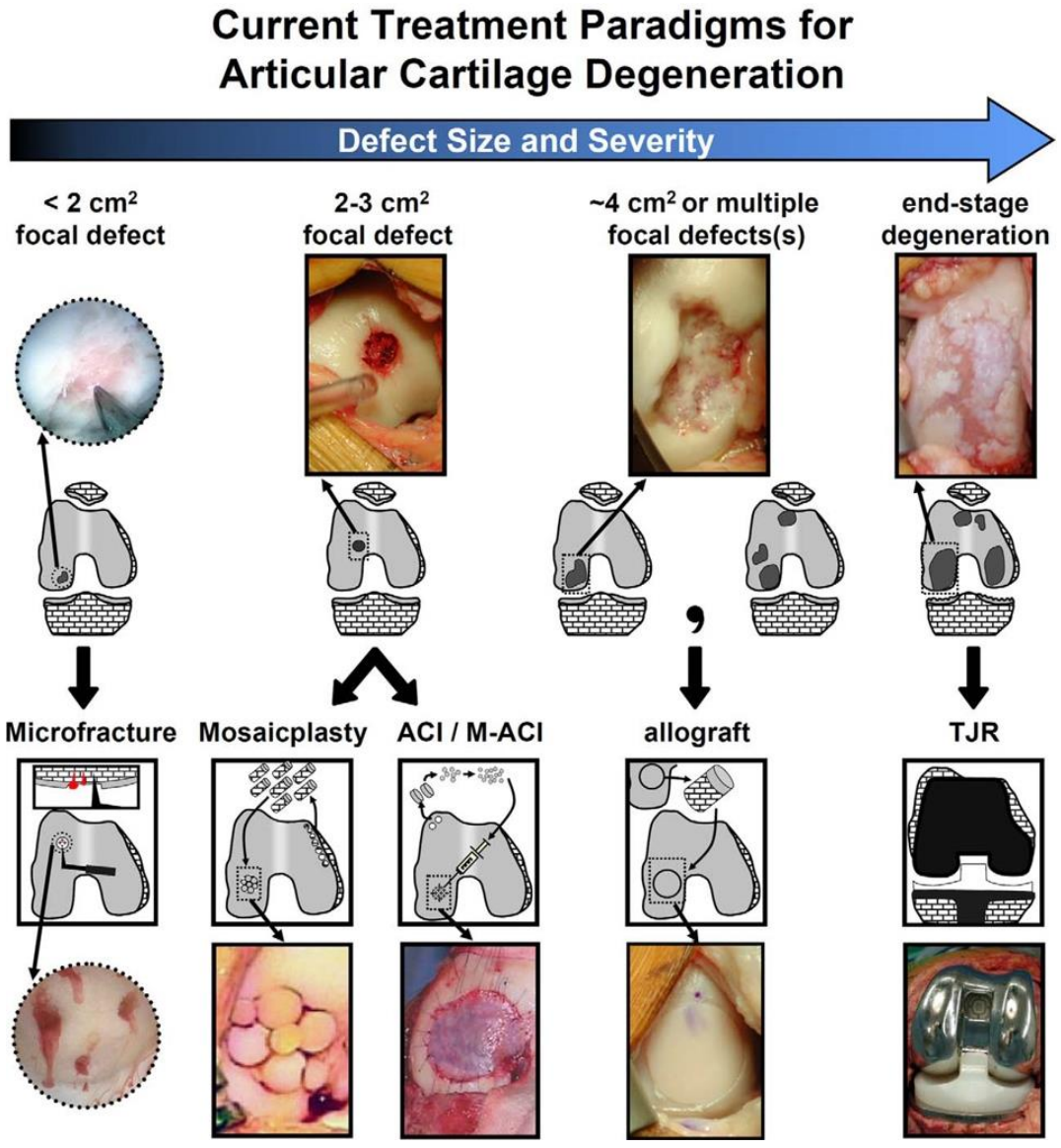

Figure 1.10 Current treatment paradigms for articular cartilage degeneration

Diagram showing the current treatment paradigms for articular cartilage degeneration depending on size and severity of the defects. [15]

1.3.1 Microfracture

Microfracture is most commonly performed for focal lesions with <2cm^2. Microfracture is a treatment option in which the damaged cartilage is removed and small holes are created deep inside the bone to allow blood cells to migrate to the injury site. These holes of approximately 2 mm in diameter and separated by 3-4 mm are created using a specially designed 45° bent awl (Figure 1.11). Microfracture has a good success rate with best long lasting results in young and less active patients with smaller defect site.

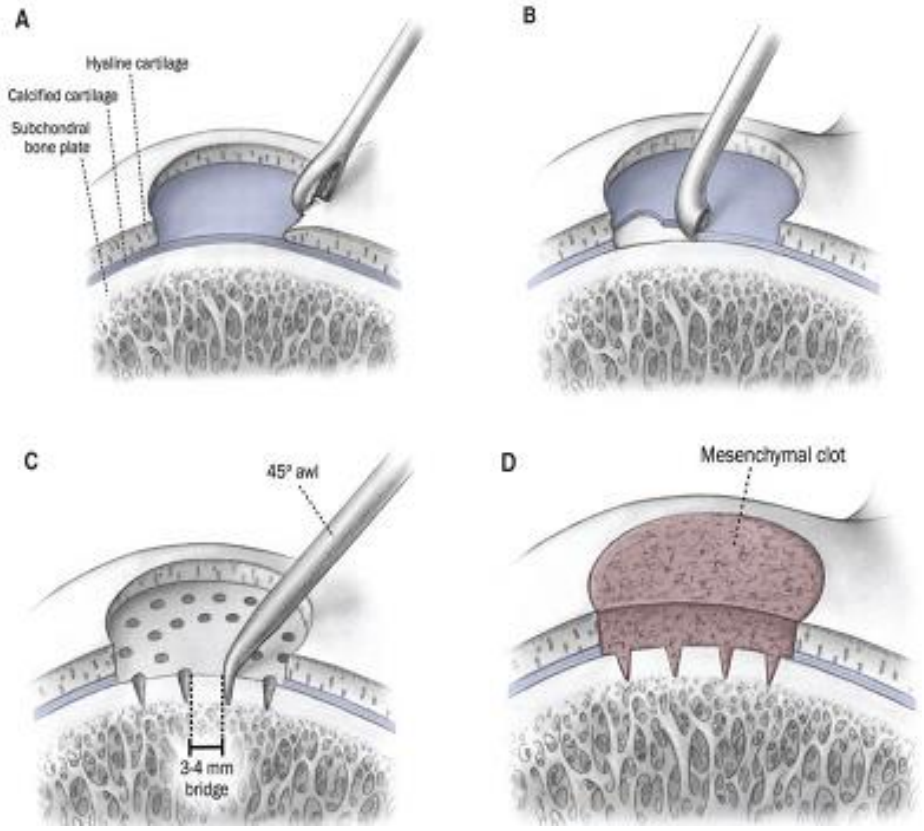

Figure 1.11 Schematic representation of microfracture process

A) removal of dead or damaged articular tissue B)calcified cartilage removal C) microfractures created using 45° bent awl D) Mesenchymal clot in the defect site for cartilage repair [16].

1.3.2 Chondroplasty

Microfracture and chondroplasty are the most commonly performed therapies to treat articular cartilage lesions [5]. Chondroplasty is the process of reshaping the joint surface by removing the damaged cartilage and stimulating the underlying undifferentiated cells to cover the damaged area with fibrocartilage. In most of the cases when chondral defects reach the bone, a scar tissue formed with fibrocartilage fills the defect. This fibrocartilage is more dense compared to articular cartilage and cannot perform functions as articular cartilage. These therapies are available to young patients with small lesions and with only limited success rate.

1.3.3 Mosaicplasty

Mosaicplasty is a surgical procedure followed to resurface the cartilage defects ranging between 2-3 cm^2 in size. In this process, autologous osteochondral grafts are harvested from a low weight bearing regions of the knee. After removing the damaged cartilage, these grafts are implanted in the defect region in a pattern that it covers the defect site. The main advantages of this procedure include autologous grafts which reduce the infection and can be performed as a single surgical procedure. The limitations of this procedure are limited availability of grafts, fitting the graft in defect site, and morbidity in the donor site [17]. As the hyaline cartilage itself is implanted directly in the defect site, mosaicplasty is preferable than autologous chondrocyte implantation, where chondrocytes are implanted in the defect region.

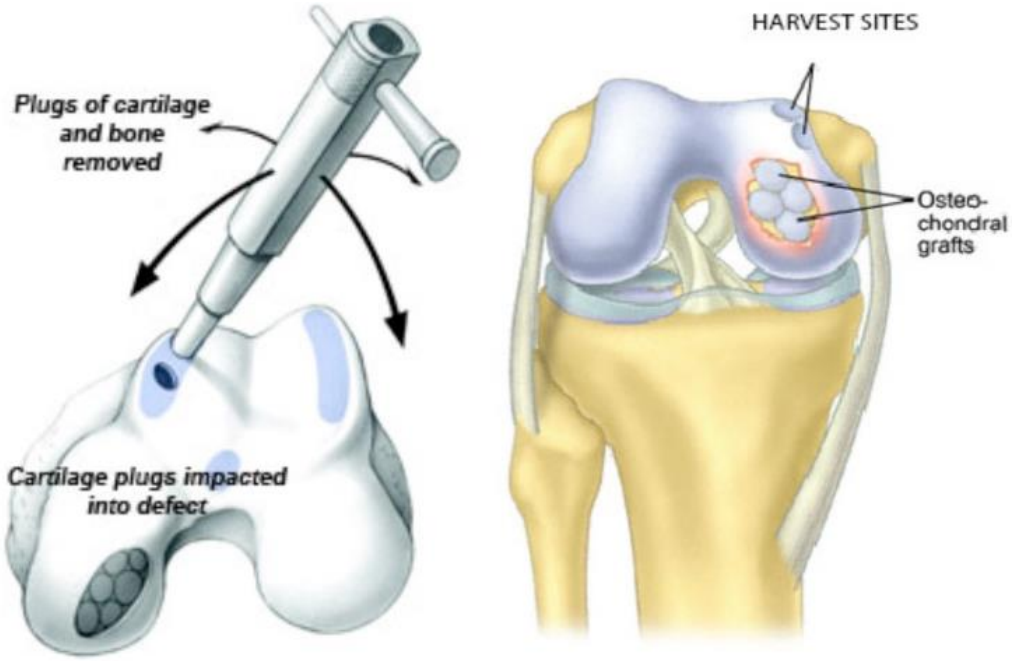

Figure 1.12 Diagram showing the process of Mosaicplatsy where autologous osteochondral grafts were implanted in defect site.

(Courtesy: http://boneandspine.com/mosaicplasty-or-osteochondral-graft-transfer-system)

1.3.4 Autologous Chondrocyte Implantation

Autologous Chondrocyte Implantation (ACI) is usually performed for a defect size ranging between 3-4 cm^2. ACI is another option for treating cartilage defects. In this process, chondrocytes are isolated from a healthy cartilage harvested from a low weight bearing region. After expanding these chondrocytes, a second surgery will be performed where these cells will be implanted in the defect site and sealed with periosteal flap. The final results of ACI have shown formation of hyaline like tissue in the defect region and there is also pain relief and restored joint function in 80-90% patients [6]. But the main drawbacks of ACI are chondrocyte leakage from the defect region, uneven distribution of chondrocytes and periosteal hypertrophy [7].

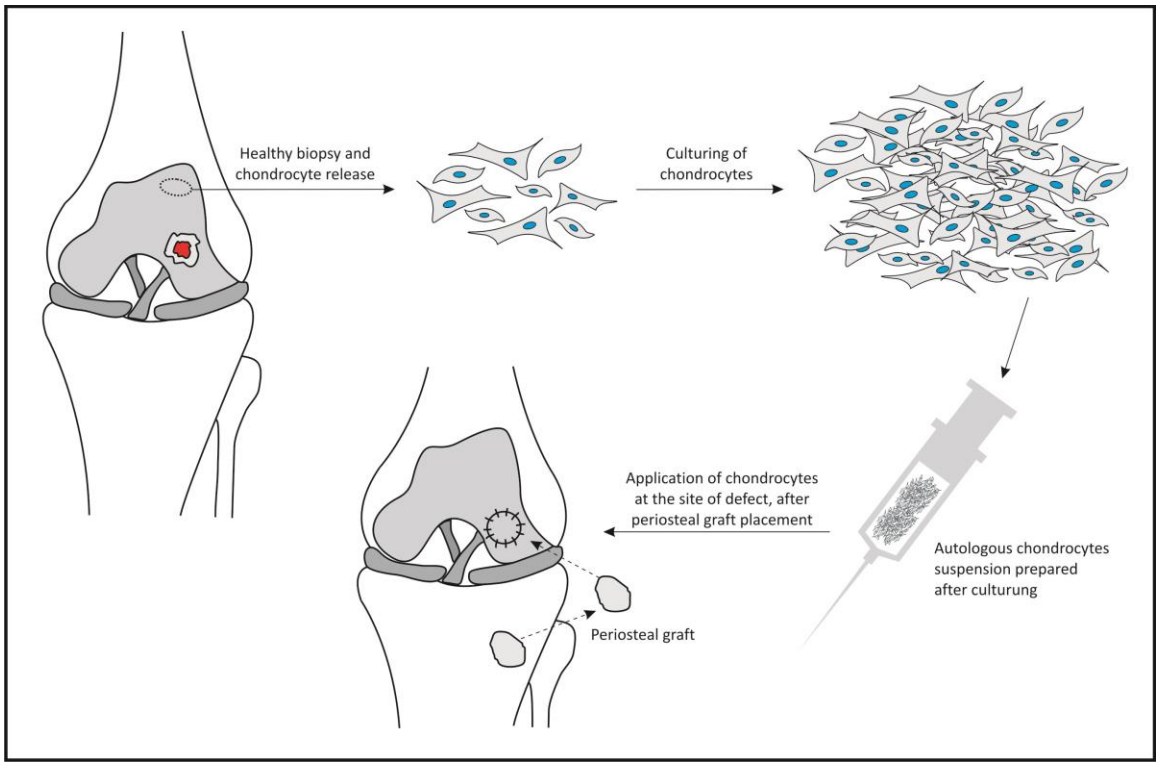

Figure 1.13 Schematic representation of Autologous Chondrocyte Implantation (ACI) [11]

1.3.5 Osteochondral grafts (allografts)

Osteochondral allograft is a procedure similar to mosaicplasty where osteochondral plugs are implanted in the defect region. This differs from mosaicplasty by collecting the osteochondral grafts from a different donor rather than from same patient as in mosaicplasty. The main advantage of this procedure is that grafts can be collected from the same site of defect from donor so that it can fix well in the defect place. Grafts can also be collected from a young donor. The main drawbacks are the immune response and disease transmission from the donor.

1.3.6 Total knee replacement

Total knee (joint) replacement or total knee arthroplasty (TKA) is the only option at the end stage of cartilage damage and there is only a 50% chance of good outcome [18]. Knee replacement is a surgical procedure where the damaged ends of femur and tibia bones will be replaced with a metal [19]. The artificial parts that are used are called prosthesis. The clinical outcome results of patients' undergone total hip replacement will start to gradually decline starting from 5 years after surgery and infection is the most common cause for failure [20].

Figure 1.14 Diagram showing a healthy knee joint and a total knee replacement (Courtesy: https://www.nlm.nih.gov/medlineplus/kneereplacement.html)

1.4 Tissue Engineering

The loss or failure of an organ or tissue is one of the most frequent, disastrous, and costly problems in human healthcare. A new field, tissue engineering, applies the principles of biology and engineering to the development of functional substitutes for damaged repair [21]. There are two main components in tissue engineering – cells to regenerate the lost or damaged tissue and scaffolds (or matrices) that allow cell attachment and tissue growth. Tissue engineering is quite challenging where the engineered tissues should contain the ECM components of the target native tissue in similar proportions and structural arrangements and also provide similar biomechanical functions. In a cartilage tissue engineering approach, cells were either encapsulated in or seeded on top of a three dimensional scaffold materials. The main goal of cartilage tissue engineering is to regenerate healthy hyaline cartilage *in vitro* and implant the tissue *in vivo* which functions similarly to the native articular cartilage.

Cell performance and ease of access are the two main specifications that need to be examined while selecting cells for cartilage repair. Different cell types including chondrocytes, mesenchymal stem cells, embryonic stem cells, and pluripotent cells have been considered for cartilage regeneration (Table 1.1). Articular chondrocytes and MSCs are the most commonly used cell sources for cartilage tissue engineering. MSCs have some advantages compared to chondrocytes, chief among them being the preservation of all healthy cartilage in the affected joint and sparing of additional trauma to that joint [22]. MSCs are hypoimmunogenic, self-renewable, and can also proliferate for long periods [23]. They also exhibit anti-apoptotic and wound healing properties [24]. MSCs are easy to harvest and can differentiate into chondrocytes when supplied with growth

factors like transforming growth factor –β1. Chondrocytes have limited potential for expansion *in vitro*, and proliferation in monolayer results in cell de-differentiation and declining chondrogenic potential [25] [26].

Table 1.1 Advantages and Disadvantages of various cell types for cartilage tissue engineering [27]

Cell type	Advantages	Disadvantages
Autologous chondrocyte	Native phenotype Minimal risk of immunological problem	Small initial cell number De-differentiation on expansion
Allogeneic chondrocyte	Larger cell number Off-the-shelf solution	Limited donor availability Risk of disease transmission
Adult mesenchymal stem cells	Potential to produce large numbers Various harvest sites Additional paracrine signaling potential	Potential for hypertrophy Heterogeneous population of cells Stable and reproducible differentiation still problematic
Induced pluripotent stem cells (iPS)	Large source of patient specific cells Multiple cell types can be produced	Stable and reproducible differentiation still problematic Potential for teratoma
Embryonic stem cells	Off-the-shelf solution Multiple cell types can be produced	Stable and reproducible differentiation still problematic Potential for teratoma Ethical considerations

Scaffolds provide a matrix for cell attachment in tissue engineering. Things need to be considered before selecting a scaffold are mechanical integrity, biocompatibility, cell attachment, degradation rate, and degradation products. Biological and synthetic based scaffolds can potentially enhance to repair or replace any tissue in musculoskeletal tissue engineering [28]. Biologically derived scaffolds are acellular tissue scaffolds (Collagen, hyaluronic acid, and chitosan) and have a limited capacity of modification. Synthetic polymer based scaffolds enable the design of scaffolds with specific mechanical and biological properties. However, the scaffold must be strong enough to provide support to the defect site until the formation of new bone. Sustained release of growth factors to promote bone growth is desirable in addition to providing a structure to

which bone cells can attach [29]. Scaffolds structurally reinforce the defect to maintain the shape of the defect and to prevent the distortion of surrounding tissue.

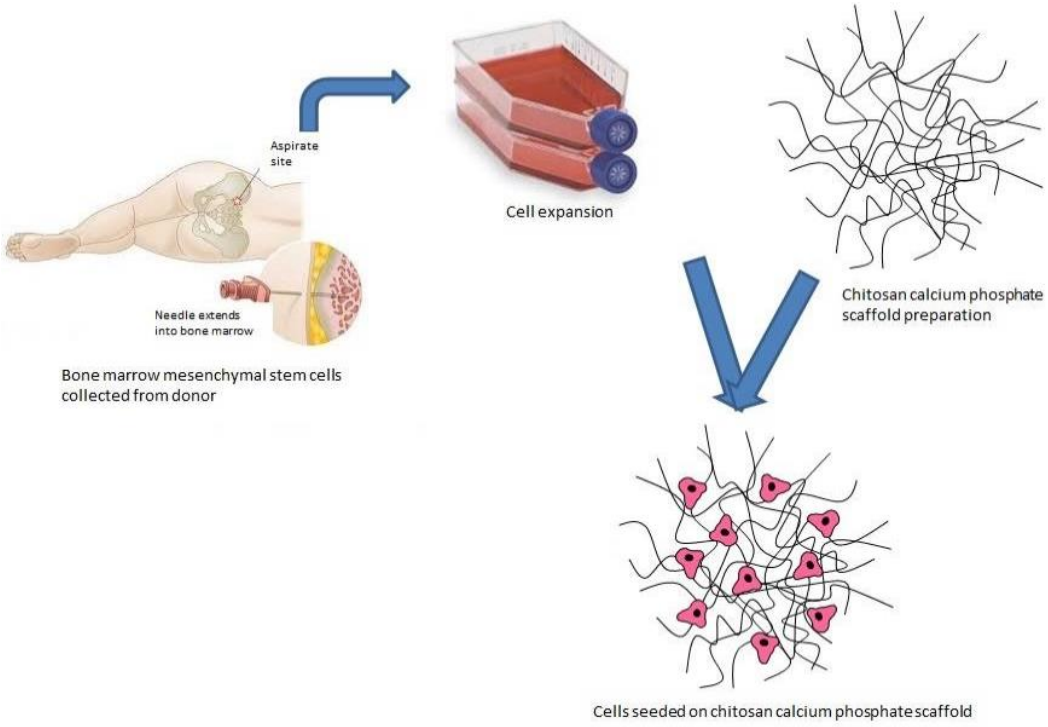

Figure 1.15 Overview of engineered cartilage on CHI-CaP scaffolds for osteochondral defects approach.

The osteoconductive scaffold we have selected for this study is made up of calcium phosphate in a chitosan matrix. Chitosan is a deacetylated derivative of chitin, found in the exoskeleton of marine crustaceans. Chitosan is a biocompatible and osteoconductive polymer with enhanced wound-healing capability [30]. Also antimicrobial properties of chitosan could reduce the bacterial infection upon implantation [31,32]. Chitosan is biodegradable and even the oligosaccharide degradation

products, liberated primarily by enzymatic hydrolysis of the acetylated residues, does not cause any damage.

Tissue engineering, a relatively new field, studies the formation of new perfectly functional tissues and organs by combining cells, biomaterials and biological factors that can be implanted in the defect region. Cartilage tissue when implanted by itself, do not easily secures to the underlying bone and the surrounding native cartilage. Cartilage is much more easily immobilized in the joint when it is attached to the scaffold and then press fit into a bony defect. Most often the subchondral bone lying below the articular cartilage defect also undergoes degeneration. It is important to repair the subchondral bone along with cartilage defect as it provides support and integrates with neocartilage [33]. The current research is a biphasic approach to cartilage tissue engineering, in which one layer supports to form subchondral bone (osteogenesis) and another support cartilage formation (chondrogenesis).

1.5 Motivation and Specific aims

Cartilage of the knee is frequently injured, often as a result of sports related trauma, but focal articular cartilage lesions do not heal spontaneously. Articular cartilage is avascular, and the chondrocytes adjacent to an injury do not proliferate or migrate into the defect. Thus the tissue has very limited capacity for intrinsic repair, and untreated focal cartilage lesions may progress to early osteoarthritis [34]. Furthermore, such defects are associated with pain, swelling, and functional deficit [35].

Focal chondral lesions are a common finding during arthroscopy. A large review of 25,124 knee arthroscopies performed from 1989 to 2004 showed that isolated cartilage lesions occurred in 18% of patients [36]. According to current clinical guidelines, patients

with an ICRS (International Cartilage Repair Society) grade III or IV chondral lesions who are under 40 years of age may be good candidates for a restorative procedure [37]. Such patients accounted for 7% of all cases in the aforementioned review. Thus grade III and IV focal chondral lesions occur in a sizeable population of relatively young patients who might benefit from hyaline cartilage restoration.

Due to the limited availability of self-healing, it motivated many researchers to regenerate healthy hyaline cartilage using tissue engineering. We propose a new treatment alternative for focal chondral lesions using a biphasic construct of autologous cartilage and an osteoconductive scaffold. Autologous mesenchymal stem cells isolated from a bone marrow or adipose tissue biopsy will be expanded in monolayer and seeded on top of a porous chitosan-calcium phosphate so as to form a scaffold-free layer of cartilage adhered to the beads of the scaffold. This biphasic constructs will then be implanted into an osteochondral defect. The scaffold is expected to facilitate attachment to the native bone and will initially serve to transmit joint forces to the underlying bone. The scaffold is biodegradable and is replaced by host bone, thereby restoring the tissue structure and mechanics of a healthy joint.

The current investigation was relevant to the regeneration of cartilage in osteochondral defects, a treatment which may prevent or delay osteoarthritis.

The first specific aim of this proposal deals with cell attachment and proliferation of mesenchymal stem cells on chitosan calcium phosphate (CHI-CaP) scaffolds. The long term aim of this proposal was to develop an osteochondral construct with engineered cartilage. In order to achieve this aim, first and fore most things to achieve was MSC attachment to CHI-CaP scaffold. The porous nature of the

chitosan/CaP scaffold facilitates anchorage for the formation of cartilage. These scaffolds have adequate mechanical strength and toughness and their degradation products were not cytotoxic. This study showed that bone marrow derived MSCs can attach and proliferate on CHI-CaP scaffolds.

In the second specific aim of this study, biphasic constructs were prepared using two different approaches to determine which approach would yield a better construct. The typical bilayered construct consists of two different scaffold materials fused together or two different cell types seeded on top and bottom halves of the scaffold. In our approach, neocartilage (chondrogenesis) was formed from MSCs by self-assembly on top of osteoconductive CHI-CaP scaffold (osteogenesis). In this aim two different approaches for creating biphasic constructs were evaluated based on tissue formation, SEM, and histology.

The third specific aim, of this proposal was to determine how scaffold porosity and collagen coating would affect the bonding between engineered cartilage and scaffold. In order to improve tissue-scaffold integration, scaffolds were coated with type I collagen, an extracellular matrix protein to which cell attachment was mediated by integrin receptors. This study suggests that MSC attachment to a collagen precoated scaffold leads to biphasic construct fully covered with neocartilage.

The fourth specific aim was to identify the best bead size to make the composite CHI-CaP scaffolds for osteochondral defects. The size of the beads wasvaried by the droplet size of the chitosan solution dropping into precipitate solution. Pore size affects the penetration depth of cells and thereby tissue formation. Porosity, swelling ratio,

mechanical testing, and degradation tests were performed on different bead size scaffolds to identify the ideal bead size.

1.6 References

[1] Alice J Sophia Fox, Asheesh Bedi, and Scott A Rodeo, "The Basic Science of Articular Cartilage Structure, Composition, and Function," Sports Health, vol. 1, no. 6, pp. 461-468, Nov 2009.

[2] J Buckwalter and H Mankin, "Articular Cartilage: Tissue Design and Chondrocyte-matrix Interactions," Instr. Course Lect, vol. 47, pp. 477-486, 1998.

[3] Johnna S Temenoff and Antonios G Mikos, "Review: Tissue Engineering for Regeneration of Articular Cartilage," Biomaterials, vol. 21, no. 5, pp. 431-440, March 2000.

[4] Van C Mow, Anthony Ratcliffe, and Robin A. Poole, "Cartilage and diarthroidal joints as paradigms for hierarchical materials and structures," Biomaterials, vol. 13, no. 2, pp. 67-97, 1992.

[5] Stephanie Grenier, Madhu M Bhargava, and Peter A Torzili, "An *In Vitro* Model for the Pathological Degradatin of Articular Cartilage in Osteoarthritis," J Biomech, vol. 47, no. 3, pp. 645-652, Feb 2014.

[6] Carey-Beth james and Timothy L Uhl, "A Review of Articular Cartilage Pathology and the Use of Glucosamine Sulfate," J Athl Train, vol. 36, no. 4, pp. 413-419, Oct 2001.

[7] Nancy S Landinez-Parra, Diego A Garzon-Alvarado, and Juan Carlos Vanegas-Acosta, "Mechanical Behavior of Articular Cartilage, Injury and Skeletal Biomechanics," in Injury and Skeletal Biomechanics, Tarun Goswami, Ed.: InTech, 2012, ch. 11, pp. 197-216.

[8] Joseph M Mansour, "Biomechanics of Cartilage," in Biomechanical Principles., 2013, ch. 5, pp. 66-79.

[9] Johannah Sanchez-Adams, Holly A. Leddy, Amy L McNulty, Christopher J O'Conor, and Farshid Guilak, "The mechanobiology of articular cartilage: Bearing the burden of osteoarthritis," Curr Rheumatol Rep, vol. 16, no. 451, October 2014.

[10] Mohamadreza Baghaban Eslaminejad and Elham Malakooty Poor, "Mesenchymal stem cells as a potential cell source for articular cartilage regeneration," World J Stem Cells, vol. 6, no. 3, pp. 344-354, July 2014.

[11] Kelc Robi, Naranda Jakob, Kuhta Matevz, and Vogrin Matjaz, "The physiology of sports and repair processes," Current issues in sports and exercise medicine, Michael Hamlin, Ed.: InTech, 2013, ch. 2, pp. 43-86.

[12] Han Xinyun Audrey, Hamid Rahmatullah Bin Abd Razak, and Tan Hwee Chye Andrew, "The truth behind subchondral cysts in osteoarthritis of the knee," Open Orthop J, vol. 8, pp. 7-10, January 2014.

[13] Stephanie K Tanamas, Anita E Wluka, Jean-Pierre Pelletier, Johanna Martel-Pelletier, and Francois Abram, "The association between subchondral bone cysts and tibial cartilage volume and risk of joint replacement in people with knee osteoarthritis: a longitudinal study.," Arthritis Res Ther, vol. 12, no. 2, March 2010.

[14] Guangyi Li et al., "Subchondral bone in osteoarthritis: insight into risk factors and microstructural changes," Arthritis Res Ther, vol. 15, no. 6, December 2013.

[15] Gregory M Williams et al., "Shape, Loading, and, Motion in the Bioengineering Design, Fabrication, and Testing of Personalized Synovial Joints," J Biomech, vol. 43, no. 1, pp. 156-165, January 2010.

[16] Timothy R McAdams, Kai Mithoefer, Jason M Scopp, and Bert R Mandelbaum, "Articular cartilage injury in athletes," Cartilage, vol. 1, no. 3, pp. 165-179, July 2010.

[17] Paul Hindle, Jane L Hendry, John F Keating, and Leela C Biant, "Autologous osteochondral mosaicplasty or TruFit plugs for cartilage repair," Knee Surg Sports Traumatol Arthrosc, vol. 22, no. 6, pp. 1235-1240, June 2014.

[18] Gillian A Hawker et al., "Which Patients Are Most Likely to Benefit From Total Joint Arthroplasty?," Arthritis & Rheumatism, vol. 65, no. 5, pp. 1243-1252, May 2013.

[19] T T Miller, "Imaging of knee arthroplasty," European J of Radiology, vol. 54, no. 2, pp. 164-177, 2005.

[20] S Jafari, C Coyle, S Mortazavi, and J Parvizi, "Revision hip arthroplasty: Infection is the most sommon cause of failure," Clin Orthoop Relat Res, vol. 468, no. 8, pp. 2046-2051, August 2010.

[21] Daniel Howard, Lee D Buttery, Kevin M Shakesheff, and Scott J Roberts, "Tissue engineering: strategies, stem cells, and scaffolds," J Anat., vol. 213, no. 1, pp. 66-72, July 2008.

[22] Ulrich Noth, Andre F Steinert, and Rocky S Tuan, "Technology insight: Adult mesenchymal stem cells for osteoarthritis therapy," Nature Clinical Practice Rheumatology, vol. 4, no. 7, pp. 371-380, July 2008.

[23] Pawan K Gupta, Anjan K Das, Anoop Chullikana, and Anish S Majumdar, "Mesenchymal stem cells for cartilage repair in osteoarthritis," Stem Cell Res Ther., vol. 3, no. 4, July 2012.

[24] AI Caplan, "Adult mesenchymal stem cells for tissue engineering versus regenerative medicine," J Cell Physiol, vol. 213, no. 2, pp. 341-347, November 2007.

[25] Steve H Elder, Anuhya Gottipati, Hillary Zelenka, and Joel Bumgardner, "Attachment, proliferation, and chondroinduction of mesenchymal stem cells on porous chitosan calcium phosphate scaffolds," The Open Orthopaedics journal, vol. 7, pp. 275-281, July 2013.

[26] Guillaume R Ragetly, Dominique J Griffon, Hae-Beom Lee, and Yong Sik Chung, "Effect of collagen II coating on mesenchymal stem cell adhesion on chitosan and on reactylated chitosan fibrous scaffolds," J Mater Sci: Mater Med, vol. 21, no. 8, pp. 2479-2490, August 2010.

[27] Brian Johnstone et al., "Tissue engineering for articular cartilage repair - The state of the art," European Cells and Materials, vol. 25, pp. 248-267, May 2013.

[28] Frances Henson and Alan Getgood, "The use of scaffolds in musculoskeletal tissue engineering," Open Orthop J, vol. 5, pp. 261-266, July 2011.

[29] b Reves, J Bumgardner, J Cole, Y Yang, and W Haggard, "Lyophilization to improve drug delivery for chitosan calcium phosphate bone scaffold construct: A preliminary investigation," J Biomed Mater Res B Appl Biomater, vol. 90, no. 1, pp. 1-10, July 2009.

[30] M Sravanthi, A Ranjith, and P Karteek, "Chitosan: A biocompatible polymer for pharmaceutical applications in various dosage forms," International J of Pharmacy & Technology, vol. 2, no. 2, pp. 186-205, June 2010.

[31] O Felt, A Carrel, P Baehni, P Buri, and R Gumy, "Chitosan as a tear substitute: A wetting agent endowed with antimicrobial efficacy," J Ocul Pharmacol Ther, vol. 16, no. 3, pp. 261-270, June 2000.

[32] G Tsai and W Su, "Antibacterial activity of shrimp chitosan against Escherichia coli," J Food Prot, vol. 62, no. 3, pp. 239-243, March 1999.

[33] H Da, S Jia , G Meng, J Cheng , and W Zhou, "The impact of compact layer in biphasic scaffold on osteochondral tissue engineering," PLoS ONE, vol. 8, no. 1, January 2013.

[34] W Maletius and K Messner, "The effect of partial meniscectomy on the long-term prognosis of knees with localized, severe chondral damage. A twelve-to fifteen-year followup," J Sports Med, vol. 24, no. 3, pp. 258-262, June 1996.

[35] Benedict A. Rogers, Lee A. David, and Tim W. R Briggs, "Sequential outcome following autologous chondrocyte implantation of the knee: A six-year follow-up," Int Orthop, vol. 34, no. 7, pp. 959-964, October 2010.

[36] W. Widuchowski, J. Widuchowski, and T. Trzaska, "Articular cartilage defects: Study of 25,124 knee arthroscopies," Knee, vol. 14, no. 3, pp. 177-182, June 2007.

[37] BJ Cole, C Pascual-Garrido, and RC Grumet, "Surgical management of articular cartilage defects in the knee," Instr Course Lect, vol. 91, no. 7, pp. 1778-1790, 2010.

CHAPTER II

ATTACHMENT AND PROLIFERATION OF HUMAN MESENCHYMAL STEM CELLS ON CHITOSAN CALCIUM PHOSPHATE SCAFFOLDS

2.1 Introduction

The purpose of this study was to conduct a preliminary investigation using a tissue engineering approach to osteochondral regeneration using composite chitosan calcium phosphate scaffolds and MSCs.

Chitosan is a deacetylated derivative of chitin found in the exoskeleton of marine crustaceans (Figure 2.1) and is the second largest biological polymer. Chitosan is one of the widely used scaffold materials for tissue engineering. It is a polysaccharide chain made up of N-acetyl-D-glucosamine and D-glucosamine linked by β(1-4) bands (Figure 2.2). Chitosan has been widely used in various biomedical applications such as tissue engineering, wound dressing, drug delivery, and cancer diagnosis [1]. Previous research also revealed that chitosan has hemostatic and cholesterol lowering properties [2]. Furthermore the material properties of chitosan can be regulated by varying the molecular weight and degree of deacetylation (DDA) [3,4,5]. Chitosan is a biocompatible and biodegradable scaffold material. Biodegradable polymers are applicable to those tissue engineering products in which tissue repair is the goal, but not where long-term materials stability is required. The degradation rate of chitosan depends on the DDA, where the

chitosan with lower DDA degrades faster [6]. Chitosan dissolves in acidic solutions with lower pH value.

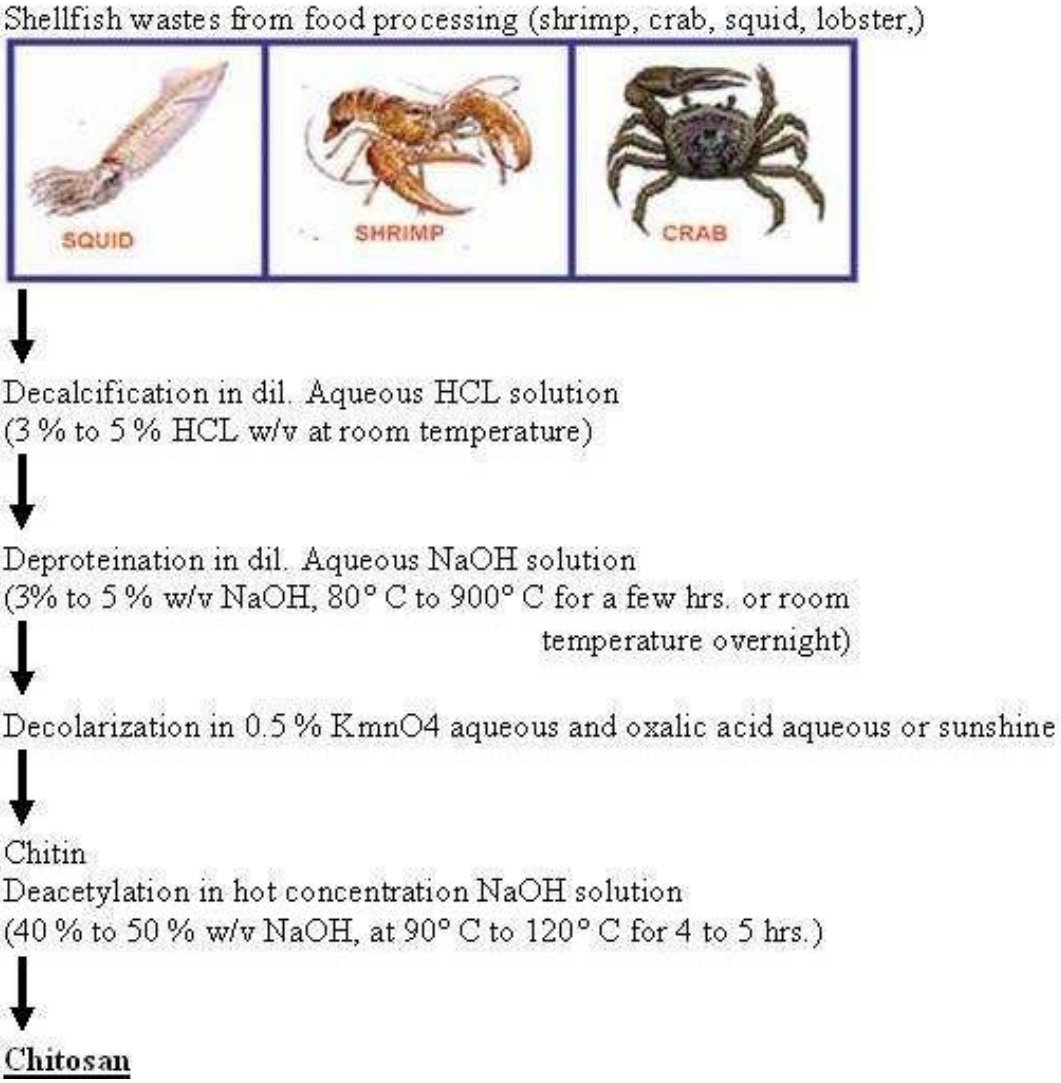

Figure 2.1 Extraction of chitosan from Shellfish wastes from food processing [7].

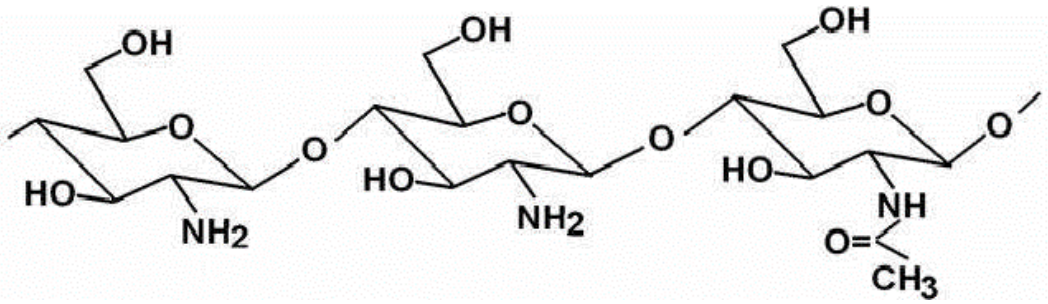

Figure 2.2 Chemical Structure of chitosan [7].

Pore size and porosity of chitosan scaffolds are approximately 100-800 μm and 35% and is sufficient for ingrowth of new tissue [6]. This porosity of the scaffolds was created by fusing small beads together by briefly washing with acetic acid. According to Chesnutt et al. the compressive modulus of theses scaffolds was 10MPa and can also undergo 50% compressive strain without breaking scaffold [6]. Compressive loading causes some matrix consolidation and fluid flow out of the tissue in the regions closest to the articular surface, which contributes to joint lubrication. Under loading for short duration, the tissue in the deeper region adjacent to bone experiences almost no deformation as load is supported by interstitial fluid pressure.

Previous investigations done by Chesnutt et al. have shown that CHI-CaP scaffolds support cell attachment and proliferation of human fetal osteoblast cells and human embryonic palatal mesenchymal cells [6,8]. Cell attachment and viability of human umbilical cord stem cells on calcium phosphate cement chitosan scaffolds was shown by Liang Zhao et al. [9]. Oliveira et al. had shown the attachment of goat bone marrow stromal cells seeded on hydroxyapatite/chitosan bilayered scaffold [10]. The current study investigates the human bone marrow mesenchymal stem cell attachment

and proliferation on composite chiotsan calcium phosphate scaffolds (CHI-CaP) prepared by co-precipitation method.

2.2 Methods

2.2.1 Scaffold fabrication

Composite CHI-CaP beads were prepared by co-precipitation method as described previously by Chesnutt et al. [6]. Chitosan solution was prepared by dissolving 3.57gm of 78.7% DDA chitosan powder (Vanson Halosource, Remond, WA) in 84 ml of 2 wt% acetic acid. 10 ml of 1 M $CaCl_2$ in 2% acetic acid and 6 ml of 1 M NaH_2PO_4 in 2% acetic acid was added to the chitosan solution to make a final Ca:P ratio of 1.67. The chitosan calcium phosphate solution was left for overnight on stirrer to get a nice consistent solution. The consistent chitosan solution was taken into a 30 ml syringe with 18G needle and was fixed to a syringe pump. The chitosan solution was added drop wise into a magnetically stirring precipitate bath at a rate of 15ml per hour (Figure 2.3). The precipitation solution was made of 20% NaOH, 30% methanol, and 50% DI water at a pH 13. These drops were precipitated into beads eventually. The beads were left in precipitate solution for 24h for the formation of crystalline hydroxyapatite, bone mineral as proposed by Rusu et al. as shown in Equation 2.1[11]. After 24 hours the precipitation solution was replaced by DI water. These beads were washed regularly in DI water until it reaches pH 7.

$$10CaHPO_4 + 12OH^- \rightarrow Ca_{10}(PO_4)_6(OH)_2 + 10H_2O + 4PO_4^{3-} \quad (2.1)$$

$$+ACP + OH^- \rightarrow Ca_{10}(PO_4)_6(OH)_2 \quad (2.2)$$

The beads were then separated individually into a large dish and air dried overnight at room temperature as shown in figure 2.4. These beads reduced to almost 60% of its original size after drying. Dried beads were packed into custom made cylindrical molds. This consists of two separate plates, where the bottom plate was flat with no holes and the top plate has cylindrical shaped holes of 6.5mm diameter × 7mm height (Figure 2.5). While making scaffolds these plates were wiped to dry and taped together so that they will not deform scaffolds. The dried beads were filled into the holes and fused into scaffolds by brief exposure to 1% acetic acid and manually applied pressure (Figure 2.6). The leftover acetic acid was washed using DI water and allowed them to dry at room temperature for 24 hours.

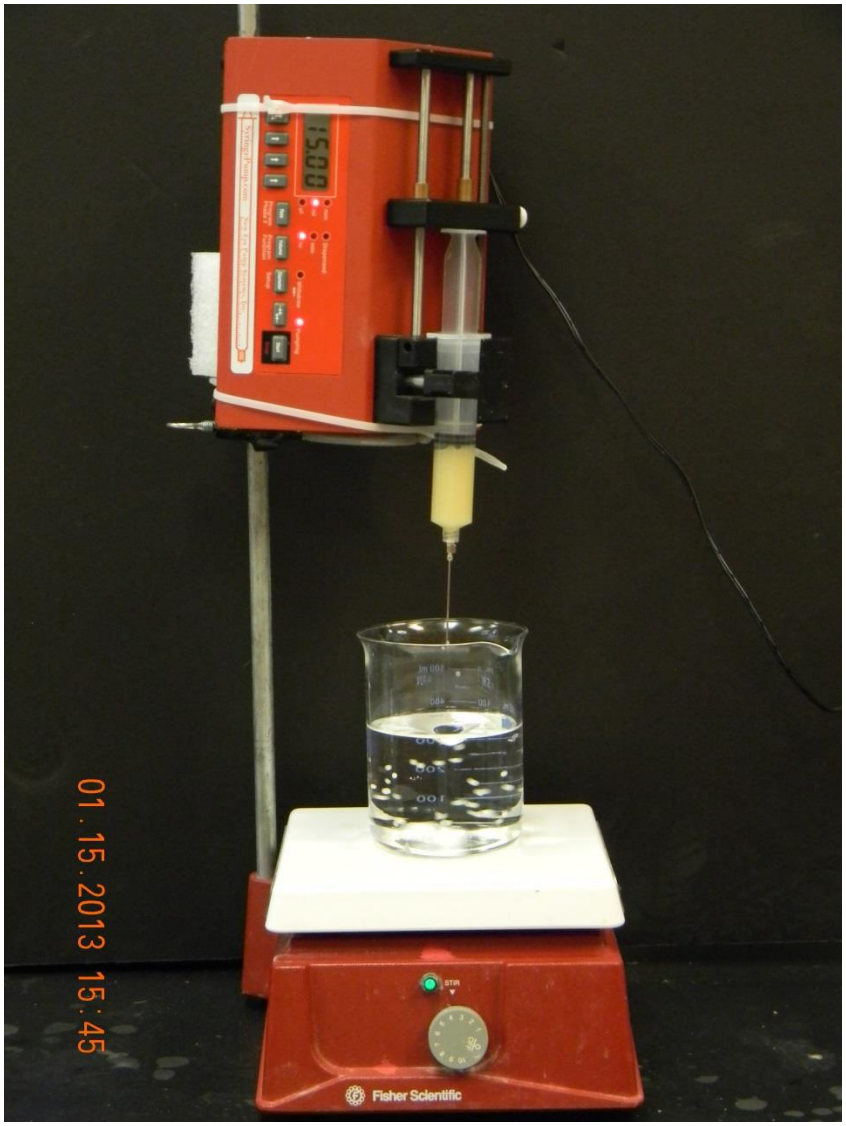

Figure 2.3 Chitosan calcium phosphate solution dripping drop wise into a magnetically stirring precipitate bath at a rate of 15ml per hour.

Figure 2.4 CHI-CaP beads separated individually into a dish and air dried overnight at room temperature.

These scaffolds were then washed in 70% ethanol for 2 hours at room temperature and allowed them to sit at room temperature for 1 hour. All the CHI-CaP scaffolds were then frozen at -20°C for 2-3 hours and lyophilized overnight. Previous study has shown that lyophilization enhances porosity, surface texture and protein absorption [12]. All these lyophilized scaffolds were collected into sterile pouches for ethylene oxide gas sterilization before seeding cells.

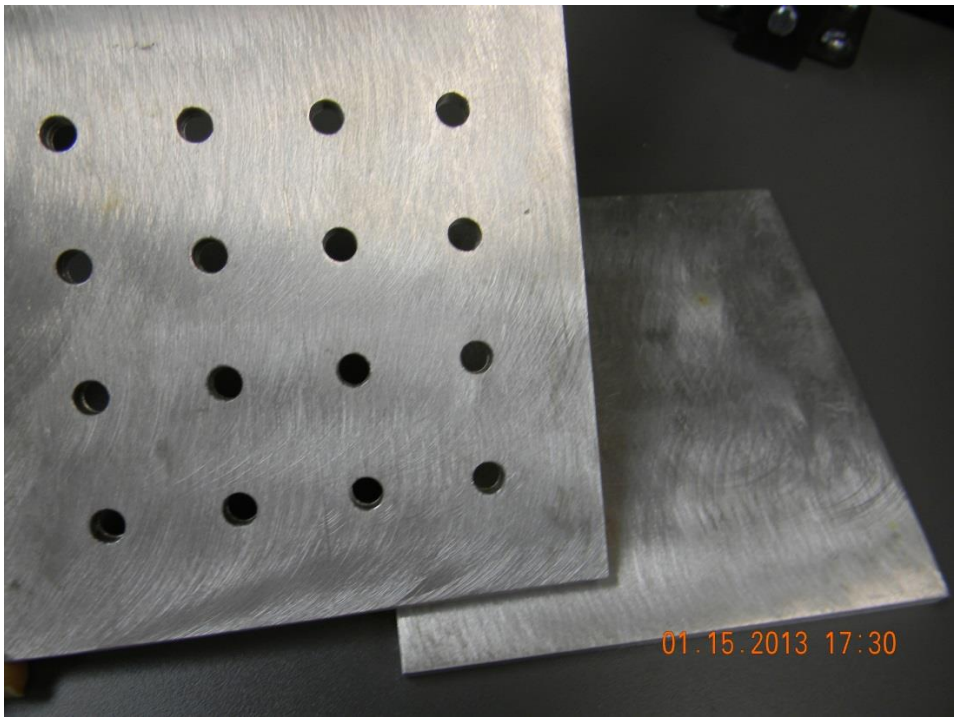

Figure 2.5 Two separate plates – one having cylindrical shape holes for scaffold fabrication to be place on top of the other flat plate.

2.2.2 Scaffold mechanical testing

The compressive modulus of cell-free scaffolds was measured. One of the main functions of bone in *in vivo* is load bearing. As these CHI-CaP scaffolds are replacing a bone part in a joint, they need to have load bearing capacity similar to native bone. In order to measure the compressive modulus, the scaffolds were first incubated for 1, 14, or 28 days in cell culture medium at 37°C. Young's modulus in the axial direction was determined by unconfined compressive loading at 5 μms^{-1}.

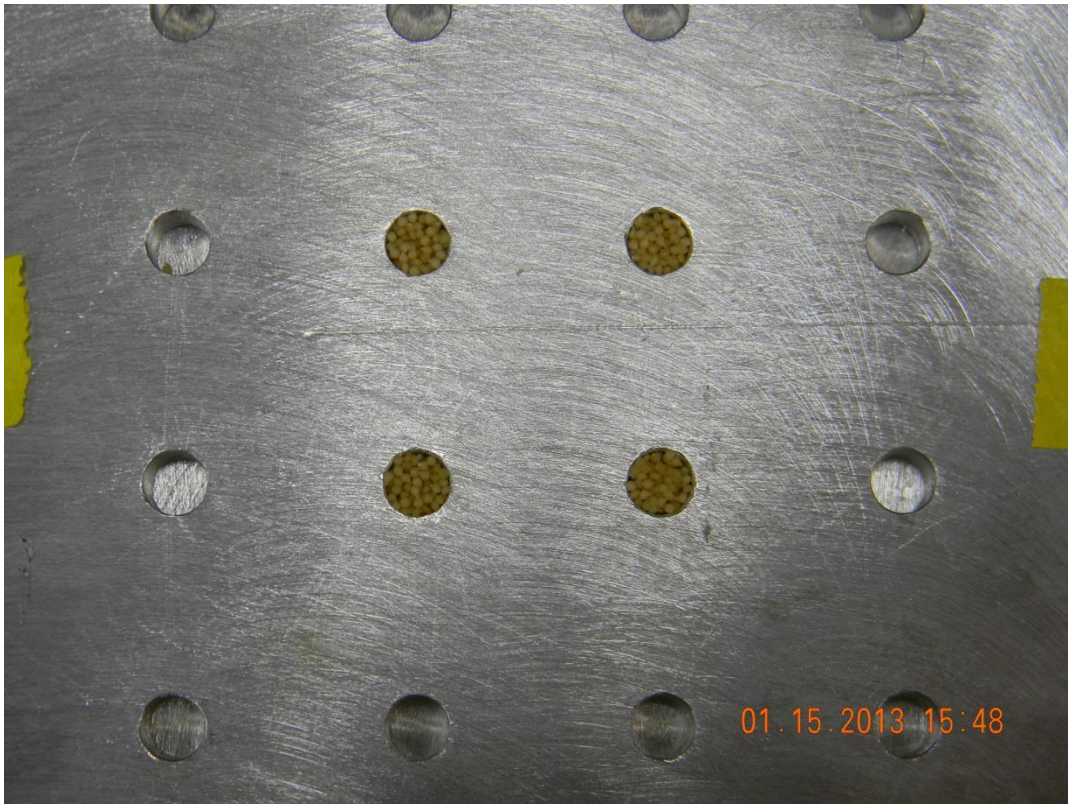

Figure 2.6 CHI-CaP beads filled into cylindrical shape molds and fused together using 2% acetic acid.

2.2.3 Cell source

Primary human bone marrow mesenchymal stem cells (MSC) were used to quantify cell attachment and proliferation on CHI-CaP scaffolds. Frozen cells of passage 1 from a 24 year old male donor were obtained from Texas A&M Health Science Center College of Medicine Institute for Regenerative Medicine at Scott & White (Temple, TX). Screening tests verified that these cells met the minimal criteria, which define human mesenchymal stem cells as established by the Mesenchymal and Tissue Stem Cell Committee of the International Society for Cellular Therapy. Cell vial was placed on ice until everything was set. Cells were thawed and plated in a new sterile cell culture flask

at approximately $5x10^3$ cells/cm^2. Cells were cultured in StemLife™ MSC Medium (Lifeline Cell Technology, Frederick, MD). Cell medium was changed every 3-4 days. Cells were subcultured before reaching confluence. Cells attached to the flask were released by enzymatic treatment using trypsin. Trypsin was added to cover the bottom layer of the flask and left in the incubator for 10 min for cell detachment from flask. Cell culture medium with 10% FBS was added to stop the action of trypsin. All the cells and medium were collected into a sterile 50 ml centrifuged at 500g for 5 min. The supernatant was discarded and the cell pellet was resuspended into fresh cell culture medium and plated again in new cell culture flasks at approximately $5x10^3$ cells/cm^2.

2.2.4 Biphasic constructs

MSCs at passage 4 were used for making biphasic constructs. After enzymatic treatment with trypsin and centrifugation, the cells were resuspended at $5x10^5$ cells/ml. 50 µl of cell suspension was pipetted directly on top of each CHI-CaP scaffold. Few 50 µl of cell suspension aliquots were frozen to determine the initial cell seeding number. These constructs were left for 30 min in the incubator at 37°C with 5% CO_2 allowing the cells to attach to the scaffold. During this time the constructs were flooded with defined chondrogenic medium (DCM). DCM consisted of high glucose Dulbecco's Modified Eagles Medium (DMEM) containing 1% ITS+Premix (BD Biosciences, San Jose, CA), 0.1 mM dexamethasone, 50 µg/mL ascorbate-2 phosphate, 1 mM sodium pyruvate, 40 µg/mL L-proline, 1% antibiotic-antimycotic solution (Sigma-Aldrich, St. Louis, MO), and 10 ng/ml human recombinant transforming growth factor-β3 (PeproTech, Rock Hill, NJ). These constructs were cultured for either 1 or 28 days in DCM. DCM was changed

every 3-4 days. Day 1 cultures were used to assess cell attachment quantitatively by measuring DNA (n = 3). Day 28 cultures were used to evaluate cell proliferation and chondroinduction based on content of DNA and GAG, respectively (n = 6). One 24 hour construct was also examined using SEM. Attachment efficiency ($T_{1/2}$) was calculated from Equation 2.2, where q_1 was the average DNA content of cells in the aliquot used for seeding, and q_2 was the DNA content on the discs after 30 minutes of seeding.

$$T_{\frac{1}{2}} = \left(\frac{q_1}{q_2}\right) 100, \tag{2.3}$$

The rate of cell population doubling time (T_d) was calculated from Equation 2.3, where q_1 and q_2 were the average DNA content at 30 minutes (t_1) seeding and DNA content on the disc at 28-day (t_2) time duration respectively.

$$T_d = (t_2 - t_1) \frac{log\, 2}{log \frac{q_2}{q_1}}, \tag{2.4}$$

2.2.5 DNA and GAG quantification

Samples designated for biochemistry (DNA/GAG) were digested in 1% papain overnight at 60°C. Samples were then centrifuged at 10,000 rpm for 3 min. One aliquot of the digested sample was used for analyzing DNA content by Hoechst dye method in DNA quantification kit (Sigma-Aldrich, St. Louis, MO). Fluorescence intensity was read in Glomax Multi detection system. DNA content was calculated from a standard curve produced with calf thymus DNA provided in the kit. By quantifying DNA we can measure cell number and cell proliferation rate. Total DNA content will be normalized to the sample wet weight. Another aliquot of the digested sample was used for GAG quantification. Total GAG content was determined by the dimethylmethylene blue

(DMMB) dye-binding method using the Blyscan™ Assay (Biocolor Ltd, Carrickfergus, United Kingdom) according to the manufacturer's instructions. The GAG content was read at 656 nm in spectrophotometer. GAG content was calculated from a standard curve produced with the chondroitin 4-sulfate standard provided in the kit. Total GAG amount was normalized to the wet weight of the sample. GAG and DNA were analyzed in the same way as mentioned in previous studies [13].

2.2.6 SEM sample preparation

The structure and the surface morphology of the constructs were examined using Scanning Electron Microscope (SEM). Constructs for SEM were fixed in 2.5% glutaraldehyde in PBS for overnight at 4°C. Later the scaffolds were dehydrated in graded ethanol (30%, 50%, 70%, and 90%) for 20 min at room temperature. Scaffolds were finally incubated in two changes of 100% ethanol and hexamethyldisilazane for 20 min each, and air dried under hood for about 30 min. These samples were then sputter coated with platinum and imaged using a JEOL JSM-6500F Field Emission Scanning Electron Microscope.

2.3 Results

2.3.1 Scaffold mechanical testing

Chitosan Calcium Phosphate scaffolds were fabricated as mentioned in experimental design. Freeze dried CHI-CaP scaffolds were approximately 6mm in diameter and 7 mm in height as shown in figure 2.7. Incubating the scaffolds in culture medium for up to 28 days had no discernible effect on their compressive Young's modulus of approximately 5 MPa (Figure 2.8), which approaches the lower range of

modulus for human trabecular bone [14]. None of the scaffolds broke during testing, but they were deformed from their original shape (Figure 2.9).

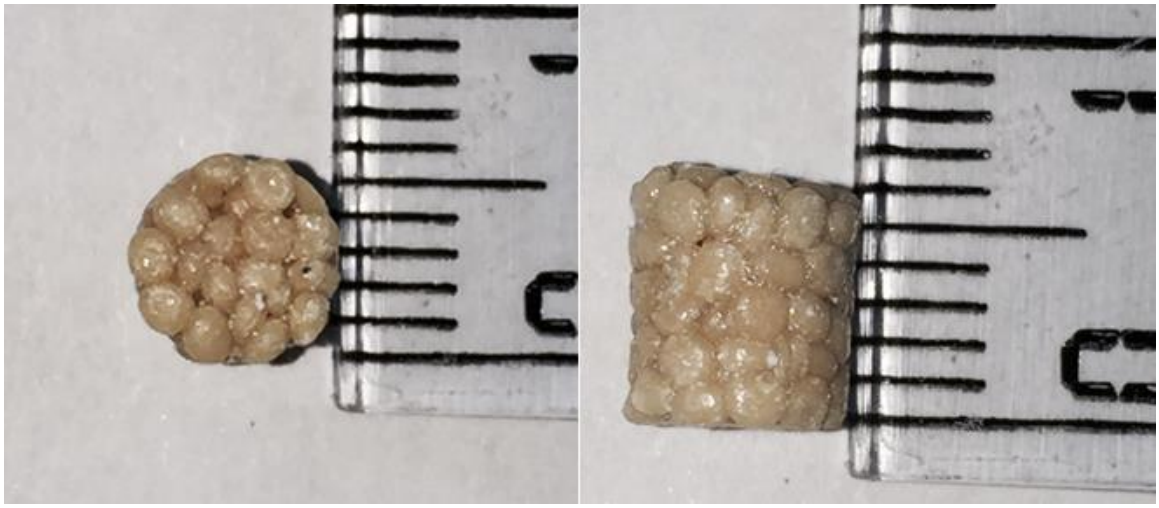

Figure 2.7 Freeze dried cylindrical shaped scaffold of approximately 6 mm in diameter and 7 mm in height.

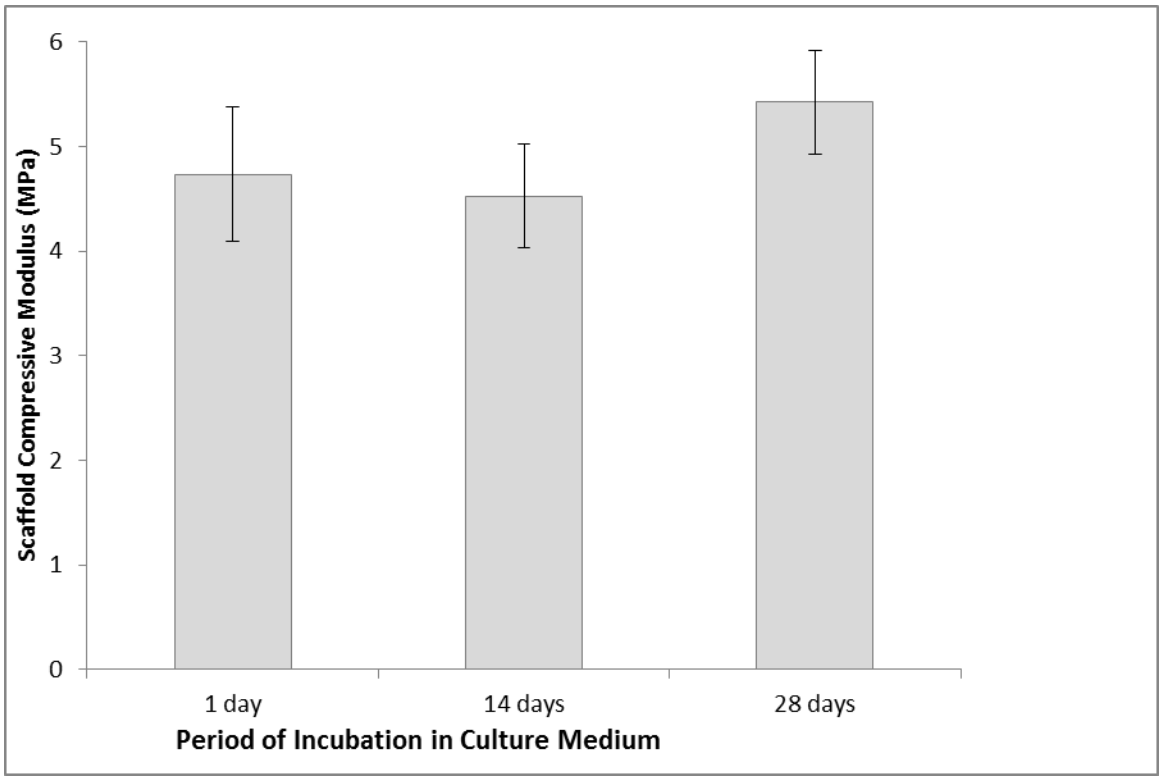

Figure 2.8 Young's modulus of scaffolds in unconfined compression

(n = 5)
Differences among groups were not statistically significant by one-way ANOVA ($p > 0.05$).

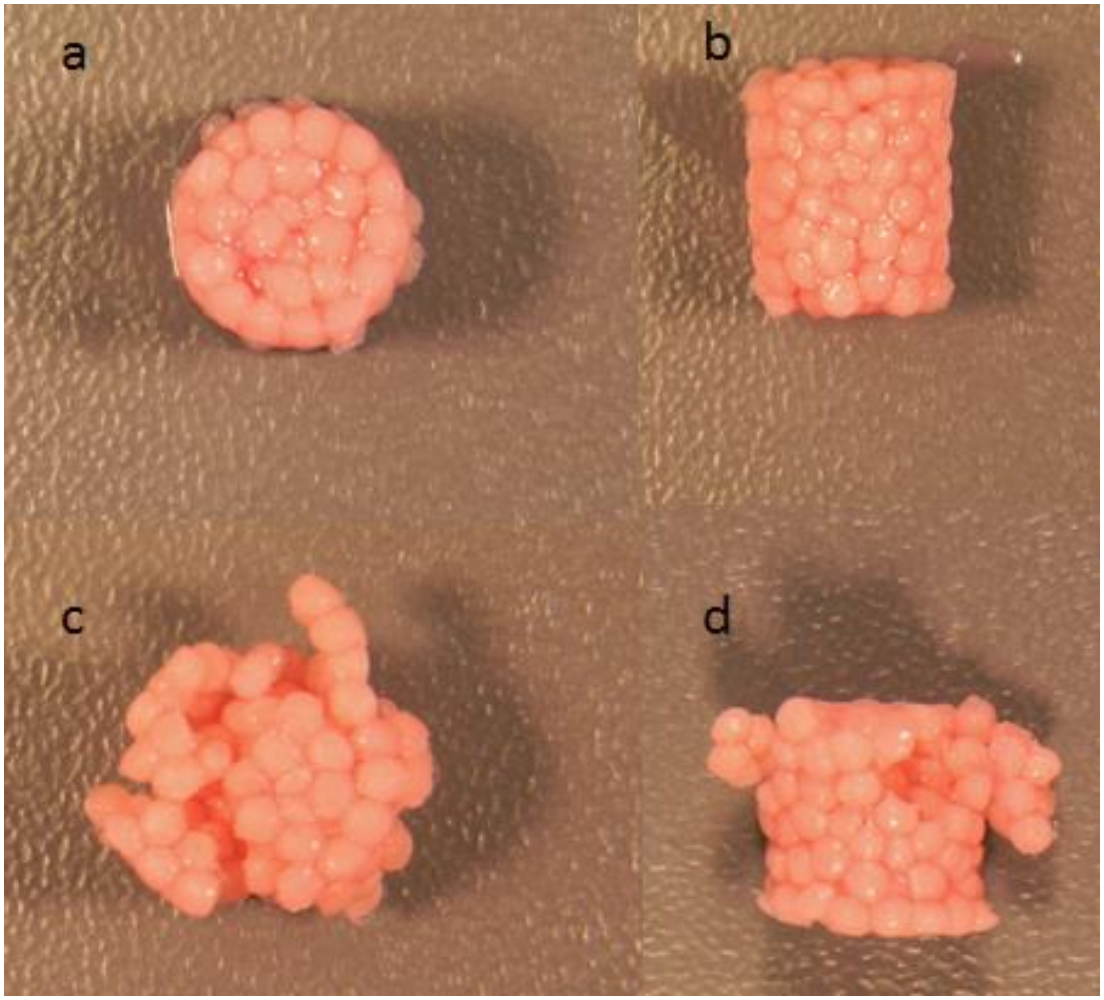

Figure 2.9 Scaffolds after mechanical testing

a) and b) are the top and side view images of the scaffold incubated for 24 h in DMEM, c) and d) are the top and side view images of (a and b) after mechanical testing. The scaffolds did not tear apart completely but they were deformed from their original shape.

2.3.2 Cell attachment and proliferation

Frozen P1 MSCs derived from the marrow of a 24 year old male were expanded to P4 in monolayer. 2.5×10^4 cells were pipetted onto a flat surface of each scaffold and allowed 30 min to attach before flooding with DCM. Seeding efficiency was expressed as the percentage of cells attached to the scaffold relative to the total number, which were seeded. The seeding or attachment efficiency of human bone marrow MSCs on CHI-CaP

scaffolds was 37.5±7.5% (mean ± standard deviation) with 95% confidence interval after 30 minutes of cell seeding. Cells attached to the CHI-CaP scaffolds proliferated as evidenced by almost 50-fold over the 4-week culture period. The cell proliferation rate results to a population doubling time of 4.84±0.09 days with 95% confidence interval. GAG was measured using dimethyl methylene blue assay and it was below the detection limit.

After 24 hours of human bone marrow mesenchymal cell seeding, cells attained a flattened and elongated or stellate morphology as shown in SEM images (Figure 2.10). SEM images also showed that some cells reached and spread the gap between adjacent CHI-CaP beads (Figure 2.11).

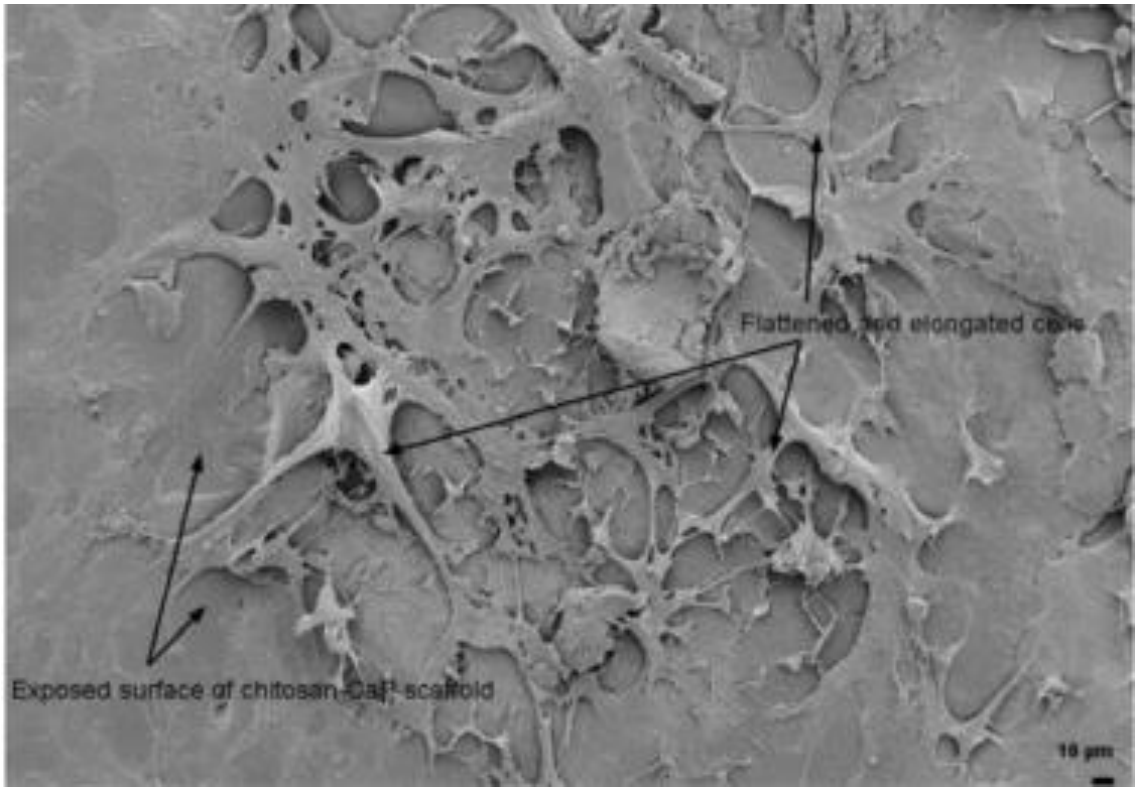

Figure 2.10 Scanning electron micrographs of human MSCs on top of a bead made up of CHI-CaP after 24 h of cell seeding (200X).

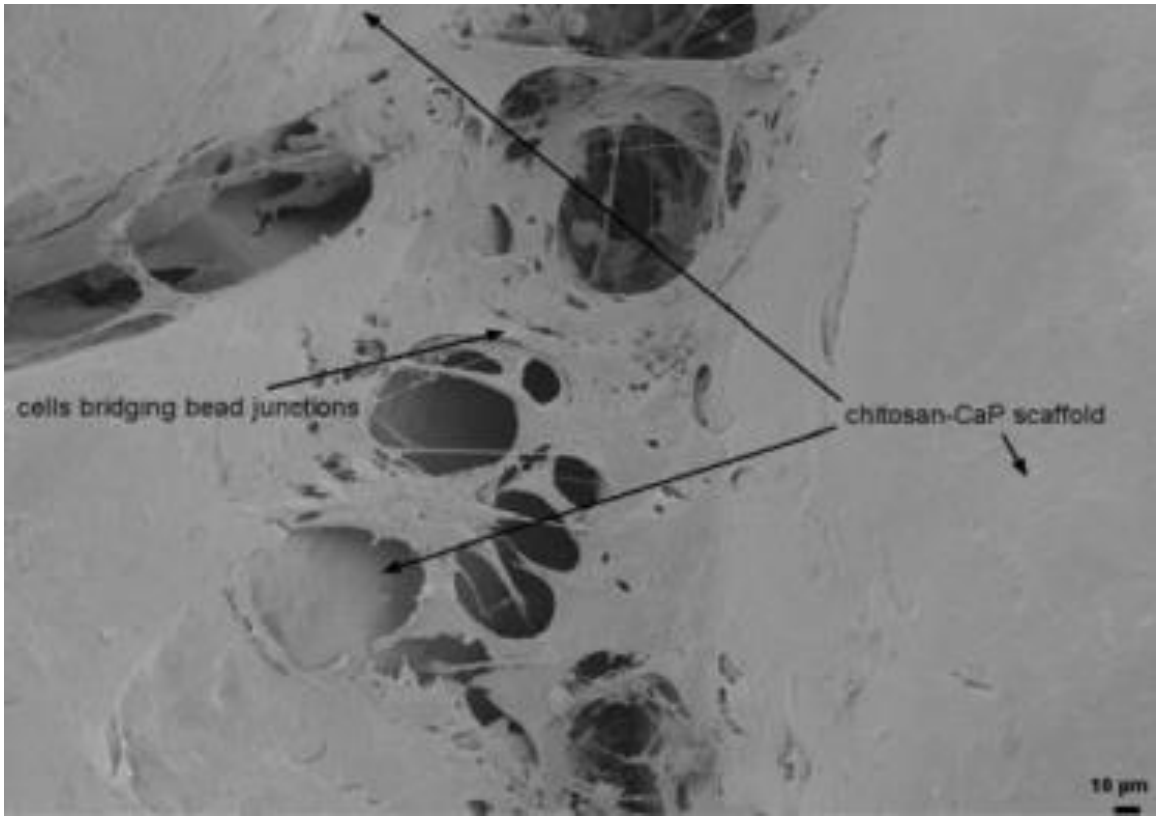

Figure 2.11 Scanning electron micrographs of human MSCs in the pore between the beads made up of CHI-CaP after 24 h of cell seeding.

2.4 Discussion

Previous studies have already shown bilayered approach for cartilage tissue engineering where one phase or layer is designed for bone formation (osteogenesis) while other supports neocartilage formation (chondrogenesis) [15,16]. In a typical bilayered approach either the scaffold is made up of two types of material or two cell types were used to make biphasic constructs. In the current study the biphasic construct was made up of only one type of material (CHI-CaP) and only mesenchymal stem cells were used to form neocartilage through self-assembly, which was similar to Waldman et al. approach for biphasic constructs [17].

The osteoconductive scaffold is fabricated by fusing chitosan calcium phosphate beads formed using co-precipitation method [6]. Chesnutt et al. also shown that the calcium and phosphate was evenly distributed through the chitosan matrix in the scaffolds fabricated using co-precipitation method. Porosity of the scaffolds was created by fusing beads and was sufficient for tissue formation and nutrient transport. The size and shape of the scaffold will be chosen depending on the defect size and it can be managed by altering the size and shape of the mold in the custom plate. The compressive modulus of the CHI-Cap scaffolds was in the lower range of the native trabecular bone modulus and falls in the midpoint of the modulus of similar type scaffolds [6].

This study demonstrates that freeze-dried chitosan-CaP scaffolds support primary human bone marrow MSC attachment and proliferation when cultured in DCM. The cells attained a flat and spindle shape, fibroblast-like morphology within 24 h of cell seeding as examined under SEM. The cell attachment or seeding efficiency of human mesenchymal stem cells was approximately 38% and is similar to human embryonic palatal mesenchymal cells on CHI-CaP scaffolds of similar composition [6]. In the current study the DNA increased to 50-fold in 28 day whereas the DNA rose to 3-fold in 4 days (from Day 3 to Day 7) of human embryonic palatal mesenchymal cells.

When seeded at relatively low density, the primary human mesenchymal stem cells attached and proliferated to cover the surface of the scaffolds, but the lack of any GAG accumulation over 28 d suggests they did not undergo chondrogenic induction, even in the presence of 10 ng/ml TGF-β3. The most likely explanation is the lack of adequate cell-cell interaction or ability to acquire a round shape. Previous studies have shown chondrogenic differentiation of MSCs when cultured in a pellet or embedded in a

hydrogel [18,19] . Further investigations need to be done to create an ideal biphasic construct with completely covered neocartilage tissue on it having chondrogenic characteristics.

2.5 References

[1] Jayakumar R, Deepthy Menon, K Manzoor, and al et, "Biomedical applications of chitin and chitosan based nanomaterials—A short review," Carbohydrate Polymers, vol. 82, no. 2, pp. 227-232, September 2010.

[2] Jiali Zhang, Wenshui Xia, Ping Liu, and al et, "Chitosan Modification and Pharmaceutical/Biomedical Applications," Open Access Marine Drugs, vol. 8, pp. 1962-1987, March 2010.

[3] S Majd, Y Yuan, S Mishra, and al et, "Effects of material property and heat treatment on nanomechanical properties of chitosan films," J Biomed Mater Res B Appl Biomater, vol. 90, no. 1, pp. 283-9, July 2009.

[4] C Tangsadthakun, S Kanokpanont, N Sanchavanakit, and al et, "The influence of molecular weight of chitosan on the physical and biological properties of collagen/chitosan scaffolds," J Biomater Sci Polymer Ed, vol. 18, no. 2, pp. 147-63, 2007.

[5] D L Nettles , S H Elder, and J A Gilbert, "Potential use of chitosan as a cell scaffold material for cartilage tissue engineering," Tissue Eng, vol. 8, no. 6, pp. 1009-16, December 2002.

[6] Chesnutt M. Besty et al., "Design and characterization of a novel chitosan/ nanocrystalline calcium phosphate composite scaffold for bone regeneration," J Biomed Mater Res A, vol. 88, no. 2, pp. 491-502, February 2009.

[7] Karteek Pesaramelli , Sravanthi Macharla, and Ranjith Anishetty, "Chitoas: A biocompatible polymer for pharmaceutical applications in various dosage form," International Journal of Pharmacy & Technology, vol. 2, no. 2, pp. 186-205, June 2010.

[8] Chesnutt M. Besty, Yuan Youling, Buddington Karyl, Haggard O. Warren, and Bumgardner D. Joel, "Composite chitosan/nano-hydroxyapatite scaffolds induce osteocalcin production by osteoblasts *in vitro* and support bone formation *in vivo*," Tissue Eng Part A, vol. 15, no. 9, pp. 2571-2579, September 2009.

[9] Zhang Liang, Weir D. Michael, and Xu H.K. Hockin, "Human umbilical cord stem cells encapsulation in calcium phosphate scaffolds for bone engineering," Biomaterials, vol. 31, no. 14, pp. 3848-3857, May 2010.

[10] Oliveira M. Joaquim et al., "Novel hydroxyapatite/chitosan bilayered scaffold for osteochondral tissue-engineering applications: Scaffold design and its performance when seeded with goat bone marrow stromal cells," Biomaterials, vol. 27, no. 36, pp. 6123-6137, December 2006.

[11] Rusu Marin Viorel et al., "Size-controlled hydroxyapatite nanoparticles as self-organized organic-inorganic composite materials," Biomaterials, vol. 26, no. 26, pp. 5414-5426, September 2005.

[12] Reves T Benjamin, Bumgardner D. Joel, Cole A. Judith, Yang Yunzhi, and Haggard O. Warren, "Lyophilization to improve drug delivery for chitosan-calcium phosphate bone scaffold construct: A preliminary investigation ," J Biomwd Mater Res B Appl Biomater, vol. 90, no. 1, pp. 1-10, July 2009.

[13] Steven H. Elder et al., "Production of hyaline like cartilage by bone marrow mesenchymal stem cells in a self-assembly model," Tissue Eng Part A, vol. 15, no. 10, pp. 3025-3036, October 2009.

[14] T M Keaveny and W C Hayes, "Mechanical properties of cortical and trabecular bone," in Bone. Boca Raton, FL: CRC Press, 1992, pp. 285-344.

[15] Theresa A. Holland et al., "Osteochondral repair in the rabbit model utilizing bilayered, degradable oligo(poly(ethylene glycol) fumarate) hydrogel scaffolds," J Biomed Mater Res A, vol. 75, no. 1, pp. 156-167, July 2005.

[16] Ching-Chuan Jiang et al., "Repair of porcine articular cartilage defect with a biphasic osteochondral composite," J Orthop Res, vol. 25, no. 10, pp. 1277-1290, June 2007.

[17] Stephen D. Waldman, Marc D. Grynpas, Robert M. Pilliar , and Rita A. Kandel, "Characteization of cartilagenous tissue formed on calcium polyphosphate substartes *in vitro*," J Biomed Mater Res, vol. 62, no. 3, pp. 323-330, January 2002.

[18] Olivia S. Beane and Eric M. Darling, "Isolation, characterization, and differentiation of stem cells for cartilage regeneration," Ann Biomed Eng, vol. 40, no. 10, pp. 2079-2097, October 2012.

[19] Hani A. Awad, M Q. Wickham, Holly A. Leddy, Jeffrey M. Gimble, and Farshid Guilak, "Chondrogenic differentiation of adipose-derived adult stem cells in agarose, alginate, and gelatin scaffolds," Biomaterials, vol. 25, no. 16, pp. 3211-3222, July 2004.

CHAPTER III

TWO DIFFERENT APPROACHES FOR MAKING BIPHASIC CONSTRUCTS

3.1 Introduction

Scaffolds in tissue engineering play an important role in supporting cell attachment and tissue regeneration. Hydroxyapatite ($Ca_{10}(PO_4)_6(OH)_2$) and chitosan are widely used as scaffold materials in musculoskeletal tissue engineering applications. Hydroxyapatite, a bone mineral salt is mainly composed of calcium and phosphate in inorganic phase which constitute to approximately 70% of calcified bone. The main advantages of using Hydroxyapatite is its bioactivity, osteoconductivity, biocompatability, and biodegradation whereas shaping it is the major drawback due to brittleness and easy to fracture nature [1,2,3]. Chitosan has weak mechanical properties when used alone as a biomaterial. Combining chitosan and hydroxyapatite improves hardness of the scaffold with load bearing capability makes an excellent osteoconductive biomaterial [4]. Moreover studies have also shown that coating chistosan with nano-hydroxyapatite improved cell proliferation on scaffolds [5,6]. Several methods have been studied to incorporate chitosan and hydroxyapatite into one biomaterial. But, the co-precipitation method [7,8] stood out as it yielded a homogenous mixture whereas other methods like mixing chitosan with hydroxyapatite/ calcium phosphate powders [9,10] or coating chitosan with hydroxyapatite resulted in inhomogeneous solutions [11].

Previous studies have shown various techniques for creating biphasic constructs for cartilage tissue engineering using one or two biomaterials and cell types. In a study, Hu Da et al. fabricated biphasic constructs using two different materials and two different cell types for osteochondral defects [12]. Biphasic constructs were also created by seeding one type of cells onto a biomaterial scaffold enclosed in a static bioreactor [13] or using vacuum infusion technique [14]. Few studies have also reported biphasic constructs formed by suspending cells in an agarose/alginate/silk hydrogels for cartilage regeneration [15,16,17,18]. Kim et al. formed multilayer constructs having zonal organization for articular cartilage defects by mixing chondrocytes from three different zones with hydrogels separately and then combining the layers using photopolymerization [19].

In our approach neocartilage (chondrogenesis) will be formed from MSCs by self-assembly on top of osteoconductive CHI-CaP scaffold (osteogenesis) [21]. In this study biphasic constructs were created using two different approaches and evaluated based on tissue formation, SEM, histology, immunohistochemistry, DNA and GAG results after 28 days culture in define chondrogenic medium (DCM).

3.2 Methods

3.2.1 Scaffold fabrication

Porous cylindrical shaped composite chitosan calcium phosphate scaffolds were fabricated as described previously by Chesnutt et al. [21]. The current method differs from Chesnutt et al. by using chitosan of 78.7% DDA, where they used 92% for scaffold fabrication. In brief, the CHI-CaP beads were made using co-precipitation method. These beads were left in the precipitate solution for 24 h for the formation of

hydroxyapatite [22] and then in DI water until it reach neutral pH. Beads were dried overnight and then fused into cylindrical shape (6mm diameter and 7 mm height) using 2% acetic acid and dried overnight. All the scaffolds were frozen at -20°C for 2 h and freeze dried overnight. Previous study has shown that freeze drying the scaffolds will increase pore size, porosity and protein absorption [23]. The scaffolds were then gas sterilized using ethylene oxide before cell seeding.

3.2.2 Scaffold characterization

Freeze-dried scaffolds were weighed before and after rehydration in PBS for 24 h. Swelling ratio was calculated as the percent increase in mass after rehydration. Porosity was calculated as shown in Equation 3.1 where Δv is the volume of methanol displaced by a scaffold and v_a is the apparent volume calculated from its measured diameter and height [21]. microCT scanning was performed on one CHI-CaP scaffold to confirm that the pores were interconnected.

$$P = \left(1 - \frac{\Delta v}{v_a}\right) \tag{3.1}$$

3.2.3 Cell source

Primary porcine bone marrow cells were used for creating biphasic constructs. These cells were collected from four femurs of two pigs, which were bought from a local meat processor. Bones were first cleaned and the entire process was done under aseptic conditions. Bones were cut open and the marrow and fat from the diaphyseal region were collected into a sterile centrifuge tubes. These tubes were centrifuged at 1000g for 10 minutes to separate marrow. Marrow was then distributed by continuous pipetting and it

was transferred into a T-175 cell culture flask. Marrow was incubated in Dulbecco's Modified Eagle Medium (DMEM) containing 10% of fetal bovine serum at 37°C. After 24 h of incubation, the media was removed, flask was rinsed thoroughly with PBS to remove any non-adherent cellular material and the cells were supplied with fresh DMEM. Before reaching confluence, cells were treated with trypsin and subcultured into a new flask. Cells at second passage were used for making biphasic constructs.

3.2.4 Biphasic constructs

In this experiment, biphasic constructs were created and compared using a higher density of porcine bone marrow derived mesenchymal stem cells in two different approaches (n=6 for each approach). For both the approaches scaffolds were fabricated in the same way. In first approach cells were seeded on top of a scaffold resting in a solidified agarose well and in second approach cells were placed in the middle of solidified agarose and the scaffold was placed on cell suspension. These biphasic constructs were cultured for 28 days in defined chondrogenic medium (DCM) and the tissue formed was evaluated quantitatively by measuring DNA and GAG and qualitatively by SEM and histological images.

3.2.4.1 Approach # 1

Wells of a 6 well plate were filled with 1.5% low gelling temperature agarose in DMEM, leaving the scaffolds in the middle of the well. Once the agarose had solidified a 4 mm biopsy punch was used to cut a cylinder shaped hole above the scaffold (Figure 3.1). The overlying agarose was removed by pasteur pipette under vacuum. Approximately $7.5x10^6$ cells of second passage were pipetted onto each scaffold. The

cells were allowed to settle for 60 min before the wells were flooded with DCM. Medium was replaced every 4-5 days.

3.2.4.2 Approach # 2

2% low gelling temperature was poured in the wells of a 6 well plate holding 10mm stainless steel rods of the same diameter as the scaffolds. The rods were gently removed after the agarose had gelled (Figure 3.1). The same number of cells as seeded in approach # 1 were pipetted into each hole and allowed to settle for 30 min. Scaffolds were then inserted into the holes and pressed gently against the cells. Later the wells were flooded with DCM. Medium was replaced every 4-5 days.

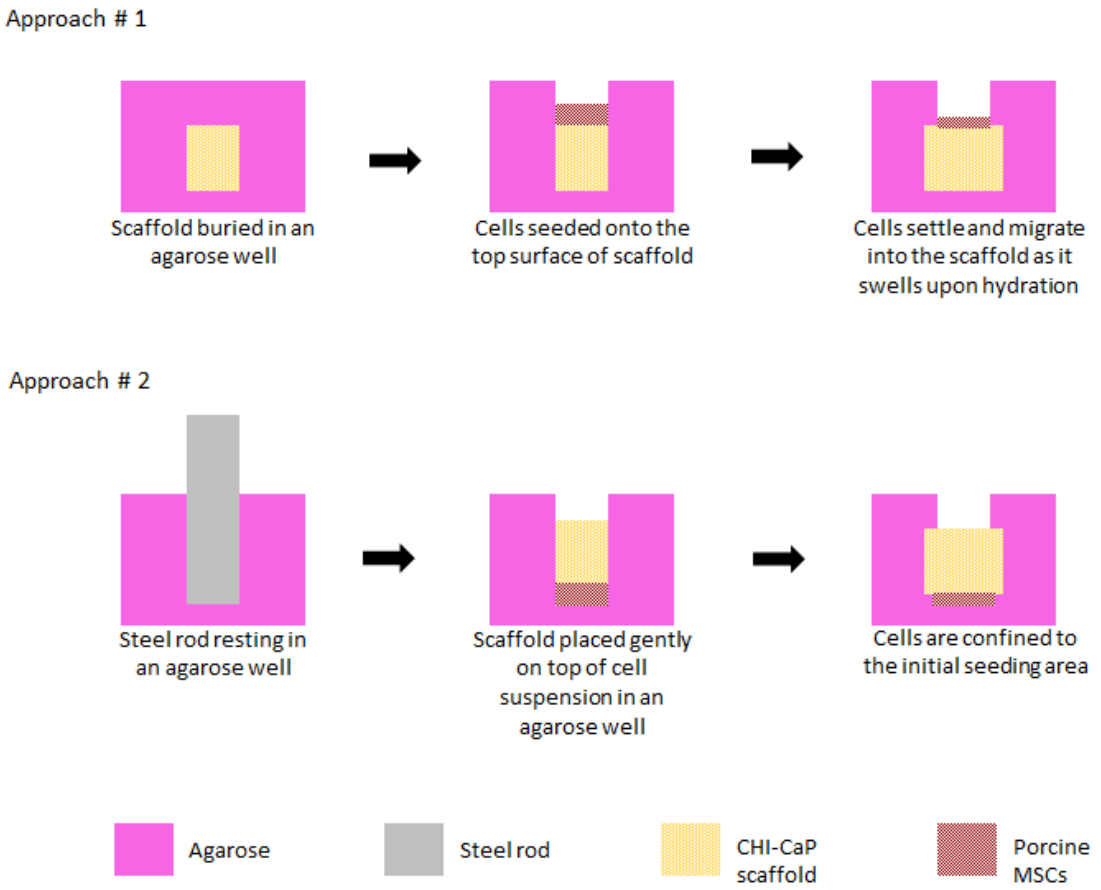

Figure 3.1 Schematic representation of crating biphasic constructs created using two different approaches.

3.2.5 SEM sample preparation

The structure and the surface morphology of the constructs were examined using scanning electron microscope (SEM). Constructs for SEM were fixed in 2.5% glutaraldehyde in PBS for overnight at 4°C. Later the scaffolds were dehydrated in graded ethanol (30%, 50%, 70%, and 90%) for 20 min at room temperature. Scaffolds were finally incubated in two changes of 100% ethanol and hexamethyldisilazane for 20 min each, and air dried under hood for about 30 min. These samples were then sputter

coated with platinum and imaged using a JEOL JSM-6500F Field Emission Scanning Electron Microscope.

3.2.6 DNA and GAG quantification

Samples designated for biochemistry (DNA/GAG) were digested in 1% papain overnight at 60°C. The samples were then centrifuged at 10,000 rpm for 3 min. One aliquot of the digested sample was used for analyzing DNA content by Hoechst dye method in DNA quantification kit (Sigma-Aldrich, St. Louis, MO). Fluorescence intensity was read in Glomax Multi detection system. DNA content was calculated from a standard curve produced with calf thymus DNA provided in the kit. Cell number and cell proliferation rate were calculated from DNA readings. Another aliquot of the digested sample was used for GAG quantification. Total GAG content was determined by the dimethylmethylene blue (DMMB) dye-binding method using the Blyscan™ Assay (Biocolor Ltd, Carrickfergus, United Kingdom) according to the manufacturer's instructions. The GAG content was read at 656 nm in spectrophotometer. GAG content was calculated from a standard curve produced with the chondroitin 4-sulfate standard provided in the kit. GAG and DNA were analyzed in the same way as mentioned in previous studies [24].

3.2.7 Histology and Immunohistochemistry

Samples for histology were fixed in paraformaldehyde. Paraffin embedded sections were sectioned along the diameter at 5 - 10 μm. All the sections were first deparaffinized by rehydrating them in xylene and graded ethanol. The sections for histology were stained with 2% toluidine blue for the detection of proteoglycans- rich

extracellular matrix. Sections for immunohistochemistry were stained to detect type II collagen. Immunohistological sections were incubated in 2mg/ml of hyaluronidase in tris-buffered saline for 30 minutes and then in 0.5mg/ml of pronase in PBS for 10 minutes for antigen retrieval. Later the sections were incubated for 2 hours at room temperature in full concentration II-II6B3 primary antibody from the Development Studies Hybridoma Bank (University of Iowa, Iowa City, IA). The staining was then continued using SuperPictureTM 3rd Gen IHC Detection Kit (Life Technologies, Grand Island, NY) following the manufacturer's recommended protocol. Sections without primary antibody were used as controls. Control sections were incubated in PBS for 2 hours at room temperature. These histology techniques were the same as those performed in previous studies [24].

3.2.8 Degradation

In vivo, the CHI-CaP scaffold would be embedded in bone and would ideally degrade at the same rate as new bone formation takes place. Lysozyme plays an important role in chitosan degradation [25,26]. CHI-CaP beads made from chitosan with a 78.7% DDA were incubated in a 1mg/ml lysozyme solution in PBS for up to 9 days. The dried beads were weighed before incubating in lysozyme. After every 3 days the beads were freeze dried for 2 days to remove any moisture and weighed. The lysozyme solution was collected to perform calcium analysis, as these beads release calcium as they degrade.

3.2.9 Statistics

The quantitative data were analyzed by independent t-tests ($\alpha = 0.05$) assuming unequal variances. Analyses were carried out using IBM SPSS Statistics (19).

3.3 Results

3.3.1 Scaffold characterization

Cylindrical shaped scaffolds were fabricated by fusing CHI-CaP beads ranging 700-900 µm in diameter. The scaffolds made were approximately 47% porous (n=1), which was measured using methanol displacement method and also the pores were interconnected as evidenced in microCT images. The mass of the scaffold increased to approximately 167% when rehydrated in PBS for 24 hours.

Table 3.1 Physical characteristics.

Increase in diameter with rehydration (%)	Increase in height with rehydration (%)	Swelling ratio (%)	Porosity of dry scaffold (%)
23.3±0.04	20.0±1.8	167.1±2.1	47.9

(n = 4, except for porosity n = 1)

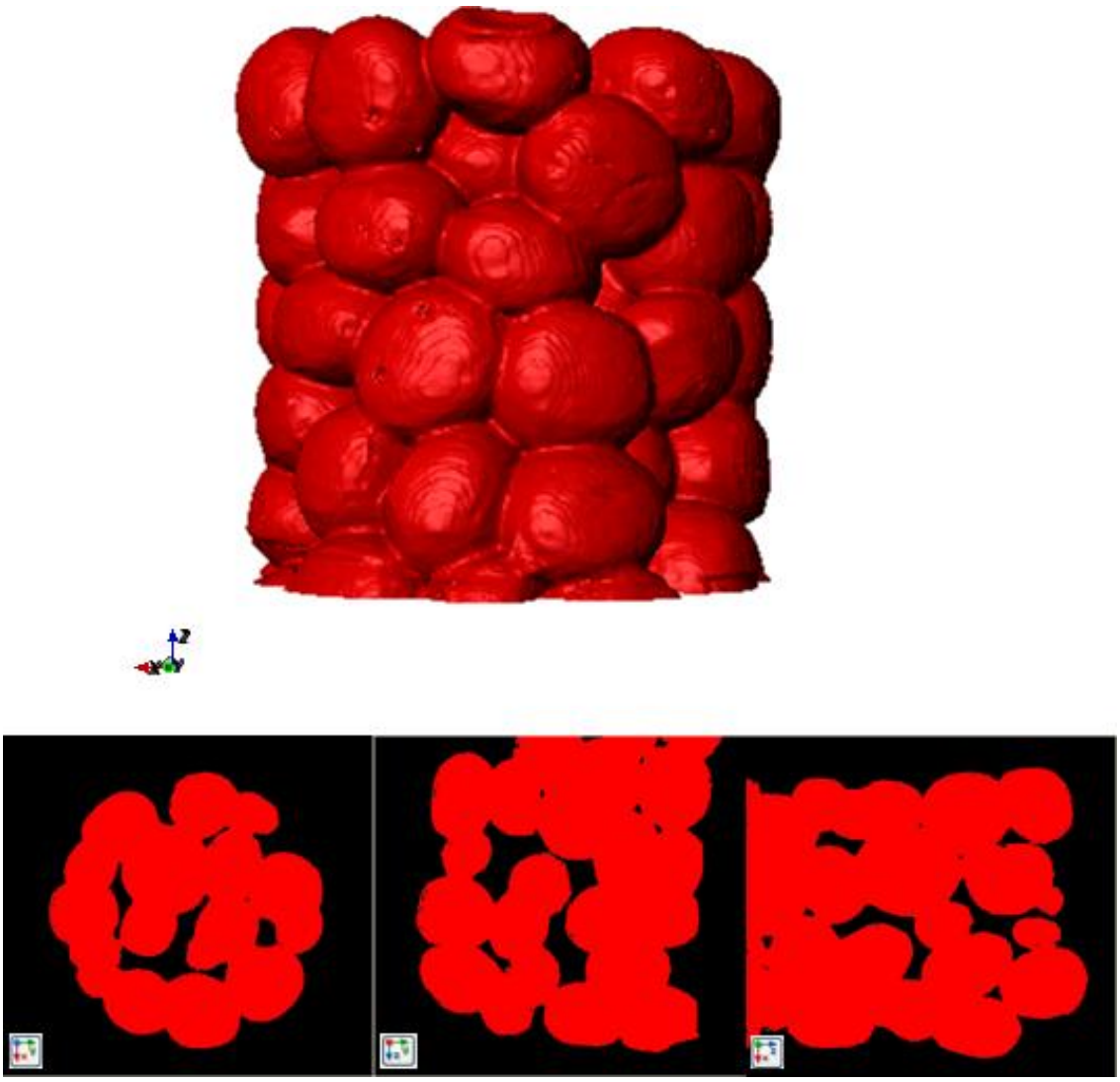

Figure 3.2 micro CT image of CHI-CaP beads fused into a cylindrical shaped scaffold showing interconnected pores.

3.3.2 Biphasic constructs

Biphasic constructs created in two different approaches using porcine bone marrow derived mesenchymal stem cells and CHI-CaP scaffolds were cultured for 28 days in DCM. There was no macroscopically visible neocartilage formation on top of scaffolds formed using approach # 1. But, the SEM images of approach # 1 scaffold

cultured for 28 days showed the beads of a scaffold were covered with a thin layer of tissue mostly comprised of fibroblast like cells (Figure 3.3). Few isolated spherical shaped cells resembling chondrocytes were observed at the gap between CHI- CaP beads (Figure 3.4).

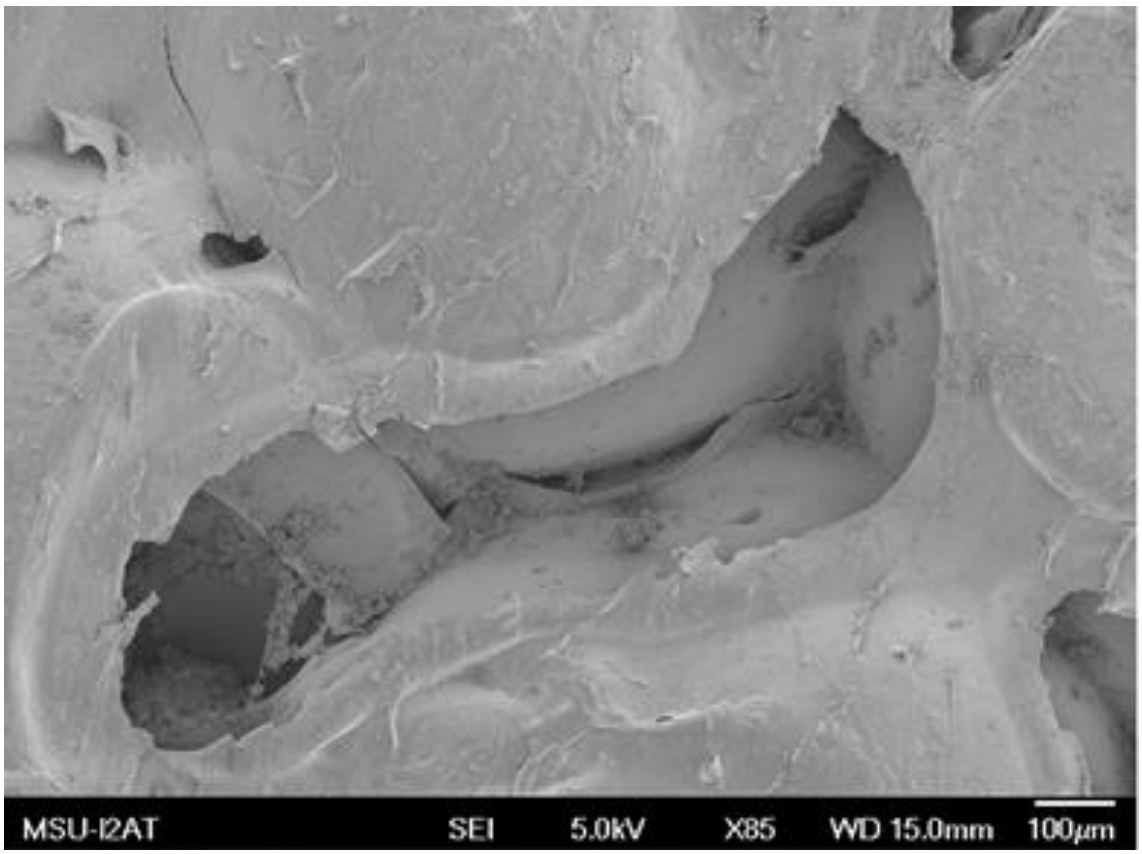

Figure 3.3 Scanning electron micrographs showing the presence of thin sheet of porcine bone marrow mesenchymal stem cells on top of CHI-CaP beads created using approach # 1 (85X).

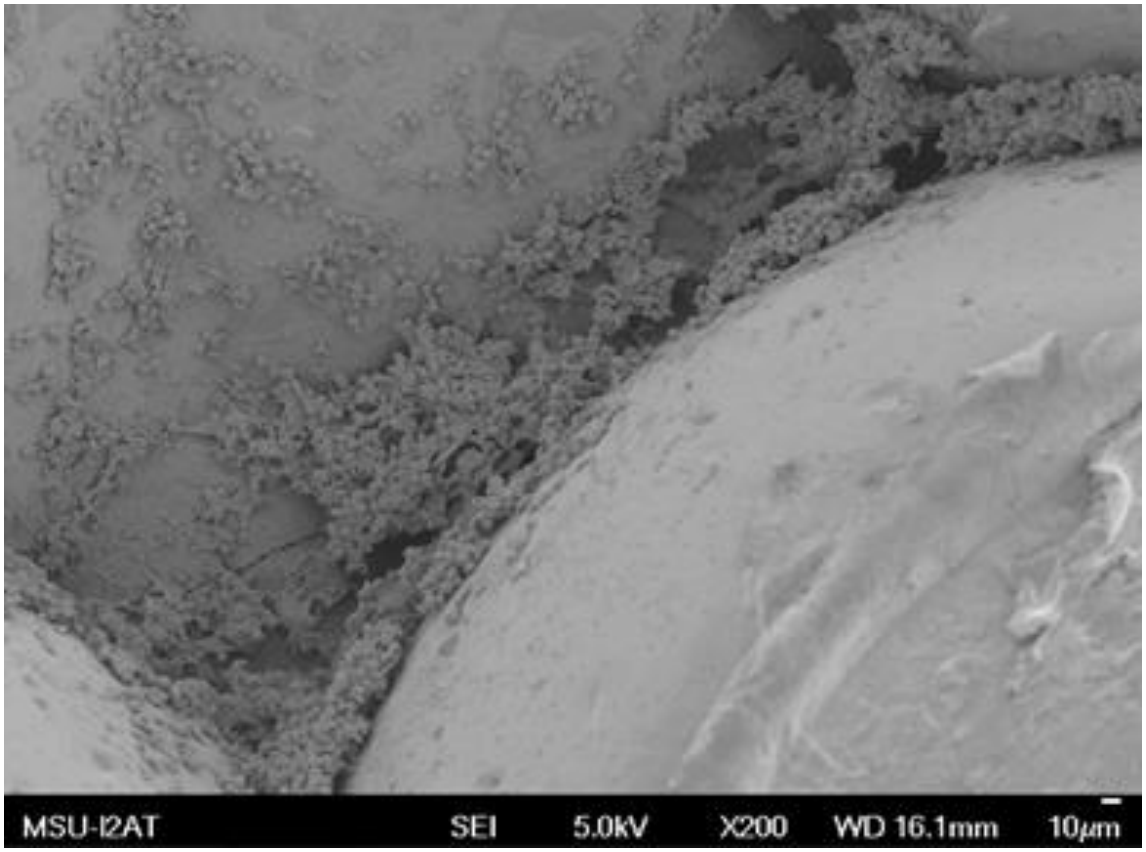

Figure 3.4 Scanning electron micrographs showing the presence of more chondrocyte like cells in the deep crevices between the beads of composite CHI-CaP scaffolds formed using approach # 1.

On the other side, the biphasic constructs formed using approach # 2 had a macroscopically visible cartilage like tissue impression after 28 d culture in DCM (Figure 3.5). The cells were more round in shape and consisted of proteoglycans which was evident in sections stained with toluidine blue (Figure 3.6). The tissue formed also showed the presence of collagen type II, which was one of the main characteristics of cartilage tissue (Figure 3.7). The main drawback of this approach would be the tissue coverage. The neocartilage like tissue formed did not cover the whole seeded area. The

approach # 2 constructs resulted in less DNA amount (or fewer cells) and has more GAG compared to approach # 1 (Table 3.2).

Figure 3.5 Neo cartilage like tissue formed on composite CHI-CaP scaffolds

Tissue on constructs created using approach # 2 after culturing for 28 d in defined chondrogenic medium using porcine bone marrow mesenchymal stem cells.

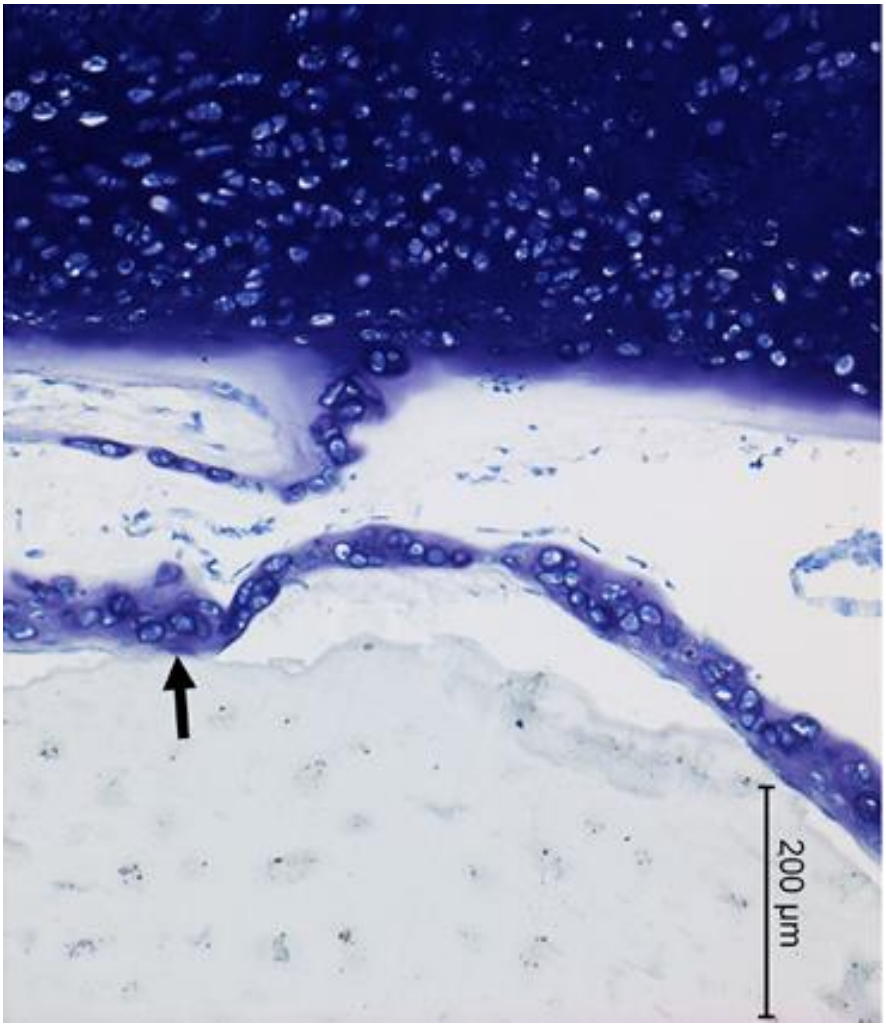

Figure 3.6 Toluidine blue stained section of cartilage like tissue formed on composite CHI-CaP

Tissue formed on constructs created using approach # 2 after culturing for 28 d in defined chondrogenic medium using porcine bone marrow mesenchymal stem cells.

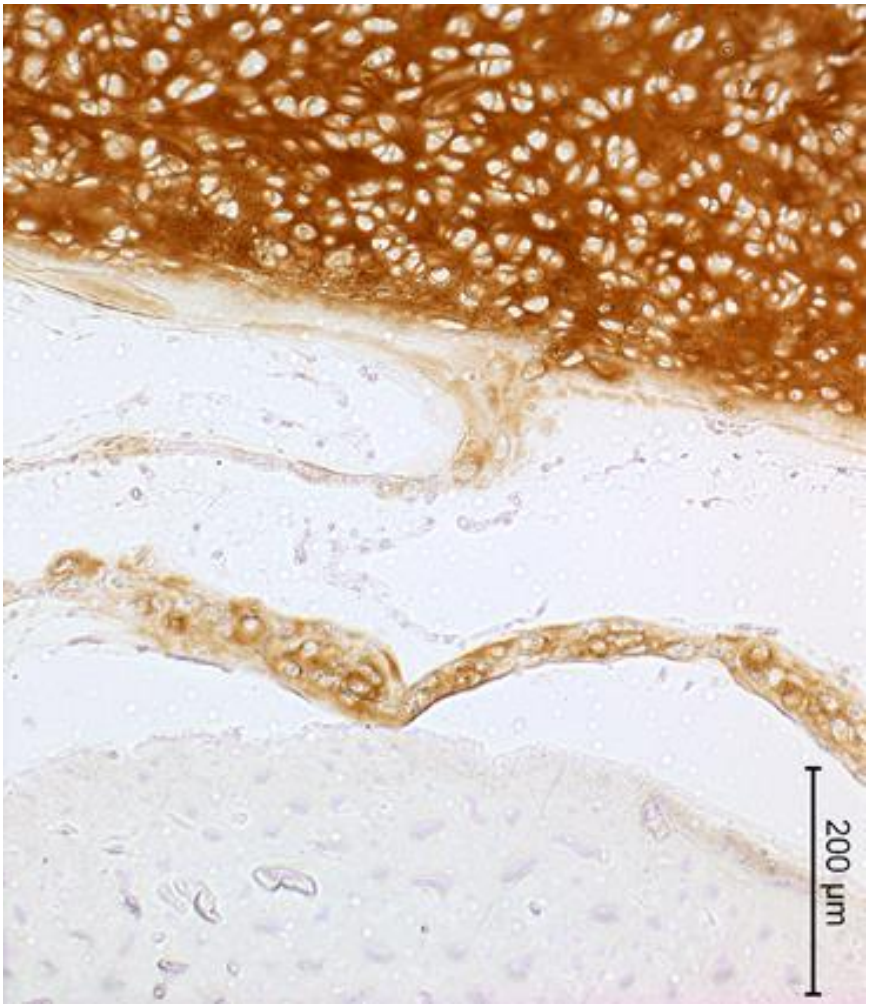

Figure 3.7 Cartilage like tissue intensively stained for collagen type II, formed on composite CHI-CaP scaffolds

Tissue formed on constructs created using approach # 2 after culturing for 28 d in defined chondrogenic medium using porcine bone marrow mesenchymal stem cells.

Table 3.2 DNA and GAG content after 28 d culture of porcine bone marrow MSCs on freeze-dried CHI-CaP scaffolds.

	DNA (µg/construct)	GAG (µg/construct)	GAG (µg)/ DNA (µg)
Approach #1	23.50±5.34	0.67±0.53	0.03±0.02
Approach #2	14.81±0.32	2.67±0.31	0.18±0.02

(mean ± standard deviation, n = 6)

3.3.3 Degradation

Chitosan calcium phosphate beads degradation was studied by incubating them in 1mg/ml of lysozyme in PBS for 9 days. The rates of calcium release and weight loss were shown in figure 3.8. There was no significant difference in the weight loss or calcium release readings. This translates to a very slow rate of degradation *in vivo*.

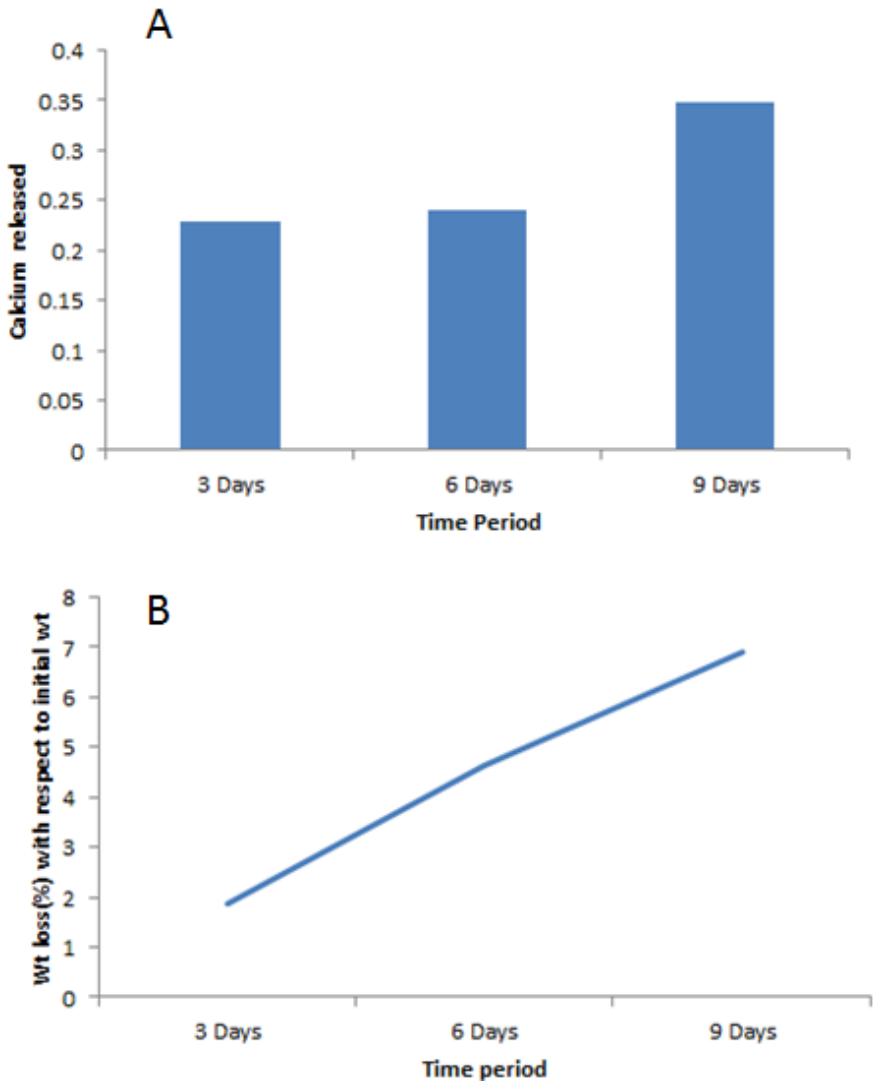

Figure 3.8 Results from CHI-CaP bead degradation using lysozyme.

Total amount of calcium released is shown in (A) and (B) shows the percentage of weight loss after incubating CHI-CaP beads in 1mg/ml of lysozyme solution in PS (n=1).

3.4 Discussion

It has been a main problem in securing the cartilaginous tissue formed *in vitro* and placing it on top of a bone *in vivo* [20]. To overcome this we propose a new therapy where neocartilage was formed on CHI-CaP scaffolds *in vitro* and the scaffold will be replaced by new bone eventually in *in vivo.* The *in vitro* cultured cartilage was found to fuse with the *in vivo* cartilage when they were in contact upon implantation [27]. It has previously been demonstrated that engineered cartilage formed by self-assembly can acquire an organized collagen architecture resembling that of native articular cartilage [24]. CHI-CaP scaffolds fabricated have interconnected pores with 47% porous which was little above the value presented by Chesnutt for similar type of scaffolds. Previous studies show that a porosity of 30-40% is enough for nutrient transport and tissue formation *in vitro* and *in vivo* [28,29]. The swelling ratio of these scaffolds was almost same as that published by Chesnutt. Degradation of CHI-CaP beads was measured over nine day time period by incubating beads in 1mg/ml lysozyme in PBS. There was no significant change in the weight loss or the calcium released. The rate of degradation will depend on several factors like – DDA, crystalline nature, and pore size [30,31].

In the current study biphasic constructs were created using two different approaches where, either the cells were seeded directly on top of a scaffold or the scaffold was gently pressed on cell suspension. The study showed that a thin layer of cartilage tissue devoid of scaffold can be formed on top of a CHI-CaP scaffold when seeded with large cell number. Biphasic constructs created using approach # 2 showed the formation of neo cartilage like tissue with round shaped cells and more proteoglycan and collagen type II. But, the tissue formed was not well adhered and did not cover the

whole seeded area. None of the approach # 1 constructs consisted of macroscopically visible tissue formation, but the SEM images showed that the scaffold was covered with a thin layer of tissue with more chondrocyte-like cells clearly seen in the junction between the beads. Approach # 2 constructs had low GAG readings compared to approach # 1 measured on scaffold. The histology sections of the tissue formed using approach #2 showed the presence of abundant proteoglycan and type II collagen with more spherical shaped cells. Presence of more proteoglycan, type II collagen and spherical shaped cells were the characteristic feature of articular cartilage tissue. These histology images showed that mesenchymal stem cells were differentiated into chondrocytes when supplied with TGF-β3.

The main advantage of approach # 1 is that the cells are in close contact with the medium for nutrient and waste transport. But the drawback is that the cells did not stay in the initial cell seeded area. They migrated through the pores of the scaffold as it expands upon rehydration in culture medium. Maintaining the porosity below 40% may help to overcome this issue. For approach # 2, the cells were confined to the initial cell seeded area, which also helps for cartilaginous extracellular matrix organization. But the cells were not in contact with the medium for nutrients.

The main limitations for both the approaches are cell adhesion and formation of continuous cartilage tissue on scaffolds. A preliminary study has shown that cell adhesion can be increased when scaffolds were coated with a protein. Scaffolds coated with 0.05% collagen and 0.02% fibronectin were created and compared against non-coated scaffolds (Figure 3.9). Same number of cells was seeded for all the groups and biphasic constructs were created using approach # 1. From these results we propose that coating scaffolds

with a protein and creating biphasic constructs using approach # 1 will be an ideal method for articular cartilage regeneration.

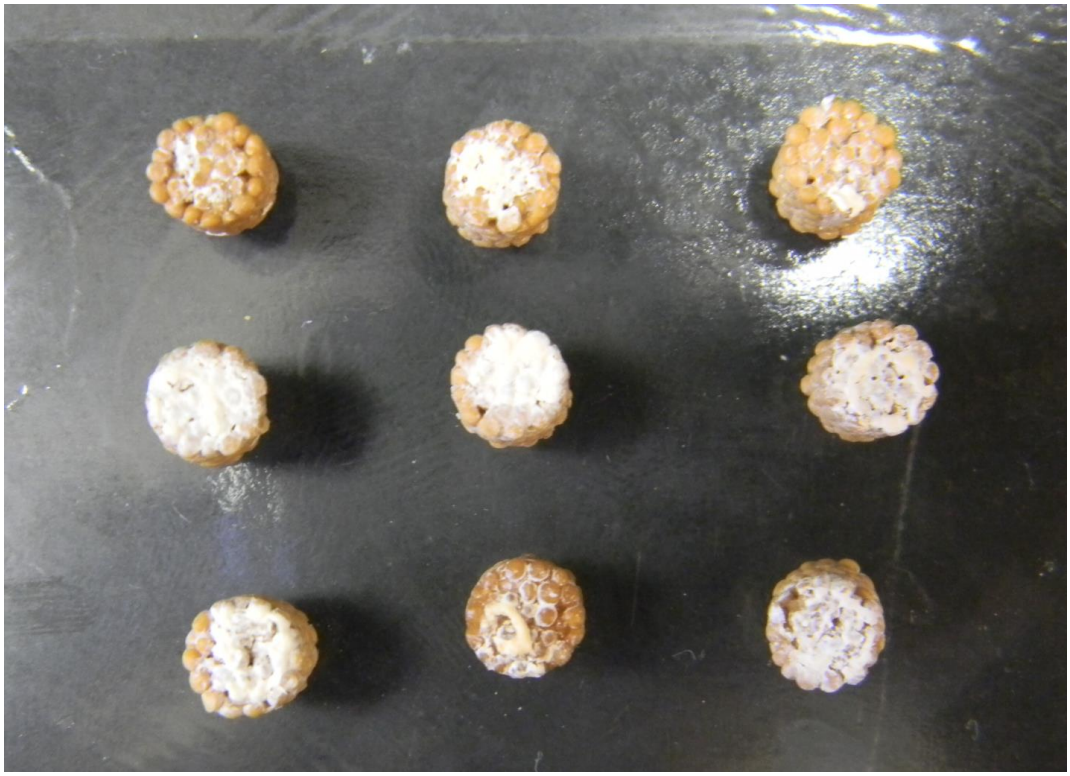

Figure 3.9 Dried biphasic constructs created using approach # 1, showing the presence of tissue covered

Top row – tissue on uncoated CHI-CaP scaffolds, Middle row – tissue on collagen coated scaffolds, Last row – tissue on fibronectin coated scaffolds.

3.5 References

[1] Luiz A Salata, Geoffery T Craig, and Ian M Brook, "Bone healing following the use of hydroxyapatite or ionomericbone substitutes alone or combined with a guided bone regeneration technique: an animal study," Int J Oral Maxillofac Implants, vol. 13, no. 1, pp. 144-151, February 1998.

[2] Chao Zhang, Yun-Yu Hu, Fu-Zhai Cui, Shu-Ming Zhang, and Di-Ke Ruan, "A study on a tissue engineered bone using rhBMP-2 induced periosteal cells with a porous nano-hydroxyapatite/ collagen/ poly(L-lactic acid) scaffold," Biomed Mater, vol. 1, no. 2, pp. 56-62, April 2006.

[3] I Yamaguchi et al., "Preparation and microstructure analysis of chitosan/ hydroxyapatite nanocomposites.," J Biomed Mater Res, vol. 55, no. 1, pp. 20-27, April 2001.

[4] Zhang Ruiyun and Ma X. Peter, "Poly(a-hydroxyl acids)/hydroxyapatite porous composites for bone-tissue engineering. I. Preparation and morphology," J Biomed Mater Res, vol. 44, no. 4, pp. 446-455, November 1999.

[5] Kong Lijun et al., "A study on the bioactivity of chitosan/ nano-hydroxyapatite composite scaffolds for bone tissue enigeering," Eur Polym J, vol. 42, no. 12, pp. 3171-3179, December 2006.

[6] Xianmiao Cheng et al., "Properties and *in vitro* biological evaluation of nanohydroxyapatite/chitosan membranes for bone guided regeneration," Mater Sci Eng C, vol. 29, no. 1, pp. 29-35, January 2009.

[7] Hu Qiaoling, Li Baoqiang, Wang Mang, and Shen Jiacong, "Preparation and characterization of biodegradable chitosan/hydroxyapatite nanocomposite rods via in situ hybridization: a potential material as internal fixation of bone fracture," Biomaterials, vol. 25, no. 5, pp. 779-785, February 2004.

[8] Kong Lijun et al., "Preparation and charaterization of nano-hydroxyapatite/ chitosan composite scaffolds," J Biomed Mater Res A, vol. 75, no. 2, pp. 275-282, March 2005.

[9] Zhang Yong and Zhang Miqin, "Synthesis and characterization of macroporous chitosan/ calcium phosphate composite scaffolds for tissue engineering," J Biomed Mater Res, vol. 55, no. 3, pp. 304-312, June 2001.

[10] Xu H.K. Hockin, Quinn B. Janet, Takagi Shozo, and ChowC. Laurence, "Synergistic reinforcement of in situ hardening calcium phosphate composite scaffold for bone tissue engineering," Biomaterials, vol. 25, no. 6, pp. 1029-1037, July 2003.

[11] Manjubala I., Scheler S, Bossert Jorg, and Jandt D. Klaus, "Mineralisation of chitosan scaffold with nano-apatite formation by double diffusion technique," Acta Biomater, vol. 2, no. 1, pp. 75-84, September 2005.

[12] Hu Da et al., "The impact of compact layer in biphasic scaffold on osteochondral tissue enigneering," PLUS ONE, vol. 8, no. 1, January 2013.

[13] Xuanhui Wang et al., "Tissue engineering of biphasic cartilage constructs using various biodegradable scaffolds: an *in vitro* study," Biomaterials, vol. 25, no. 17, pp. 3681-3688, August 2004.

[14] Franklin T. Moutos and Farshid Guilak, "Functional Properties of Cell-Seeded Three-Dimensionally Woven Poly(ε-Caprolactone) Scaffolds for Cartilage Tissue Engineering," Tissue Eng Part A, vol. 16, no. 4, pp. 1291-1301, April 2010.

[15] Benjamin A. Byers, Robert L. Mauck, Ian E. Chang, and Rocky S. Tuan, "Transient exposure to TGF-β3 under serum-free conditions enhances the biomechanical and biochemical maturation of tissue-engineered cartilage," Tissue Eng Part A, vol. 14, no. 11, pp. 1821-1834, November 2008.

[16] Hani A. Awad, M. Quinn Wickham, Holly A. Leddy, Jeffrey M. Gimble, and Farshid Guilak, "Chondrogenic differentiation of adipose-derived adult stem cells in agarose, alginate, and gelatin scaffolds," Biomaterials, vol. 25, no. 16, pp. 3211-3222, July 2004.

[17] David R. Diduch, Louis C.M. Jordan, Cay M. Mierisch, and Gary Balian, "Marrow stromal cells embedded in alginate for repair of osteochondral defects," Arthroscopy: The Journal of Arthroscopic & Related Surgery, vol. 16, no. 6, pp. 571-577, September 2000.

[18] Pen-Hsiu Grace Chao et al., "Silk hydrogel for cartilage tissue engineering," J Biomed Mater Res B Appl Biomater, vol. 95, no. 1, pp. 84-90, October 2010.

[19] T. Kim et al., "Experimental model for cartilage tissue engineeing to regenerate the zonal organization of articular cartilage," Osteoarthritis and Carilage, vol. 11, no. 9, pp. 653-664, September 2003.

[20] S Waldman, M Grynpas, R Pilliar, and R Kandel, "Characterization of cartilagenous tissue formed on calcium polyphosphate substartes *in vitro*," J Biomed Mater Res, vol. 62, no. 3, pp. 323-330, December 2002.

[21] B Chesnutt, A Viano, Yuan Y, and al et, "Design and characterization of a novel chitosan/nanocrystalline calcium phosphate composite scaffold for bone regeneration," J Biomed Mater res A, vol. 88, no. 2, pp. 491-502, February 2009.

[22] Viorel Marin Rusu et al., "Size-controlled hydroxyapatite nanoparticles as self-organized organic-inorganic composite materials," Biomaterials, vol. 26, no. 26, pp. 5414-5426, September 2005.[23] Benjamin T. Reves, Joel D. Bumgardner, Judith A. Cole, Yunzhi Yang, and Warren O. Haggard, "Lyophilization to improve drug delivery for chitosan-calcium phosphate bone scaffold construct: A preliminary investigation," J Biomed Mater Res B Appl Biomater, vol. 90, no. 1, pp. 1-10, July 2009.

[24] Steven H. Elder et al., "Production of hyaline like cartilage by bone marrow mesenchymal stem cells in a self-assembly model," Tissue Eng Part A, vol. 15, no. 10, pp. 3025-3036, October 2009.

[25] Eugene Khor, Chitosan: Fulfilling a Biomaterial's Promise. Oxford, UK: Elsevier, 2001.

[26] Hockin H.K. Xu and Carl G. Simon Jr, "Fast setting calcium phosphate-chitosan scaffold: mechanical properties and biocompatibility," Biomaterials, vol. 26, no. 12, pp. 1337-1348, April 2005.

[27] R. A. Kandel et al., "Repair of osteochondral defects with biphasic cartilage-calcium polyphosphate constructs in a Sheep model," Biomaterials, vol. 27, no. 22, pp. 4120-4131, August 2006.

[28] M Borden, M. Attawia, Y. Khan, SF El-Amin, and CT Laurencin, "Tissue-engineered bone formation *in vivo* using a novel sintered polymeric microsphere matrix," J Bone Joint Surg Br, vol. 86, no. 8, pp. 1200-1208, November 2004.

[29] M Borden, M Attawia, and CT Laurencin, "The sintered microsphere matrix for bone tissue engineering: *in vitro* osteoconductivity studies," J Biomed Mater Res, vol. 61, no. 3, p. 42429, September 2002.

[30] Thomas Freier, Hui Shan Koh, Karineh Kazazian, and Molly S. Shoichet, "Controlling cell adhesion and degradation of chitosan films by N-scetylation," Biomaterials, vol. 26, no. 29, pp. 5872-5878, February 2005.

[31] Malgorzata Jaworska, Kensuke Sakurai, Pierre Gaudon, and Eric Guibal, "Influence of chitosan characteristics on polymer properties. I: Crystallographic properties," Polymer International, vol. 52, no. 2, pp. 198-205, January 2003.

CHAPTER IV

MESENCHYMAL STEM CELL MEDIATED CHONDROGENESIS ON CHITOSAN - CALCIUM PHOSPHATE SCAFFOLDS: EFFECT OF COLLAGEN COATING

4.1 Introduction

As previously mentioned, there is a need for an alternative approaches to articular cartilage repair. Our approach to cartilage tissue engineering is a biphasic construct, in which one layer supports to form subchondral bone (osteogenesis) and another supports cartilage formation (chondrogenesis) [1,2]. The goal is to create a tissue engineered biphasic osteochondral plug by seeding human bone marrow mesenchymal stem cells (hbMSCs) (chondrogenic layer) on top of a porous chitosan-calcium phosphate (CHI-CaP) scaffold (osteogenic layer). The scaffold provides a 3D environment and structure for the delivery of cells, and it must have similar interconnected porosity as that of bone to support not only the ingrowth of tissue but also the nutrient transportation to cells and removal of waste products. However, the scaffold must be strong enough to provide support to the defect site until the formation of new bone.

The scaffold currently under investigation in our laboratory is made from chitosan, a deacetylated derivative of chitin found in the exoskeleton of marine crustaceans. Chitosan has a wide range of biomedical applications. Previous research revealed that chitosan has hemostatic and cholesterol lowering properties [3]. Chitosan is a biocompatible and osteoconductive polymer with enhanced wound-healing capability

[4,5]. Also, antimicrobial properties of chitosan could reduce bacterial infection upon implantation [6,7]. Combining chitosan with calcium phosphate, a calcium salt found in the inorganic phase of bone mainly as hydroxyapatite, improves osteoconductivity, strength, and rigidity of the scaffold [8]. CHI-CaP scaffolds can be fabricated with at least 35% porosity, which is sufficient to support new tissue ingrowth. Our aim is to create a biphasic construct by high density seeding of hbMSCs onto a CHI-CaP scaffold.

Previous investigations done by Chesnutt et al. have shown that CHI-CaP scaffolds support cell attachment and proliferation of human fetal osteoblast cells and human embryonic palatal mesenchymal cells [9,10]. From our previous study, we have also shown that hbMSCs and porcine mesenchymal stem cells can attach and proliferate on CHI-CaP scaffolds [11], but weak attachment led to poor cartilage tissue integration and minimal coverage of the scaffold surface. Previous studies have shown an increase in cell attachment and viability when scaffolds are coated with extracellular matrix protein [12], and we hypothesized that the CHI-CaP scaffold would similarly benefit from such a coating. A pilot experiment suggested type I collagen coating could effectively enhance cell adhesion. Collagen type I provides a structural framework for connective tissue and helps in the formation of new bone [13]. Previous studies have shown that enhanced mesenchymal stem cell adhesion and survival on collagen enhancement was mediated by transmembrane integrins [14].

The main purposes of this study were to determine what effects coating the CHI-CaP scaffold with type I collagen would have on hbMSCs cell adhesion and chondrogenesis and how it would affect the physical characteristics of the scaffolds. It was hypothesized that collagen coating would promote cell attachment and

chondrogenesis on CHI-CaP scaffolds with minimal alteration of the scaffold's physical properties. To test this hypothesis, coated and uncoated scaffolds were characterized based on microscopic appearance, porosity, swelling ratio, and hydrophobicity/hydrophilicity. In addition, coated and uncoated scaffolds were seeded with hbMSCs and analyzed for cell proliferation and chondrogenesis.

4.2 Methods

4.2.1 Fabrication of composite chitosan calcium phosphate scaffolds

Composite CHI-CaP beads were prepared by a co-precipitation method as described previously [9]. In short, these were made by dissolving 3.57gm of 78.7% degree of deacetylation (DDA) chitosan powder (Vanson Halosource, Redmond, WA) in 84ml of 2 wt% acetic acid having $CaCl_2$ and NaH_2PO_4 to make a final Ca:P ratio of 1.67. Using a syringe pump and an 18G needle, the chitosan solution was added drop wise into a magnetically stirred precipitate bath at 15ml per hour. The precipitating solution consisted of 20% NaOH, 30% methanol, and 50% DI water (pH 13). These drops precipitated into beads. The beads were left in the precipitate solution for 24 hours for the formation of crystalline hydroxyapatite. The precipitating solution was replaced by DI water regularly until it reached pH 7. The beads were then separated and air dried overnight. The dried beads were packed into cylindrical molds and fused into scaffolds by brief exposure to 1% acetic acid and manually applied pressure. The scaffolds were extensively washed with DI water to remove any traces of acetic acid and air dried overnight. They were then washed in 70% ethanol for 2 hours at room temperature and the residual ethanol was washed out using DI water. Scaffolds were then frozen at -20°C for 3 hours and lyophilized overnight to enhance porosity, surface texture, and protein

adsorption [8]. The scaffold fabrication technique in the current study is distinguished from Chesnutt et al, as we incorporated lyophilization. The scaffolds to be coated were soaked in 0.05% type I collagen from rat tail (Sigma, St. Louis, MO) in phosphate-buffered saline (PBS) for 3 hours at room temperature and air dried overnight. All the scaffolds were EtO gas sterilized before use. The resulting scaffolds were approximately 6 mm in diameter and 7 mm in height.

4.2.2 Scanning Electron Microscopy

The surface morphology of composite CHI-CaP scaffolds was examined under the scanning electron microscopy (SEM). The scaffolds designated for SEM were fixed in 2.5% glutaraldehyde in PBS, dehydrated in graded ethanol and hexamethyldisilazane, and air dried. These scaffolds were then sputter coated with platinum and imaged on a JEOL JSM-6500F Field Emission Scanning Electron Microscope.

4.2.3 Porosity and Swelling ratio

Freeze dried scaffolds were weighed and dimensions were measured using digital calipers. Porosity was determined by volume displacement using methanol as described previously [9]. Three scaffolds of known dimensions were taken into a tube having 300µl of methanol. Porosity was calculated from Equation 4.1, where Δv is the volume of methanol displaced by scaffolds and v_a is the apparent volume calculated from the diameter and height of the scaffolds. The scaffolds were weighed, and dimensions were measured again after rehydrating them in PBS for 24 hours at 37°C. The porosity of hydrated scaffolds was measured similarly, by volume displacement of water. Starting volume of water was 800µl water. In Equation 4.1, Δv was the volume of water

displaced by hydrated scaffolds and v_a was the apparent volume calculated from the diameter and the height of the hydrated scaffolds. The swelling ratio was calculated as the percentage increase in weight upon rehydration. The porosity and the swelling ratio of collagen coated scaffolds were compared against uncoated scaffolds.

$$P = (1 - \Delta v/v_a) \tag{4.1}$$

4.2.4 Contact angle

To eliminate the effect of surface irregularity, contact angle measurements were made on solid collagen-coated and uncoated CHI-CaP discs having a final diameter of approximately 7 mm. Solid CHI-CaP discs were identical in composition to the porous scaffolds. Discs were made by filling wells of a 6-well polystyrene culture plate with chitosan solution and overlaying the precipitating solution for 24 hours. The precipitating solution was replaced by DI water until a neutral pH was reached. Discs were removed from the plate and placed into a custom press, which prevented them from warping during lyophilization. Half of the total number of discs were coated with 0.05% type I collagen in the same manner as porous scaffolds were coated. A 15µl drop of water was pipetted onto the center of the disc, and a digital photograph was captured within 7-10 seconds after pipetting. The image was processed using drop analysis LB-ADSA plugin of ImageJ software [15].

4.2.5 Human mesenchymal stem cell culture

Biphasic constructs were prepared using primary human bone marrow mesenchymal stem cells. Frozen passage 1 hbMSCs from a 22-year old healthy male donor were obtained from the Texas A&M Health Science Center College of Medicine

Institute for Regenerative Medicine at Scott & White (Temple, TX). The cells met the minimal criteria which define mesenchymal stem cells as established by the Mesenchymal and Tissue Stem Cell Committee of the International Society for Cellular Therapy [16]. The cells were thawed and plated at approximately 5-6×10^3 cells/cm^2. They were expanded in Dulbecco's modified Eagle Medium (DMEM) (Sigma, St. Louis, MO) containing 5% Fetal Bovine Serum, 1% Mesenchymal Stem Cell Growth Supplement (ScienCell Research Laboratories, Carlsbad, CA), and 1% antibiotic-antimycotic solution (Sigma, St. Louis, MO). The cells were subcultured using trypsin before reaching confluence.

4.2.6 Cell attachment and proliferation

To avoid inadvertent loss of any part of the inoculating cell suspension and to control for variability in scaffold architecture, cell attachment and proliferation rate studies were conducted using non-porous solid discs. HbMSCs were seeded onto circular flat CHI-CaP discs of approximately 20mm in diameter which were fabricated as described for contact angle measurements. Collagen coating and sterilization were performed in the same way as for porous scaffolds. Third passage hbMSCs were resuspended at 1×10^5 cells/ml in defined chondrogenic medium (DCM), and 0.5ml of cell suspension was pipetted onto the central region of each disc. Additional 0.5ml aliquots were frozen to establish the DNA content of the seeded cells. DCM consisted of high glucose DMEM containing 1% ITS+Premix (BD Biosciences, San Jose, CA), 0.1 mM dexamethasone, 50 µg/mL ascorbate-2 phosphate, 1 mM sodium pyruvate, 40 µg/mL L-proline, 1% antibiotic-antimycotic solution (Sigma-Aldrich, St. Louis, MO), and 10 ng/ml human recombinant transforming growth factor-β3 (PeproTech, Rock Hill, NJ)

[17,18]. At 60 minutes and 7 days following cell seeding non-adherent cells were removed by gentle rinsing with PBS, and attached cells were recovered by trypsinizing. Frozen aliquots were lysed and DNA was quantified similar to that of the trypsinized cells. DNA was quantified using the Hoechst assay to determine attachment efficiency and proliferation rate, respectively. In addition, viability staining using the PromoKine Live/Dead Cell Staining Kit II (PromoCell GmbH, Heidelberg, Germany) was performed on one disc from each group after a time period of 3 days. Attachment efficiency ($T_{1/2}$) was calculated from Equation 4.2, where q_1 was the average DNA content of cells in the aliquot used for seeding, and q_2 was the DNA content on the discs after 60 minutes of seeding.

$$T_{\frac{1}{2}} = \left(\frac{q_1}{q_2}\right) 100 \tag{4.2}$$

The rate of cell population doubling time (T_d) was calculated from Equation 4.3, where q_1 and q_2 were the average DNA content at 60 minutes seeding and DNA content on the disc at 7-day time duration respectively.

$$T_d = (t_2 - t_1) \frac{log\, 2}{log \frac{q_2}{q_1}}, \tag{4.3}$$

4.2.7 Creation and Evaluation of Biphasic Osteochondral Constructs

To investigate chondrogenesis *in vitro,* porous coated and uncoated scaffolds were first embedded in 1.5% agarose in a 6-well plate. Thus the scaffolds were buried underneath a layer of agarose approximately 4 mm thick. A biopsy punch was used to make a 4mm diameter cylindrical cut through the agarose overlying the scaffold. The agarose in that region was removed by Pasteur pipette under vacuum, thereby exposing

an area for cell seeding. A pilot study was performed to observe tissue formation and to measure the effect of coating on cell proliferation. A 50 µl aliquot of cell suspension containing approximately 4×10^6 passage 6 hbMSCs was pipetted on top of each scaffold, and the cells were permitted 4 hours for self-assembly before any additional medium was added. These constructs were cultured for 21 days in DCM, at which time they were digested for 12 h at 60 °C in 100 mM Na_2HPO_4, 10 mM Na_2EDTA, 10 mM L-cysteine, and 0.125 mg/mL papain. DNA in the supernatant was precipitated using 3M sodium acetate and 100% ethanol, resuspended in water, and quantified by measuring the optical absorbance at 285nm on a Nanodrop 2000c spectrophotometer (Thermo Fisher Scientific Inc., Waltham, MA).

Constructs to be used for evaluation of chondrogenesis were created in the same way using fourth passage hbMSCs. These constructs were cultured for 28 days in DCM, and the medium was changed every 2-3 days. The cells produced an opaque layer of tissue which as easily distinguished in digital photographs. ImageJ software was used to measure the projected surface area of the engineered tissue after manually outlining its perimeter. The cultured constructs were also processed for histology and immunohistochemistry. Formalin-fixed, paraffin-embedded and plastic-embedded sections of all the constructs were stained with toluidine blue for proteoglycan detection (2% toluidine blue in 1% glacial acetic acid) and with picro-sirius red to stain collagen (0.1% Sirius red in a saturated aqueous solution of picric acid). Picro-sirius red-stained sections were imaged under cross polarization, which reveals strongly oriented collagen fibers as birefringent. At evenly spaced sites across each of 3 sections from 3 different coated constructs, the angle of preferential collagen fiber alignment was measured in the

upper 20% and lower 30% (adjacent to scaffold) of the tissue using the OrientationJ plugin to ImageJ [19]. Sections of coated constructs were not amenable to measurements of collagen fiber alignment. Additional sections of collagen-coated and uncoated constructs were immunostained for type II collagen. Antigen retrieval was performed by incubating sections for 30 min at 100 °C in 10 mM sodium citrate buffer pH 6.0, followed by incubation for 10 min at 37 °C in 0.5 mg/ml pronase in PBS. The collagen epitope was exposed by incubating for 30 min at 37 °C in 2 mg/ml hyaluronidase in tris-buffered saline. Sections were incubated in a monoclonal anti-type II collagen primary antibody overnight at 4° C (undiluted culture supernatant) (II-II6B3, Development Studies Hybridoma Bank, University of Iowa, Iowa City, IA). The Superpicture 3rd Generation IHC Detection Kit (Invitrogen, Carlsbad, CA) was then used according to the manufacturer's instructions.

4.2.8 Statistics

The quantitative data were analyzed by an independent t-test at α=0.05, and p-values < 0.05 were considered statistically significant (IBM SPSS Statistics 19).

4.3 Results

4.3.1 Scaffold Characterization

The surface morphology of platinum sputter coated CHI-CaP scaffolds, collagen coated and uncoated, were examined under SEM. SEM images showed a slightly bumpy surface with nanoscale features, which was not affected by collagen coating (Figure 4.1). There was no significant difference in physical properties between the collagen coated and uncoated scaffolds (Table 4.1), with the exception of contact angle (Figure 4.2). The

porosity of the dry collagen coated scaffold (36.06±3.62) was similar to that of the dry uncoated scaffold (38.73±1.84), which was measured using methanol volume displacement method. The porosity of the hydrated collagen coated scaffold (75.67±8.97) was similar to the hydrated uncoated scaffold (69.01±6.55), which was measured using water volume displacement. The swelling ratio, which was calculated as the increase in mass upon rehydration, was also similar in both the groups (Table 4.1). Water contact angle was significantly influenced by collagen coating. The contact angle on uncoated CHI-CaP was 107.81°±13.09°, and on collagen coated discs it was 78.2°±8.71° ($p<0.05$).

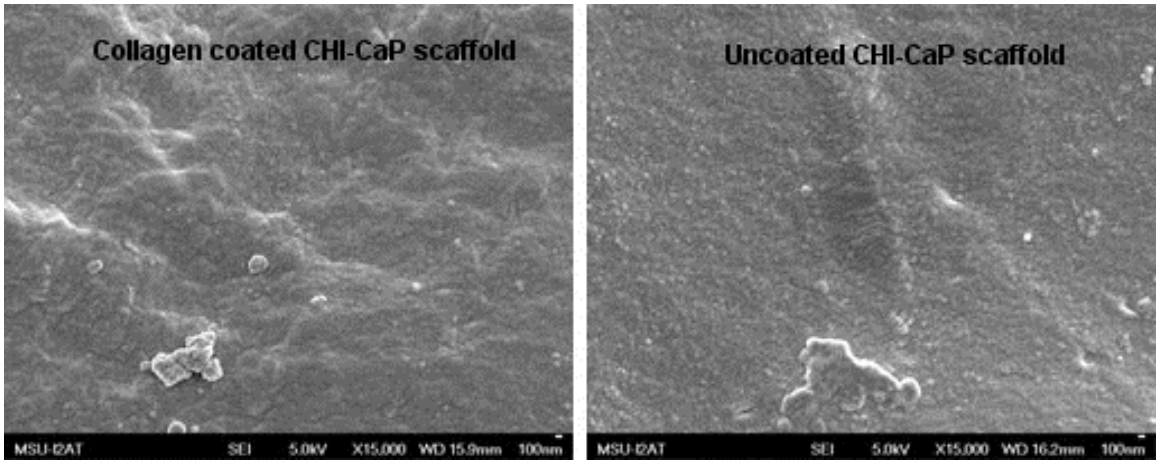

Figure 4.1 Scanning Electron micrograph of freeze dried collagen coated and uncoated composite CHI-CaP scaffold showing a slightly bumpy surface at 15000X magnification.

Table 4.1 Physical characteristics of collagen coated and uncoated scaffolds.

Characteristic	**Collagen Coated Scaffolds**	**Uncoated Scaffolds**
Porosity of dry scaffold (%) (n=5)	36.06±3.62	38.73±1.84
Porosity of hydrated scaffold (%) (n=5)	75.67±8.97	69.01±6.55
Swelling ratio (%) (n=5)	75.65±0.79	77.01±1.59
Increase in diameter after hydrating (%) (n=5)	19.40±1.07	20.38±1.58
Increase in height after hydrating (%) (n=5)	20.79±1.42	20.12±0.58
Increase in volume after hydrating (%) (n=5)	72.23±3.90	74.17±5.22

(values=mean±stdev)

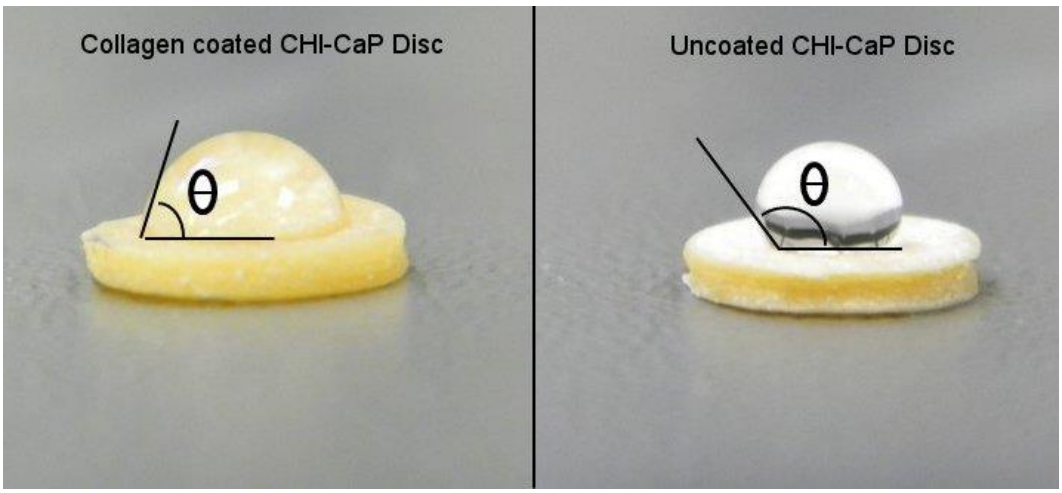

Figure 4.2 Contact angle measurement on colalgen coated and uncoated CHI-CaP discs.

Image caputered within 7-10 seconds after dropping 15 µl of water on a collagen coated and an uncoated CHI-CaP disc for contact angle measurement using ImageJ.

4.3.2 Cell attachment and proliferation

Composite CHI-CaP discs supported the attachment and the proliferation of hbMSCs. More cells were attached to the collagen coated discs than to the uncoated ones. The attachment efficiency for collagen-coated scaffolds was 70.88%±4.75% and for the uncoated scaffolds was 51.07%±4.04% after 60 min of cell seeding ($p<0.05$) (Figure 4.3). Cells in both groups proliferated as evidenced by 3-fold increases in recovered DNA between 60 min and 7 days. However, there was no difference in population doubling time ($p=0.422$), indicating equivalent rates of proliferation. More DNA, indicating a greater number of cells, was recovered from collagen coated constructs on Day 7 than from uncoated scaffolds ($p<0.05$). Many green fluorescent (live) cells, but no red fluorescent (dead) cells were observed on the coated and uncoated discs on Day 3 (Figure 4.4).

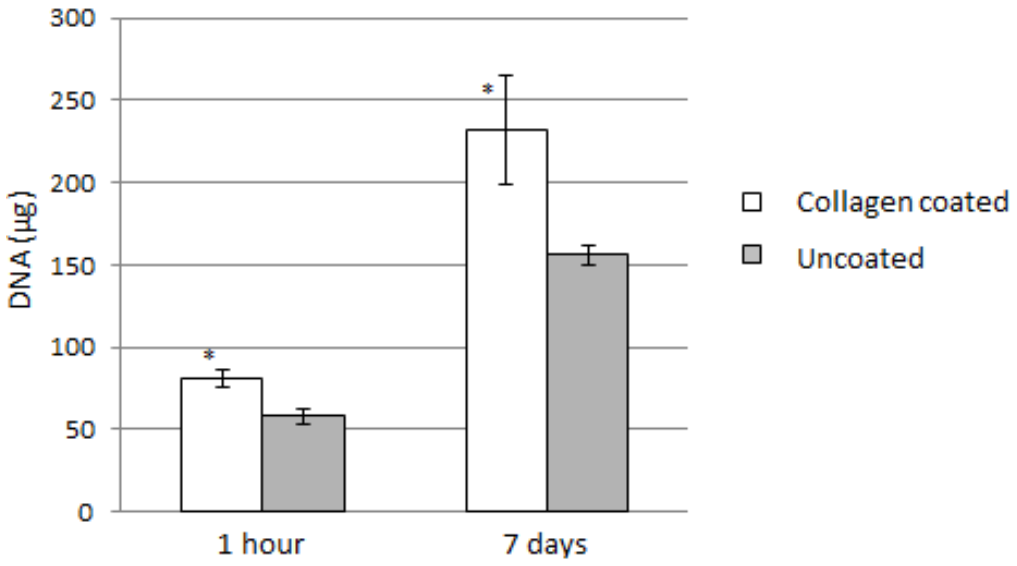

Figure 4.3 The bar graph shows the amount of DNA on collagen coated and uncoated scaffolds at 1 hour and 7 day time interval.

(*indicates both the groups are statistically different, $p<0.05$).

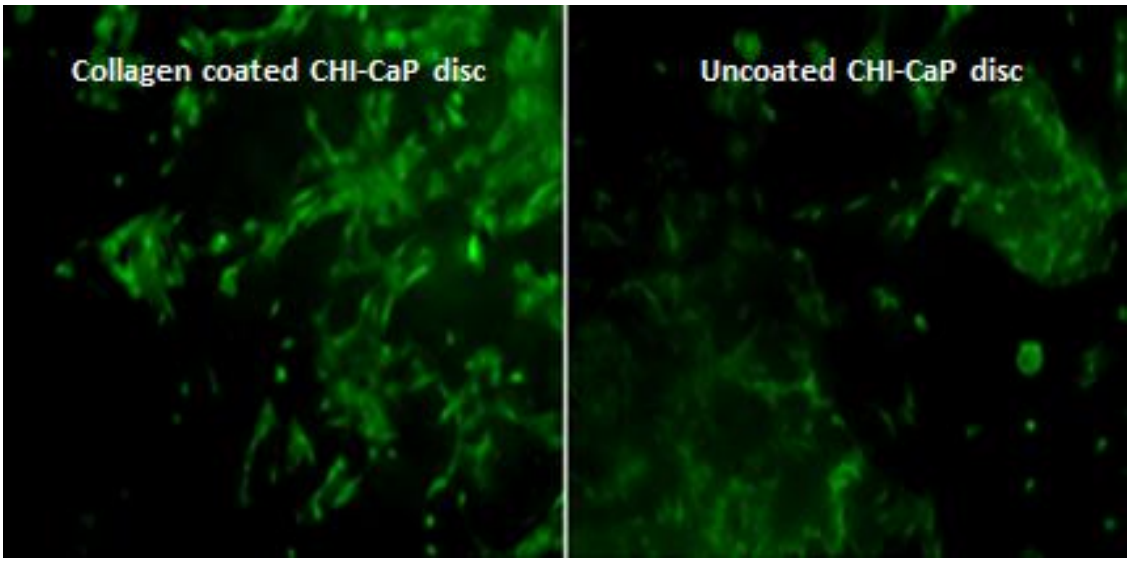

Figure 4.4 Live dead staining of hbMSCs on CHI-CaP discs

Live dead staining of hbMSCs seeded at 1×10^5 cells/ml density on a collagen coated and an uncoated composite CHI-CaP disc after 3 day time period (10X objective).

4.3.3 Biphasic constructs- DNA quantification

On Day 21, the cells had formed semi-translucent to opaque patches of tissue, the sizes of which were much smaller on the uncoated scaffolds than on the collagen-coated ones. There was somewhat more DNA in biphasic constructs made from collagen-coated scaffolds than from uncoated scaffolds (2.04±0.44, and was 1.54±0.69 µg per construct, respectively). However, due the relatively small sample size, a statistically significant difference was not demonstrated.

4.3.4 Chondrogenesis

By Day 28, hbMSCs seeded on top of CHI-CaP scaffolds had synthesized a tissue similar in to hyaline cartilage. The tissue on uncoated scaffolds was contracted into a spherical mass which was easily dislodged. It covered a small fraction of the initial

seeding area. On the other hand, the tissue on the coated scaffolds was a circular patch of approximately uniform thickness. It appeared to cover the entire area onto which cells had been seeded (Figure 4.5). Tissue area covered on collagen coated scaffolds was 11.09±2.25 mm^2 and it was only 2.76±0.38 mm^2 for uncoated scaffolds. As shown in figure 5, the average projected surface area of tissue was 75% greater in the collagen-coated group compared to the uncoated group ($p<0.05$).

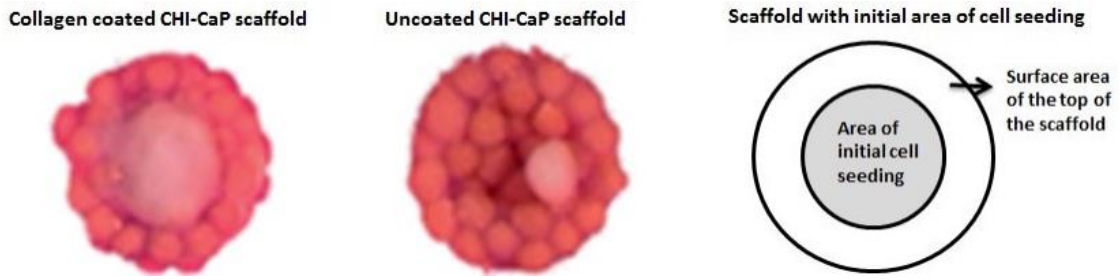

Figure 4.5 Area of neocartilage formed on collagen coated and uncoated composite CHI-CaP scaffolds.

Cartilage like tissue formed was extended into the pores on a collagen coated scaffold while the tissue contracted into a spherical mass on uncoated scaffold. Area of the tissue covered was statistically different between two groups, $p<0.05$.

4.3.5 Histology

In most of the uncoated constructs, the tissue detached from the scaffold during the embedding process because it was not well adhered to the scaffold. On coated scaffolds, but not uncoated ones, the tissue extended into the pores so that the tissue contour matched the scaffold contour at their interface. The tissue on collagen coated and uncoated scaffolds demonstrated strong metachromatic toluidine blue staining, especially in the deep zone (Figure 4.6). Tissue formed on the control scaffolds did not cover sufficient surface area for collagen orientation analysis. On collagen-coated

scaffolds, the directions of preferential fiber alignment in the superficial and deep zones were significantly different (0.30° vs. 95.5° with respect to the top surface, $p<0.05$), a pattern which is similar to that observed in native articular cartilage (Figure 4.7). Positive staining for type II collagen (brown color) was far more intense in the tissue grown on collagen coated CHI-CaP than on the uncoated scaffolds (Figure 4.6), indicating a much greater proportion of type II collagen in the extracellular matrix.

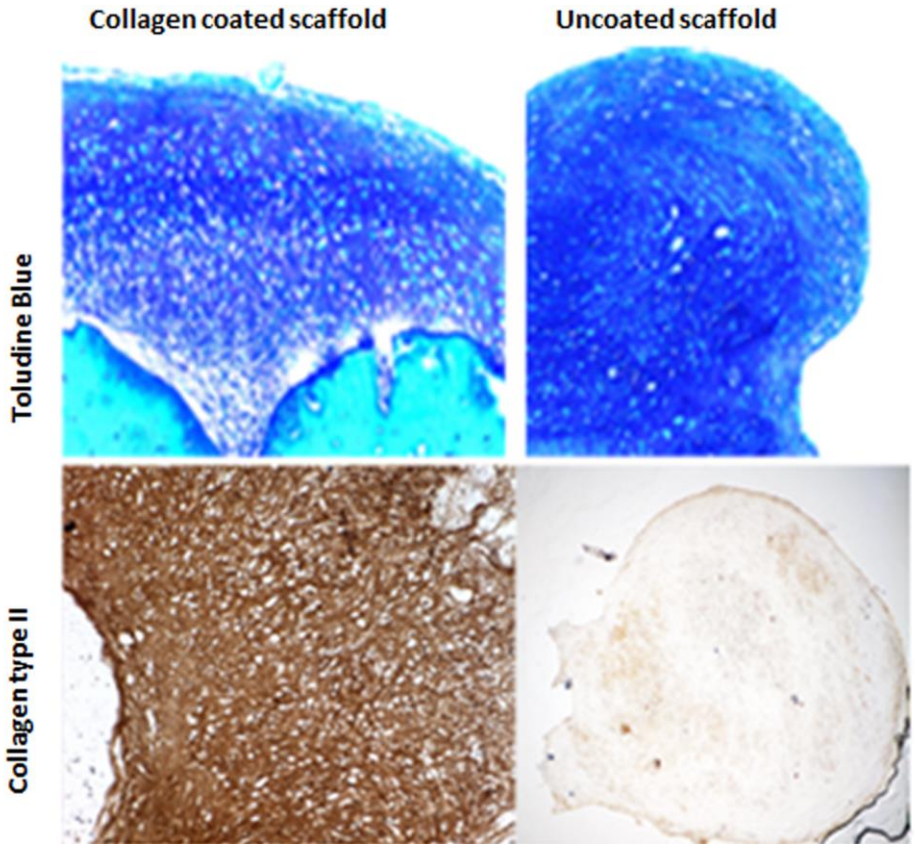

Figure 4.6 Toluidine blue and collagen type II staining on the neocartilage formed on collagen coated and uncoated CHI-CaP scaffolds.

Histological sections of engineered cartilage formed on CHI-CaP scaffolds stained with toluidine blue showed a strong metachromatic staining at deep zones, a circular patch of tissue extended into pores on collagen coated scaffold and tissue contracted into a spherical mass on uncoated scaffold. Immunohistochemistry sections, positive staining for type II collagen was intense in the tissue grown on collagen coated CHI-CaP than the uncoated scaffolds at 10X magnification.

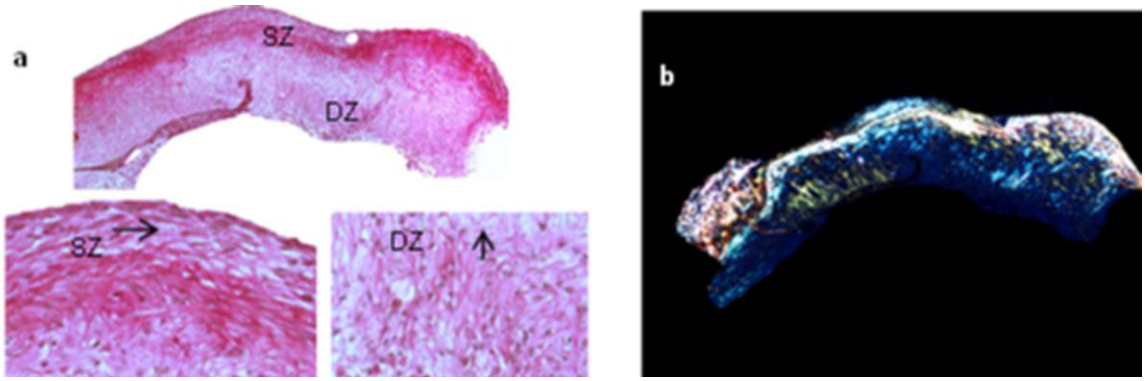

Figure 4.7 Picosirius red stained neocartilage on collagen coated scaffolds.

Digitally isolated engineered cartilage on collagen coated scaffold stained for a) picosirius red showing collagen fiber orientation in the superficial and deep zones b) polarized light microscopy images showing birefringent collagen fibers alignment on collagen coated scaffold.

4.4 Discussion

The current investigation advances a biphasic approach to cartilage tissue engineering, in which one layer is designed to support osteogenesis (bone growth), and another promotes chondrogenesis (cartilage regeneration). The osteoconductive phase is a porous CHI-CaP scaffold. An extremely high density suspension of MSCs is layered on top of the scaffold so that it will form a cartilaginous phase through self-assembly. It is similar to the system previously described by Waldman et al., which involved the seeding of articular chondrocytes onto a porous calcium polyphosphate substrate [20]. Our approach is distinguished by use of a less brittle scaffold and by the use of MSCs. This scheme is different from most other bilayered designs, which typically involve the fusion of two different scaffold materials and/or incorporation of different cell types [21,22,23,24].

Based on previous studies, chitosan has been regarded as a promising biopolymer in tissue engineering. The main reason for choosing chitosan as a scaffold is its chemical

similarity and its ability to interact with glycosaminoglycans of cartilage. Properties of chitosan scaffolds, such as crystallinity, mechanical strength, and degradation, can be varied by altering molecular weight and the degree of deacetylation [3]. Composite CHI-CaP scaffolds were found to have a significantly greater compressive modulus than scaffolds of pure chitosan [9]. Furthermore, the modulus is approximately 10 MPa, which is at the lower end of the range for human cancellous bone [25], and should be sufficient for the initial transmission of joint forces to the underlying bone. In a study done by Chesnutt et al., CHI-CaP scaffolds with DDA 92.3% seeded with human fetal osteoblast cells were implanted in rat calvarial defect. After 12 weeks of study, the histology images revealed the formation of new bone, but the chitosan scaffold had undergone little degradation. In the current study, the scaffolds were fabricated using chitosan of 78.7% DDA, which is expected to degrade faster [10]. Ideally, the rate of scaffold degradation would match the rate of new bone formation.

In this study human bone marrow MSCs were used to generate the chondrogenic layer of the biphasic scaffold. Autologous chondrocytes and MSCs are the most commonly used cell sources for cartilage tissue engineering. Chondrocytes have limited potential for expansion *in vitro*, and proliferation in monolayer results in cell de-differentiation and declining chondrogenic potential [26,27]. On the other hand, use of MSCs preserves all healthy cartilage in the affected joint and spares it from additional trauma. MSCs are hypoimmunogenic, self-renewable, and can also proliferate for long periods [10]. They also exhibit anti-apoptotic and wound healing properties [13]. We have previously demonstrated that MSCs can be chondroinduced with high efficiency when exposed to either TGF-β1 or TGF-β3 [17].

Our previous study revealed that inefficient cell attachment to porous CHI-CaP scaffolds was a hindrance to formation of a functional cartilage layer [11]. It was hypothesized that coating the scaffolds with type I collagen would significantly improve MSC adhesion. Collagen is roughly a third of the total body protein, and is abundant in cartilage, bone, blood vessels, skin and many other tissues. It has both mechanical and physiological functions. Mechanically it is excellent at resisting tensile loads, and physiologically it supports cell attachment. Collagen type I was of particular interest. It is the predominant type of collagen in bone, and the attachment of MSCs to collagen type I is mediated by α1β2, α2β1, and α11β1 integrin receptors [28]. It has specifically been shown to be superior to chitosan for enhancing cell attachment to PLGA scaffolds [29]. In a monolayer culture model, MSC attachment and proliferation on collagen type I was compared to fibronectin, laminin I, and poly-L-lysine. MSCs adhered to collagen type I with very high efficiency within 45 minutes, and collagen supported the highest rate of cell proliferation [14]. Furthermore, collagen type I and type II coatings were found to be equivalent in terms of promoting cartilaginous extracellular matrix production by human articular chondrocytes [30].

This study demonstrated that coating the CHI-CaP scaffolds with collagen type I serves to make them hydrophilic but does not otherwise alter their physical properties including porosity, swelling ratio, and dimensional changes upon rehydration. The porosity of these CHI-CaP scaffolds measured by methanol displacement method was approximately 35%, irrespective of coating, and was similar to the porosity of chitosan scaffolds fabricated by Chesnutt et al [10]. Although a greater void fraction is likely to be advantageous, it is expected that this porosity is sufficient to support bone ingrowth

[31]. Interconnectivity of the porous structure has been directly observed under microCT scanning (data not shown). MSC adhesion was greater to the discs coated with collagen, and proliferation was similar on collagen-coated and uncoated discs. Efficiency of attachment to uncoated CHI-CaP was similar to that observed by Chesnutt et al. on composite scaffolds [19], but lower than previously reported for collagen-coated tissue culture plastic [14]. The improved adhesion is attributed to better scaffold wettability and also to the abundance of ligands for MSC integrin receptors. Surface topography was likely not a factor, as the surfaces of coated and uncoated scaffolds displayed similar nanoscale features upon examination by SEM.

In this study, fourth passage human bone marrow MSCs was seeded directly on top of a composite CHI-CaP scaffold within a circular agarose mold. After 4 weeks of culture in defined chondrogenic medium containing TGF-β3, the cells had formed a firm, white tissue resembling hyaline cartilage on top of collagen-coated and uncoated scaffolds. The tissue formed on coated scaffolds was a layer of approximately uniform thickness tightly adhered to the surface and covering the entire area of cell seeding. In contrast, tissue formed on uncoated scaffolds was concentrated in a spherical mass which occupied a small portion of the initial cell seeding area and which had a fragile attachment to the scaffold. Contraction of the cell mass started approximately 48 h after cell seeding. At the end of the culture period, the tissue on coated scaffolds covered 5 times as much surface area as the tissue on uncoated scaffolds. Complete coverage of neotissue over the entire cell seeding area is essential for eventual application of this approach to cartilage repair.

Histology showed that the tissue on coated scaffolds conformed to the scaffold's shape, thereby covering a larger surface area than the projected area measured from macroscale photograhs. On coated scaffolds, the tissue was approximately 400-500 μm thick over the entire area of cell seeding. It displayed noticeably more metachromatic staining with toluidine blue compared to tissue on uncoated scaffolds, which suggests a higher proteoglycan concentration. It also stained intensely for collagen type II, in contrast to the faint staining exhibited by the tissue on uncoated scaffolds. These findings indicate that the collagen coating not only promoted cell adhesion, but chondrogenesis as well. In fact, the tissue that formed on the collagen-coated scaffolds displayed a distinct pattern of collagen fiber orientation. In a very narrow zone at the upper surface, it was parallel to the upper surface. In a relatively wide zone adjacent to the scaffold, it was roughly perpendicular to the upper surface. These zones were separated by a zone of indistinct orientation. This pattern of alignment is very similar to that found in articular cartilage with its superficial, transition, and deep zones containing collagen that is aligned parallel, randomly, and perpendicular to the joint surface, respectively. It is also the same pattern we previously observed in tissue engineered cartilage formed by self-assembly of MSCs [17]. With respect to chondrogenesis, our results are consistent with those of Ragetly et al., who demonstrated that coating chitosan fibrous scaffolds with type II collagen increased MSC seeding efficiency, cartilaginous extracellular matrix production, and surface area covered by extracellular matrix [12]. Thus coating with collagen may be generally beneficial to cartilage tissue engineering approaches involving chitosan-based scaffolds.

Our results clearly demonstrate that the collagen coating improves MSC adhesion and promotes formation of a continuous cartilage layer on the scaffold's surface. However, the effect of collagen coating solution concentration was not investigated. The 0.05% concentration used in this study was considerably lower than the concentrations used in a previous study to coat chitosan fibrous scaffolds, but that study found little benefit to raising the concentration from 0.2% to 0.4%. Therefore we speculate that collagen concentration-dependent effects on cell adhesion and chondrogensis may be observed in our model within the range of 0.05% to 0.2%. Another limitation of the current study was the inability to quantify the tissue-scaffold adhesive strength. Tissue maturation, in terms of stiffness and thickness, was not adequate for mechanical testing. Future studies will aim not only to optimize concentration of the collagen coating solution but also the size of the beads from which scaffolds are created. Bead size affects porosity, pore size, and surface morphology and is therefore predicted to strongly influence tissue coverage and strength of adhesion to the scaffold.

4.5 References

[1] Jiang C, Chiang H, Liao C, Lin Y, Kuo T. Repair of porcine articular cartilage defect with a biphasic osteochondral composite. J Orthop Res. 2007;25:1277-1290.

[2] Tampieri A, Sandri M, Landi E, Pressato D, Francioli S. Design of graded biomimetic osteochondral composite scaffolds. Biomaterials. 2008;29:3539–3346.

[3] Nettles D, Elder S, Gilbert J. Potential use of chitosan as a cell scaffold material for cartilage tissue engineering. Tissue Eng. Dec 2002;8(6):1009-16.

[4] Karteek P SMRA. Chitosan: A Biocompatible Polymer for Pharmaceutical Applications in Various Dosage Forms. International Journal Of Pharmacy & Technology. June 2010;2(2):186-205.

[5] ASlam R SASD. Microspheres-a tool for drug delivery system. Novel Science International Journal Of Pharmaceutical Science. 2013;2(5-6):97-103.

[6] Felt O, Carrel A, Baehni P, Buri P, Gurny R. Chitosan as a tear substitute: a wetting agent endowed with antimicrobial efficacy. J Ocul Pharmacol Ther. June 2000;16(3):261-70.

[7] Tsai G, Su W. Antibacterial activity of shrimp chitosan against Escherichia coli. J Food Prot. March 1999;62(3).:239-43.

[8] Reves B, Bumgardner J, Cole J, Yang Y, Haggard W. Lyophilization To Improve Drug Delivery For Chitosan-Calcium Phosphate Bone Scaffold Construct: A Preliminary Investigation. J Biomed Mater Res B Appl Biomater. July 2009;90(1):1-10.

[9] Chesnutt B, Viano A, Yuan Y, al e. Design and characterization of a novel chitosan/nanocrystalline calcium phosphate composite scaffold for bone regeneration. J Biomed Mater Res A. Feb 2009;88(2):491-502.

[10] Chesnutt B, Yuan Y, Buddington K, Haggard W, Bungardner J. Composite chitosan/nano-hydroxyapatite scaffolds induce osteocalcin production by osteoblasts *in vitro* and support bone formation *in vivo*. Tissue Eng Part A. Sep 2009;15(9):2571-9.

[11] Elder S, Gottipati A, Zelenka H, Bumgardner J. Attachment, Proliferation, and Chondroinduction of Mesenchymal Stem Cells on porous chitosan calcium phosphate scaffolds. The Open Orthopaedics Journal. Jul 2013;7:275-81.

[12] Ragetly G, Griffon D, Lee H, Chung Y. Effect of collagen II coating on mesenchymal stem cell adhesion on chitosan and on reacetylated chitosan fibrous scaffolds. J Mater Sci: Mater Med. Aug 2010:2479-90.

[13] Yang X, Bhatnagar R, Li S, Oreffo R. Biomimetic collagen scaffolds for human bone cell growth and differentiation. Tissue Eng. Jul-Aug 2004;10(7-8):1148-59.

[14] Popov C RTHFea. Integrins α2β1 and α11β1 regulate the survival of mesenchymal stem cells on collagen I. Cell Death Dis. July 2011;2:e186.

[15] Stalder A, Melchior T, Muller M, Sage D, Blu T, Unser M. Low-Bond axisymmetric drop shape analysis for surface tension and contact angle measurements of sessile drops. Colloids and Surfaces A: Physicochemical and Engineering Aspects. Jul 2010;364(1-3):82-81.

[16] Dominici M LBKMIea. Minimal criteria for defining multipotent mesenchymal stromal cells. The International Society for Cellular Therapy position statement. Cytotherapy. 2006;8(4):315-7.

[17] Elder S, Cooley J, Borazjani A, Sowell B, To H, Tran S. Production of hyaline like cartilage by bone marrow mesenchymal stem cells in a self-assembly model. Tissue Eng Part A. Oct 2009;15(10):3025-36.

[18] Murdoch A, Grady L, Ablett M, et al. Chondrogenic differentiation of human bone marrow stem cells in transwell cultures: generation of scaffold-free cartilage. Stem Cells. Nov 2007;25(11):2786-96.

[19] Rezakhaniha R, Agianniotis A, Schrauwen J, et al. Experimental investigation of collagen waviness and orientation in the arterial adventitia using confocal laser scanning microscopy. Biomech Model Mechanobiol. August 2010.

[20] Waldman S, Grynpas M, Pilliar R, Kandel R. Characterization of cartilagenous tissue formed on calcium polyphosphate substrates *in vitro*. J Biomed Mater Res. Dec 2002;62(3):323-30.

[21] Yan LP, Silva-Correia J, Oliveira MB, al e. Bilayered silk/silk-nanoCaP scaffolds for osteochondral tissue engineering: *In vitro* and *in vivo* assessment of biological performance. Acta Biomater. January 2015;12:227-41.

[22] Lam J, Lu S, Lee EJ, al e. Osteochondral defect repair using bilayered hydrogels encapsulating both chondrogenically and osteogenically pre-differentiated mesenchymal stem cells in a rabbit model. Osteoarthritis cartilage. Sep 2014;22(9):1291-300.

[23] Lam J, Lu S, Ville V, al e. Generation of osteochondral tissue constructs with chondrogenically and osteogenically predifferentiated mesenchymal stem cells encapsulated in bilayered hydrogels. Acta Biomaterialia. March 2014;10(3):1112-1123.

[24] Oliveira JM, Rodrigues MT, Silva SS, al e. Novel hydroxyapatite/chitosan bilayered scaffold for osteochondral tissue-engineering applications: Scaffold design and its performance when seeded with goat bone marrow stromal cells. Biomaterials. December 2006;27(36):6123-6137.

[25] Keavney TM HW. Mechanical Properties of Cortical and Cancellous Bone. 285p ed. Boca Raton: CRC Press; 1992.

[26] Natalia Martins Breyner AAZea. Cartilage Tissue Engineering Using Mesenchymal Stem Cells and 3D Chitosan Scaffolds - *In vitro* and *in vivo* Assays. In: Pignatello R, ed. Biomaterials Science and Engineering: INTECH; 2011:211-226.

[27] C. Csaki PRASMS. Mesenchymal stem cells as a potential pool for cartilage tissue engineering. Annals of Anatomy - Anatomischer Anzeiger. November 2008;190(5):395-412.

[28] Barczyk M, Cerracedo S, Gullberg D. Integrins. Cell Tissue Res. 2010;339(1):269-280.

[29] Wu Y, Shaw S, Lin H, Lee T, Yang C. Bone tissue engineering evaluation based on rat calvaria stromal cells cultured on modified PLGA scaffolds. Biomaterials. Feb 2006;27(6):896-904.

[30] Rutgers M, Saris D, Vonk L, et al. Effect of collagen type I or type II on chondrogenesis by cultured human articular chondrocytes. Tissue Eng Part A. 2013;19(1-2):59-65.

[31] Karageorgiou V, Kaplan D. Porosity of 3D biomaterial scaffolds and osteogenesis. Biomaterials. 2005;26(27):5474-5491.

CHAPTER V

EFFECT OF BEAD SIZE ON SCAFFOLD CHARACTERISTICS

5.1 Introduction

Several studies have investigated engineering cartilage tissue using various scaffold materials [1,2]. The scaffold material and architecture plays an important role in tissue engineering. Scaffolds need to be fabricated in such a way that supports cell proliferation, tissue formation, and nutrient and waste material transportation [3]. It acts as an interim substitute and provides mechanical strength until new tissue formation takes place. Pore size plays a major role in scaffold designing and it controls several factors like tissue growth, mechanical integrity, degradation, nutrient, and waste material diffusion [3,4,5]. Various methods have been discussed for creating porous scaffolds – freeze drying [6], gas foaming [7], 3D printing [8], electrospinning [9], and phase separation [10]. However, the perfect tissue engineered graft should possess almost same structure and perform similar functions of a native tissue [11].

The scaffold material we are interested in is chitosan, a biocompatible, biodegradable, and osteoconductive polymer with wound healing and antimicrobial properties [12,13,14]. Chitosan along with calcium and phosphate was known to increase the mechanical integrity of the scaffolds [15]. Previous studies have shown the potential use of chitosan as a scaffold material for cartilage tissue engineering [16,17,18]. Chitosan is also known to support cell attachment for various cell types [15,16,19] and cell

attachment increased when coated with an extracellular matrix protein [20]. Chesnutt et al. fabricated chitosan calcium phosphate scaffolds by fusing individual beads with approximately 35% porous having 100-800 μm pore sizes [15]. By varying the bead size, the pore size and porosity also varies, which reflects the design and architecture of the scaffolds. A previous study has shown that freeze-drying of similar type of scaffolds increased porosity and pore size [6].

Articular cartilage defects are classified into two types – chondral and osteochondral defects. In chondral defects, the cartilage damage is limited to the cartilage tissue; whereas in osteochondral defects, subchondral bone lying below the cartilage defect also gets damaged. Several studies have shown the use of biphasic constructs for treating osteochondral defects, where one phase represents bone and other cartilage. In a traditional biphasic constructs, either two types of scaffold materials were fused together [21,22,23] or two types of cells were seeded on top and bottom halves of the scaffold [11,21,24]. In the current study, we are developing a tissue-engineered approach for treating osteochondral defects using one biomaterial, chitosan calcium phosphate scaffolds (CHI-CaP) and two different cell types, osteosarcoma and chondrocytes. The scaffolds were first incubated with osteosarcoma cell line for the deposition of bone mineral on the scaffold and later porcine chondrocytes were used to regenerate cartilage tissue on top of these mineral deposited CHI-CaP scaffolds. The main objective of this study was to understand the influence of CHI-CaP bead size on the porosity, swelling ratio, mechanical strength, degradation, and neocartilage tissue formation.

5.2 Methods

5.2.1 Scaffold fabrication

Porous cylindrical shaped composite chitosan calcium phosphate scaffolds were fabricated using co-precipitation method as described previously by Chesnutt et al. [15]. Our study differs from Chesnutt et al. by using chitosan powder of 78.7% DDA, where they used 92% for scaffold fabrication. In the current study, scaffolds with three different bead sizes were fabricated. Bigger size beads were made by dripping the chitosan calcium phosphate solution directly from the nozzle of a 30 ml syringe (no needle was used). Medium size beads were made in the similar way but using an 18G needle [19]. Smaller size beads were made by using an 18G needle and by focusing a jet of air directly at the tip of the needle in order to dislodge each CHI-CaP droplet from the needle before it grows large enough to fall under its own weight. These beads were collected and left in the precipitate solution, a mixture of methanol, NaOH, and water at a pH 13 for 24 h for the formation of hydroxyapatite [25]. The beads were then washed in DI water regularly, until it reaches neutral pH. Beads were dried overnight and then fused into cylindrical shape (6mm diameter and 7 mm height) using 2% acetic acid and dried overnight. All the scaffolds were frozen at -20°C for 2 h and freeze dried overnight. All the scaffolds designated for making biphasic constructs were soaked in 0.05% of type I collagen from rat tail in PBS for 3 h and air dried overnight. The scaffolds were then gas sterilized using ethylene oxide before cell seeding.

5.2.2 Porosity and swelling ratio

Three freeze dried scaffolds from each group were imaged using micro computed tomography (microCT). After imaging, the same scaffolds were rehydrated in PBS for 24

h at 37°C and imaged again under microCT. The images were reconstructed into a 3 dimensional model using scanIP software and masked depending on the density of the material (grey scale). The dimensions of the scaffold and the volume of the mask covered for each scaffold were recorded. Porosity of dry and hydrated scaffolds was calculated using Equation 5.1, where v_a is the apparent volume of the scaffold calculated from dimensions of the scaffold and v_m is the volume of mask covered (volume of beads). The swelling ratio was calculated as the percentage increase in mass upon rehydration for 24 h in PBS.

$$P = \left(\frac{v_a - v_m}{100}\right) v_a \tag{5.1}$$

5.2.3 Mechanical testing

One of the main functions of bone in *in vivo* is load bearing. As the scaffold replaces the bone, compression modulus of the cell-free composite CHI-CaP scaffolds were measured using Mach I. In order to measure the compressive modulus, six scaffolds from each group were incubated for 24 h, 14 d, or 28 d in cell culture medium at 37°C. Young's modulus in the axial direction was determined by unconfined compressive loading at 5 μms^{-1}. The compression modulus was calculated from the slope of stress-strain curve.

5.2.4 Degradation

Lysozyme is the enzyme that helps in chitosan degradation in *in vivo*. Three scaffolds (6 mm diameter x 7 mm height) from each group were incubated at 37°C in 1mg/ml of lysozyme in PBS. The lysozyme solution was collected at every three-day time interval and the scaffolds were dried completely until they attained stable weight

before adding fresh lysozyme solution. The lysozyme solution at every 3 d time interval was used to measure the amount of calcium released into the solution based on colorimetric assay using Calcium LiquiColor kit, Stanbio laboratory. Total dry weight loss with respect to their initial dry weights was also calculated at each time point.

5.2.5 Mouse Osteosarcoma cell line

Osteosarcoma cells at 8th passage were obtained from another lab. These cells were cultured in Dulbecco's Modified Eagle's Medium (DMEM) medium having 10% fetal bovine serum (FBS) and 1% antibiotic and antimitotic factors (ABAM). When cells reach 90% confluence, they were treated enzymatically with trypsin and seeded into new flasks. Cells at tenth passage were used for this study.

5.2.6 Porcine chondrocytes

Chondrocytes were collected and cultured from femoral condyles of one healthy matured pig. First, the articular cartilage tissue was carefully removed from the femoral condyles and digested in DMEM containing 1% type 2 collagenase, 5% FBS, and 2% ABAM for overnight at 37°C and 5% CO_2. Cartilage tissue digestion solution was filtered using a cell suspension filter and centrifuged at 500g for 5 min. The cell pellet was then resuspended in DMEM containing 10% FBS and 1% ABAM and seeded in a T175 cell culture flask. Before reaching confluence, cells were treated with trypsin and subcultured into a new flask. Cells at second passage were used for making biphasic constructs.

5.2.7 Biphasic constructs

Twelve Freeze dried, collagen coated, and gas sterilized scaffolds of each bead size were used for making biphasic constructs. Two scaffolds of same bead size were incubated together in 10×10^6 cells/ml of tenth passage mouse osteosarcoma cell suspension for 24 hours in a sterile 15ml centrifuge tube. The cell suspension in the tubes was resuspended by slowly shaking the tube for every 15 min for 2 h to achieve maximum cell attachment to the scaffolds. The scaffolds were then incubated in osteogenic medium in a 6 well cell culture plate for 6 weeks, replacing medium every 4 days. At the end of 3 week and 6 week time period one scaffold from each group was fixed in 2.5% glutaraldehyde for SEM. The remaining scaffolds were air dried for several hours before seeding porcine chondrocytes. Each dried scaffold was placed in an individual well of a 6 well plate and covered with 1.5% agarose in DMEM. Once the agarose was gelled, 5mm hole was made on top of the scaffold using biopsy punch and the agarose was removed using pasteur pipette. 3.5×10^6 of second passage porcine chondrocytes suspended in 40µl of DMEM were then seeded on top of each scaffold resting in an agarose well (Figure 5.1). Chondrocytes were allowed to settle for 30 min and then the wells were flooded with defined chondrogenic medium (DCM). DCM consisted of high glucose DMEM containing 1% ITS+Premix (BD Biosciences, San Jose, CA), 0.1 mM dexamethasone, 50 µg/mL ascorbate-2 phosphate, 1 mM sodium pyruvate, 40 µg/mL L-proline, 1% antibiotic-antimycotic solution (Sigma-Aldrich, St. Louis, MO), and 10 ng/ml human recombinant transforming growth factor-β3 (PeproTech, Rock Hill, NJ) [26]. These biphasic constructs were cultured for 4 weeks in DCM, replacing medium every 4 days. At the end of 4 weeks, the tissue formed on top of two biphasic

constructs of each group was slowly scrapped to see how well the tissue was adhered to scaffold and the scaffolds were fixed in 2.5% glutaraldehyde for SEM. Three biphasic constructs from each group with the tissue were also fixed in 2.5% glutaraldehyde for SEM and microCT imaging.

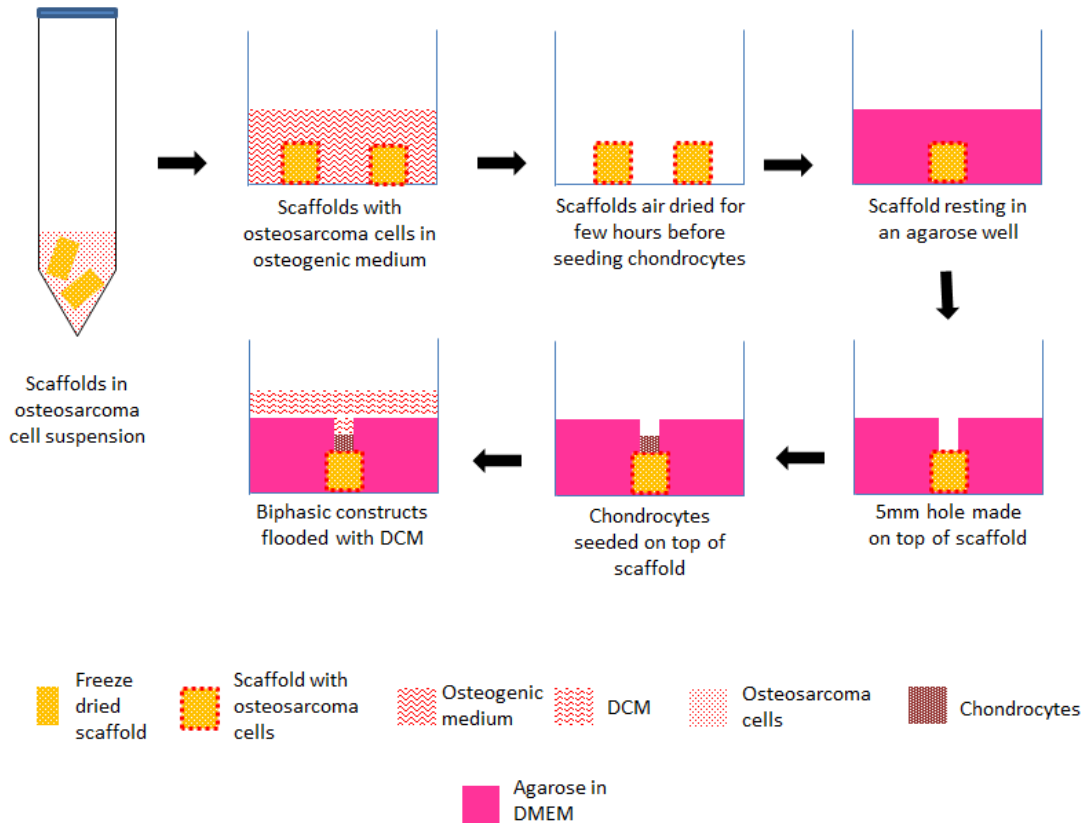

Figure 5.1 Schematic representation of the formation of biphasic constructs using collagen coated CHI-CaP scaffolds.

5.2.8 SEM sample preparation

The structure and the surface morphology of the cell free scaffolds, scaffolds with osteosarcoma cells and final bipasic constructs were examined using a scanning electron microscope (SEM). SEM gives a clear view of tissue covered on a scaffold. All the

samples designated for SEM were fixed in 2.5% glutaraldehyde in PBS for overnight at 4°C. Later the scaffolds were dehydrated in graded ethanol (30%, 50%, 70%, and 90%) for 20 minutes at room temperature. Scaffolds were finally incubated in two changes of 100% ethanol and hexamethyldisilazane for 20 minutes each, and air dried under hood for about 30 minutes. These samples were then sputter coated with platinum and imaged using a JEOL JSM-6500F Field Emission Scanning Electron Microscope.

5.2.9 Statistics

All the quantitative data reported were analyzed using turkey test in SPSS, and p-values < 0.05 were considered as statistically significant (IBM SPSS statistics 23).

5.3 Results

5.3.1 Scaffold characteristics

Scaffolds with three different bead sizes were fabricated as mentioned earlier. The diameter of big, medium, and small size beads were approximately 1.49±0.09 mm, 0.984±0.11 mm, and 0.76±0.06 mm respectively. The final dimensions of scaffolds in all the groups were approximately 6 mm in diameter and 7 mm in height. SEM images of cell free scaffolds showed a clear surface morphology of freeze dried CHI-CaP with porous architecture (Figure 5.2, 5.3) and there was no difference in the surface morphology between the three groups. The microCT images gave a clear view of the bead size and porosity (Figure 5.4, 5.5). Porosity of dry and hydrated scaffolds of the big bead size was greater than other two groups (Table 5.1). Pore sizes range from 250 to 1300 and 200 to 750 µm for big and small bead size scaffolds (Figure 5.6). Porosity of dry and hydrated scaffolds of big size beads was significantly different from small size

beads. Swelling ratio, which was measured as the increase in mass upon rehydration was also greater in bigger bead size scaffolds. No statistical difference was observed for swelling ratio between the groups.

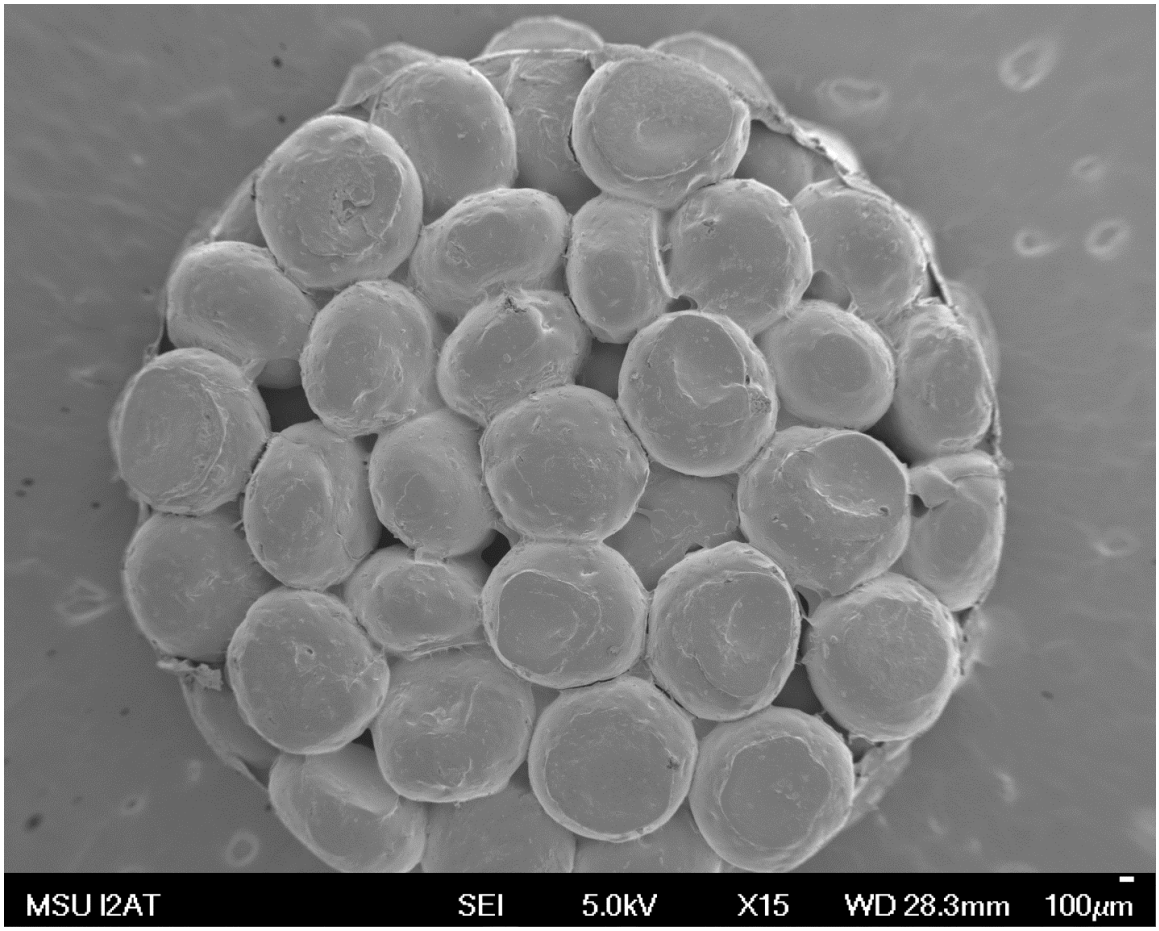

Figure 5.2 Scanning electron micrograph of a porous CHI-CaP scaffold formed by fusing medium size beads using acetic acid.

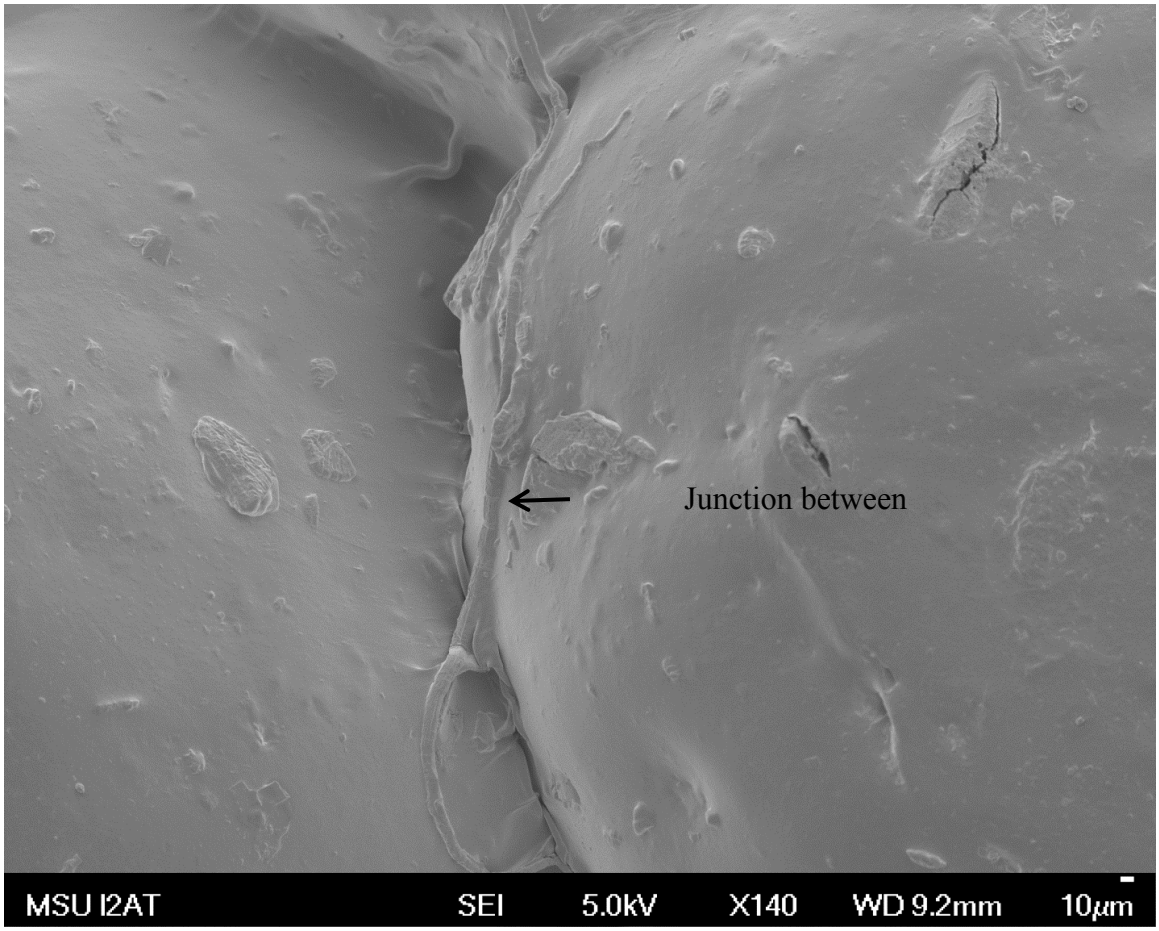

Figure 5.3 Scanning electron micrograph showing the junction between two medium size beads fused together.

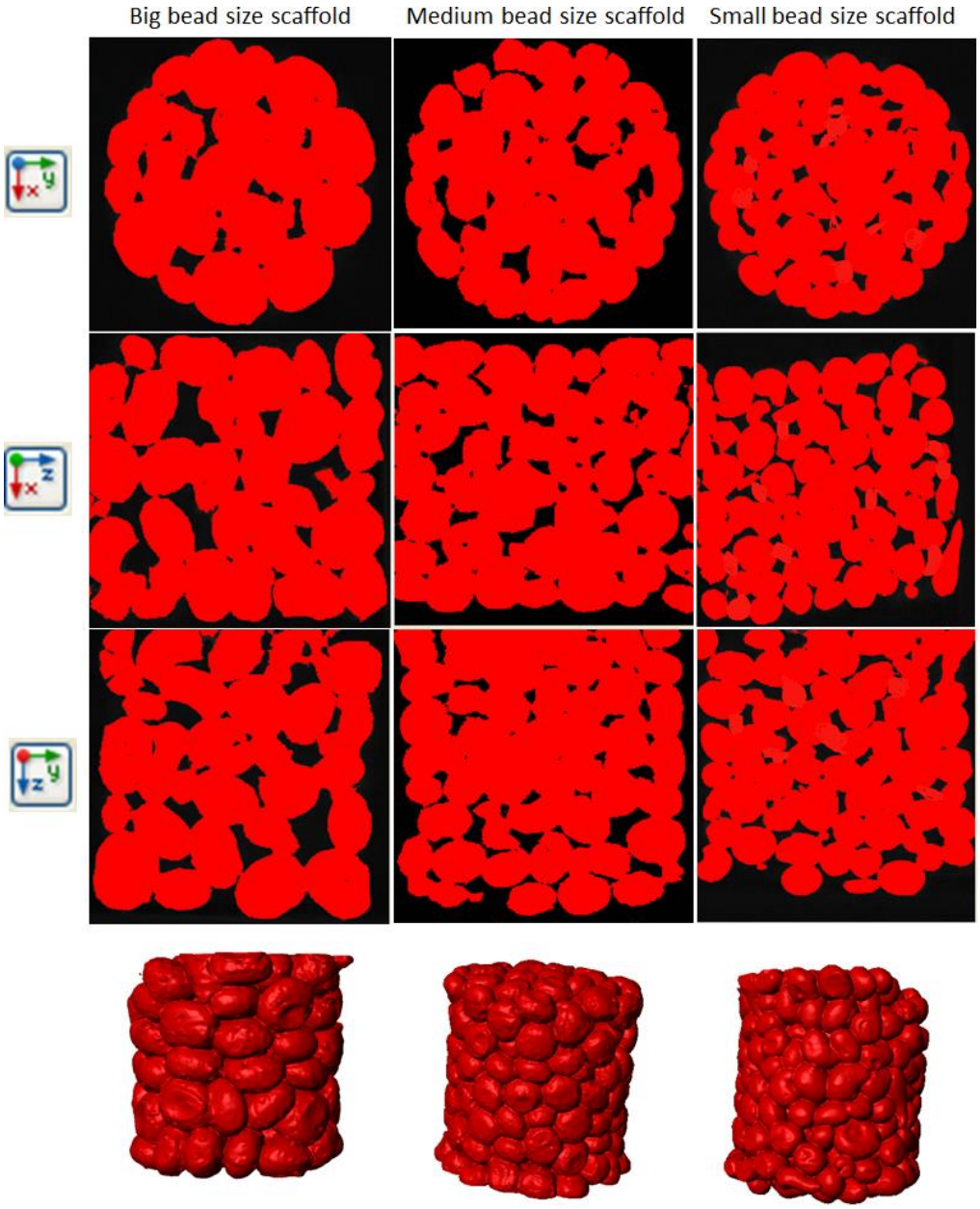

Figure 5.4 Micro computed tomography images of freeze dried CHI-CaP scaffolds formed using three different bead sizes.

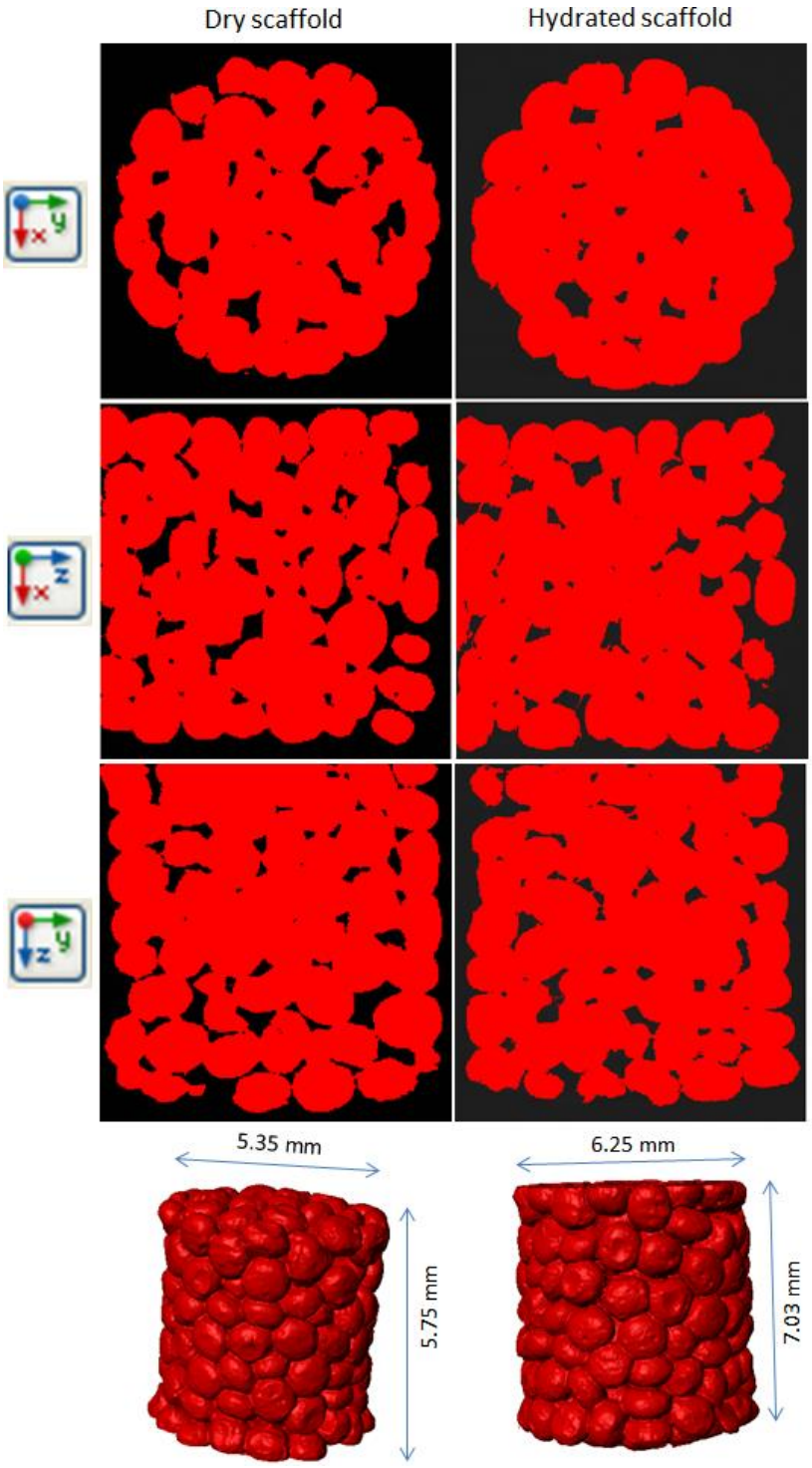

Figure 5.5 Micro computed tomography images of freeze dried and hydrated CHI-CaP scaffold formed using medium size beads.

Table 5.1 Physical characteristics of CHI-CaP scaffolds formed using three different bead sizes.

Characteristic	Big bead size scaffold	Medium bead size scaffold	Small bead size scaffold
Average bead size (n=25)(mm)	1.49 ± 0.09^{A}	0.984 ± 0.11^{B}	0.76 ± 0.06^{C}
Porosity of dry scaffold (%) (n=3)	43.02 ± 5.86^{A}	34.24 ± 4.50^{AB}	30.29 ± 3.20^{B}
Porosity of hydrated scaffold (%) (n=3)	116.53 ± 19.06^{A}	85.26 ± 9.61^{AB}	73.09 ± 5.60^{B}
Pore range of dry scaffold (n=30) (µm)	$250 - 1200^{A}$	$200 - 900^{AB}$	$200 - 750^{B}$
Pore range of hydrated scaffold (n=30) (µm)	$400 - 1500^{A}$	$300 - 1150^{AB}$	$250 - 950^{B}$
Swelling ratio (%) (n=6)	94.28 ± 2.80^{A}	90.09 ± 2.55^{AB}	87.19 ± 5.05^{B}
Increase in diameter after hydrating (%) (n=6)	24.15 ± 1.72^{A}	22.71 ± 1.53^{A}	22.14 ± 2.33^{A}
Increase in height after hydrating (%) (n=6)	24.08 ± 3.02^{A}	22.97 ± 1.97^{A}	22.41 ± 1.38^{A}
Increase in volume after hydrating (%) (n=6)	91.25 ± 5.22^{A}	85.23 ± 6.51^{A}	82.67 ± 7.01^{A}

(values= mean±stdev). Letters represent statisctical significance.

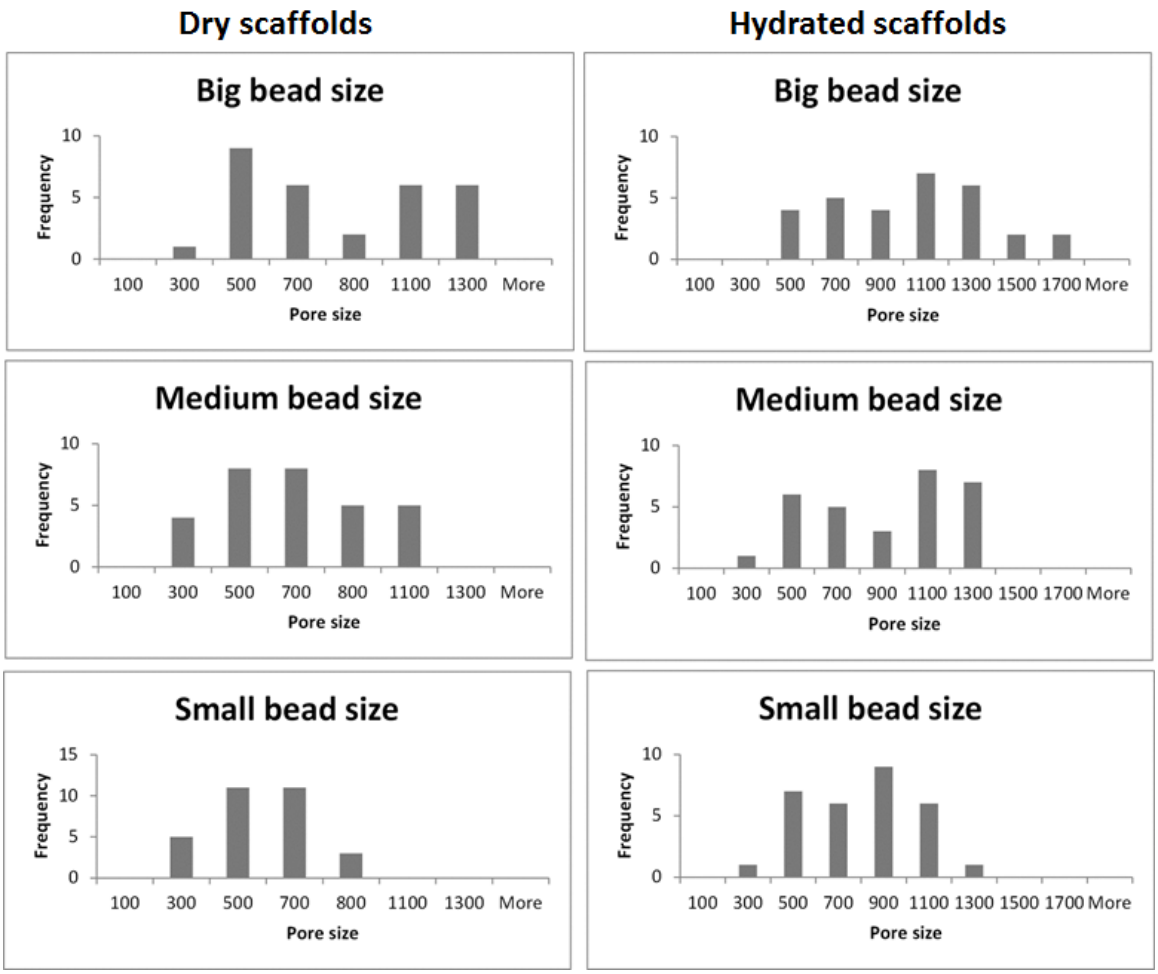

Figure 5.6 Histograms showing the pore size range in dry and hydrated CHI-CaP scaffolds of different bead sizes.

5.3.2 Mechanical testing

The compressive modulus of CHI-CaP scaffolds rehydrated in culture medium for 24 h, 2 weeks and 4 weeks was measured by performing unconfined compression testing. Results from mechanical testing revealed that the compression modulus for the small size scaffolds rehydrated in culture medium for 4 weeks was higher (8.31±1.45) whereas the bigger bead size scaffolds rehydrated for 2 weeks has the least (5.36±0.44) than all other

groups (Figure 5.7). The overall compressive modulus of big bead size scaffolds was significantly lower from other groups, whereas no significant difference was noticed between medium and small size groups. The hydrated scaffolds were not delicate and all the scaffolds reached the end point without fracture. Scaffolds were more consolidated and compacted while testing.

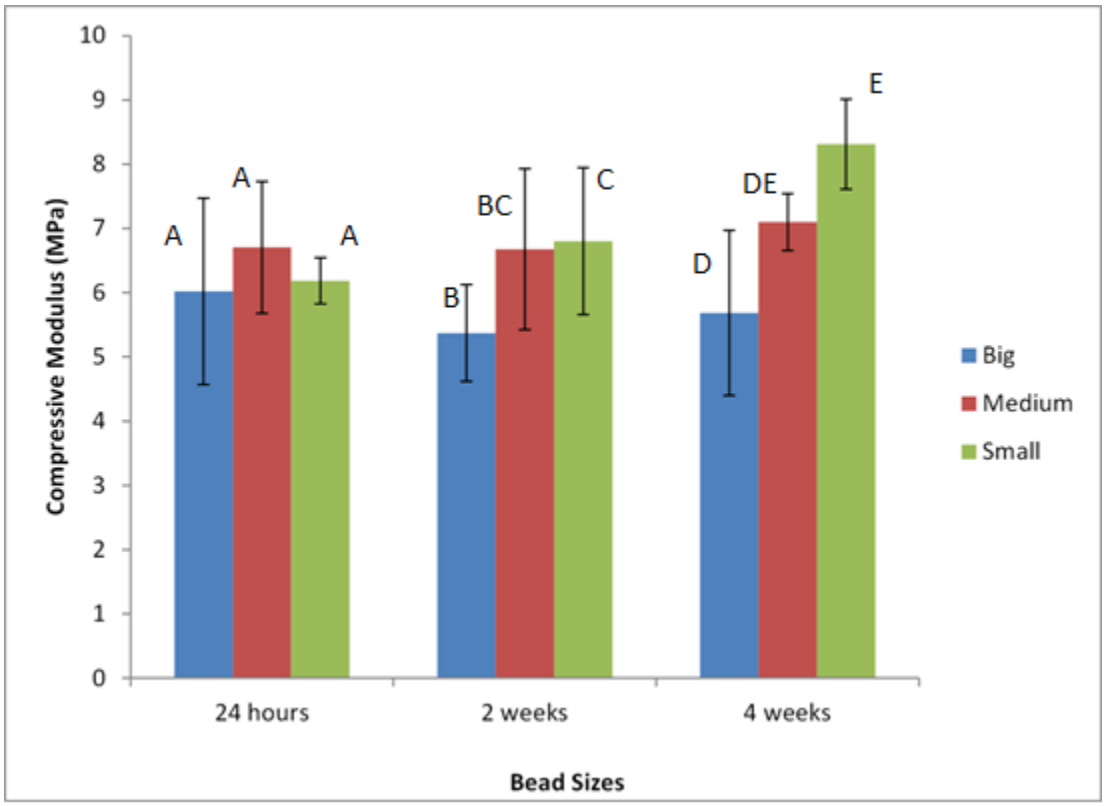

Figure 5.7 Compressive modulus of different bead size CHI-CaP scaffolds after rehydrating in culture media for 24 h, 2 weeks or 4 weeks.

Letters represent the statistical significance at respective time period

5.3.3 Degradation

CHI-CaP scaffolds of different bead sizes were digested in 1mg/ml of lysozyme solution in PBS. After every 3 day time interval, scaffolds were dried completely and

weighed before adding fresh lysozyme solution. The rate of degradation was estimated from the amount of calcium released into the solution and the weight loss with respect to initial dry weight of the scaffolds. The amount of calcium released was significantly increased with bead size with more calcium released from big size beads. The total weight loss increased with an increase in bead size and a statistical increase was seen from small to big size beads.

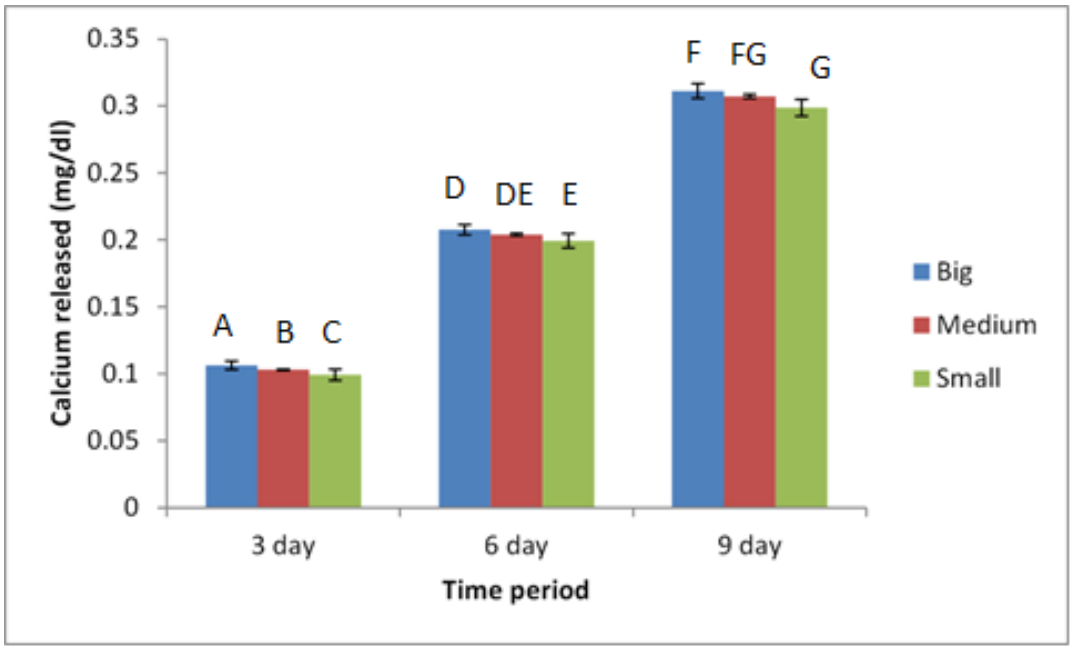

Figure 5.8 Total amount of calcium released after 3 d, 6 d, and 9 d of incubation in lysozyme solution.

Letters represent statistical significance at respective time period.

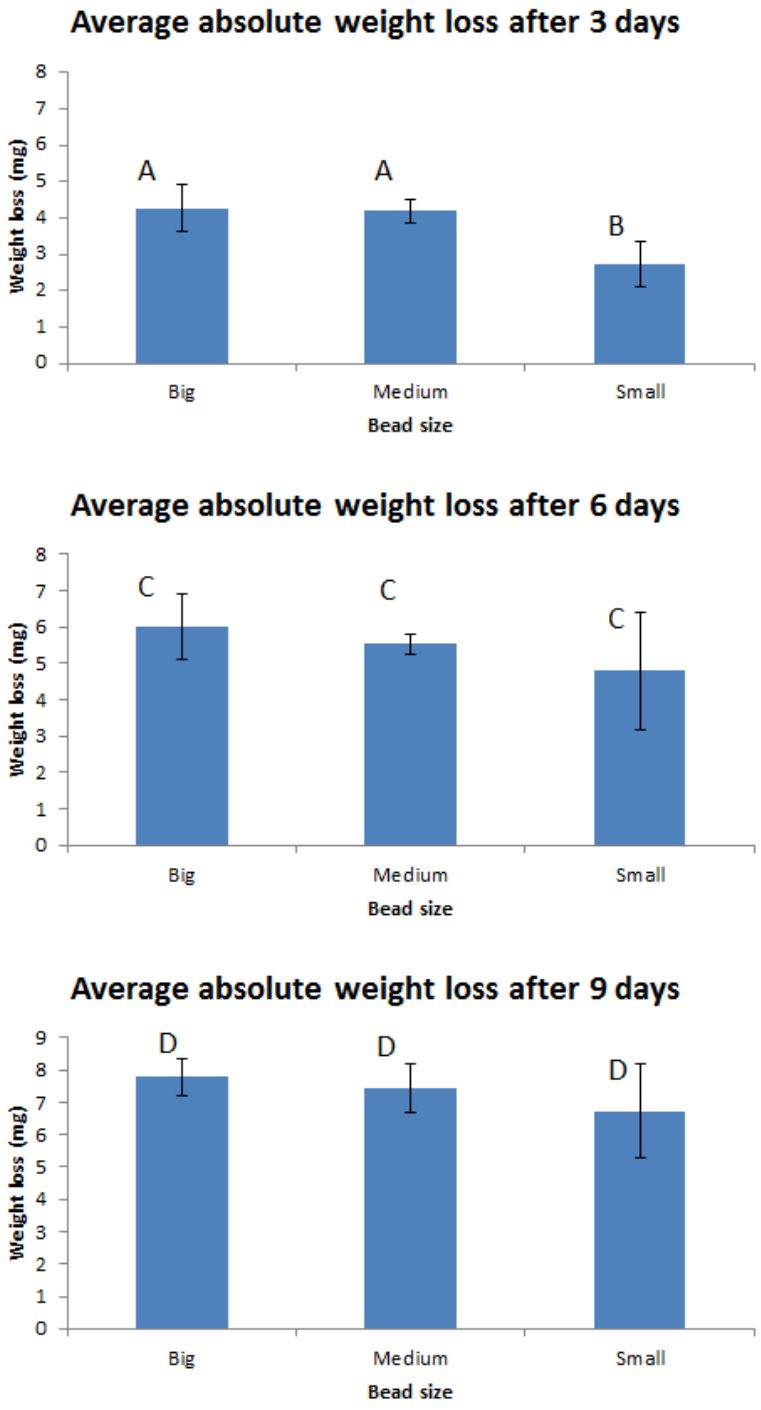

Figure 5.9 Average absolute weight loss with respect to initial weight after 3 d, 6 d, and 9 d of incubation in lysozyme solution.

Letters represent statistical significance at respective time period.

5.3.4 Biphasic constructs

Scaffolds with three different bead sizes were used to make biphasic constructs. Scaffolds were first incubated in a mouse osteosarcoma cell line for 6 weeks. One scaffold from each group was taken for SEM at 3 week and 6 week time periods. All the scaffolds at the 3 week time period showed a huge mass of fibroblasts stretched over the scafoold (Figure 5.10). SEM images at the 6 week time period showed more mineral deposition compared to 3 week time period (Figure 5.11). SEM images of all the scaffolds with mineral deposition were almost the same with no effect on bead size. Porcine chondrocytes were then seeded on these mineral deposited scaffolds for neocartilage formation. After culturing these biphasic constructs in DCM for 4 weeks, a white cartilage like tissue was observed on all of the scaffolds macroscopically (Figure 5.13). The tissue formed was not uniform on big sized bead scaffolds when observed macroscopically, but the SEM images showed neotissue covering the seeded area. Tissue formed on two biphasic constructs of all bead sizes was slowly scrapped to see how well the tissue was adhered. The tissue formed on all the groups adhered at almost same rate. Small amounts of tissue remnants attached to scaffold after scrapping the tissue were observed under SEM (Figure 5.14). SEM images of the final biphasic constructs showed the presence of cartilage like tissue on the beads covering almost the whole chondrocyte seeded area. One biphasic construct with osteosarcoma and chondrocytes was fixed in 2.5% glutaraldehyde and imaged under microCT image. The images were reconstructed and masked depending on density (grey scale). The final images showed that in all the three experimental groups, beads were covered with cellular material (mineral deposition from osteosarcoma cell line) (Figure 5.15) but there is no clear separation of cellular

material from osteosarcoma and chondrocytes in big and small bead size scaffolds (Figure 5.16). In medium size bead scaffolds, the area of chondrocytes seeded was clearly noticeable (Figure 5.17).

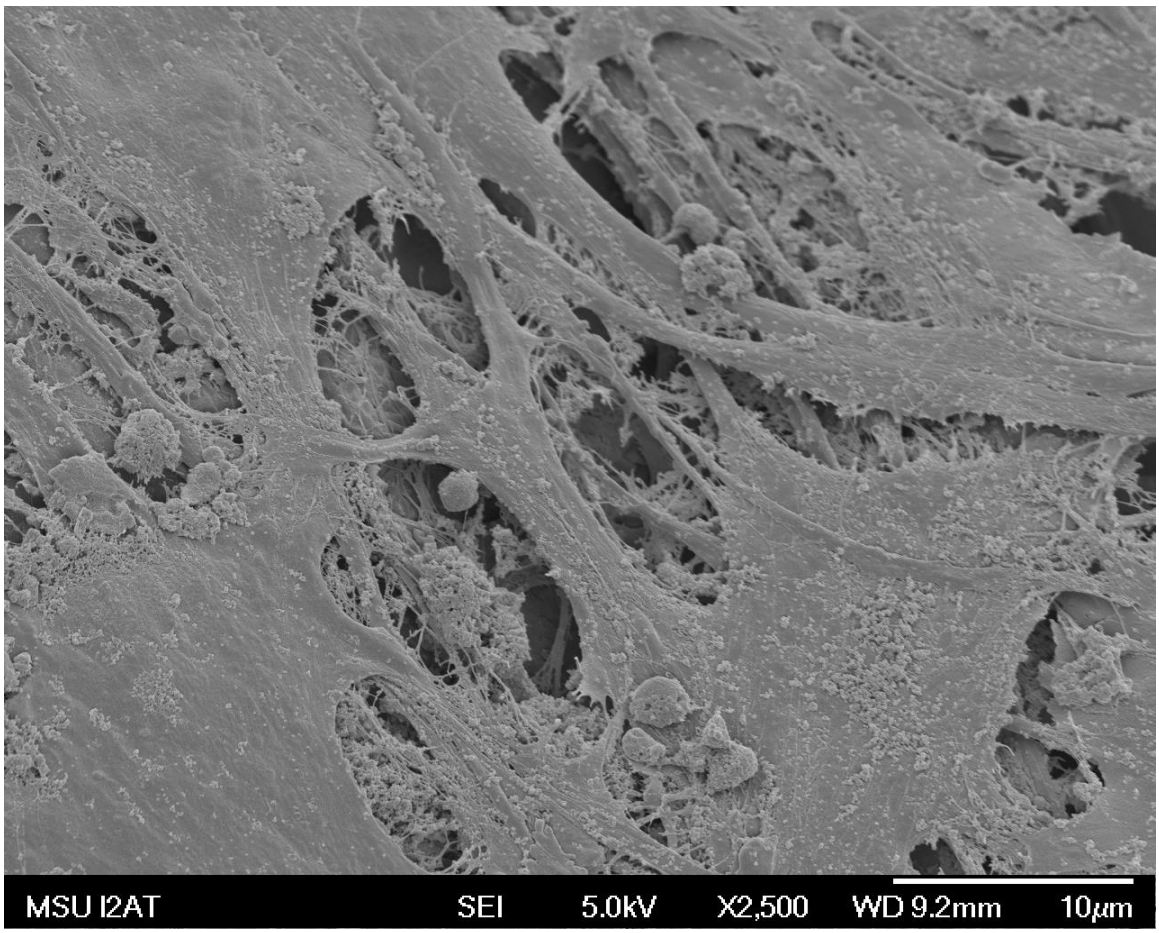

Figure 5.10 SEM images showing fibroblast like cell coverage on big bead size CHI-CaP scaffolds after incubating scaffolds in osteosarcoma cell suspension for 3 weeks.

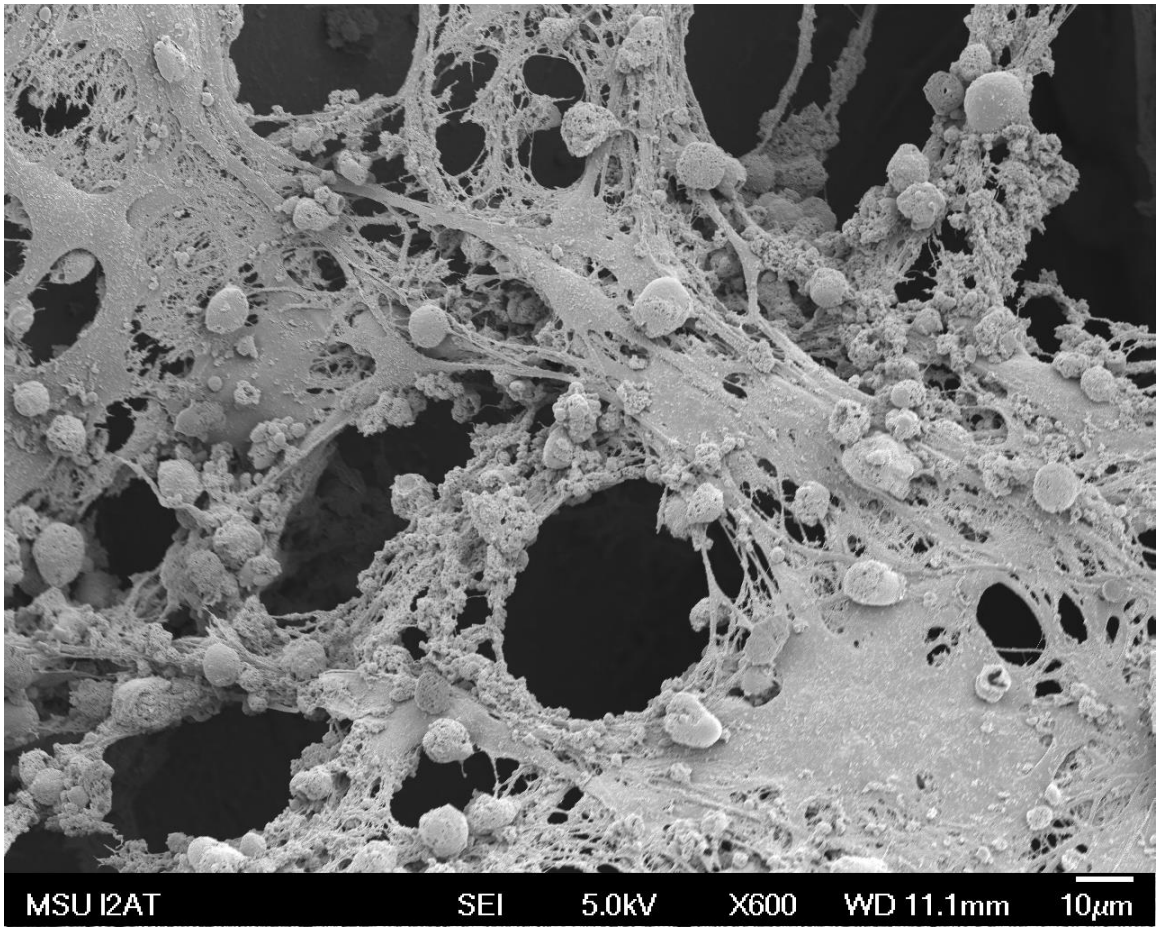

Figure 5.11 SEM images showing increased mineral deposition on big bead size CHI-CaP scaffolds after incubating scaffolds in osteosarcoma cell suspension for 6 weeks.

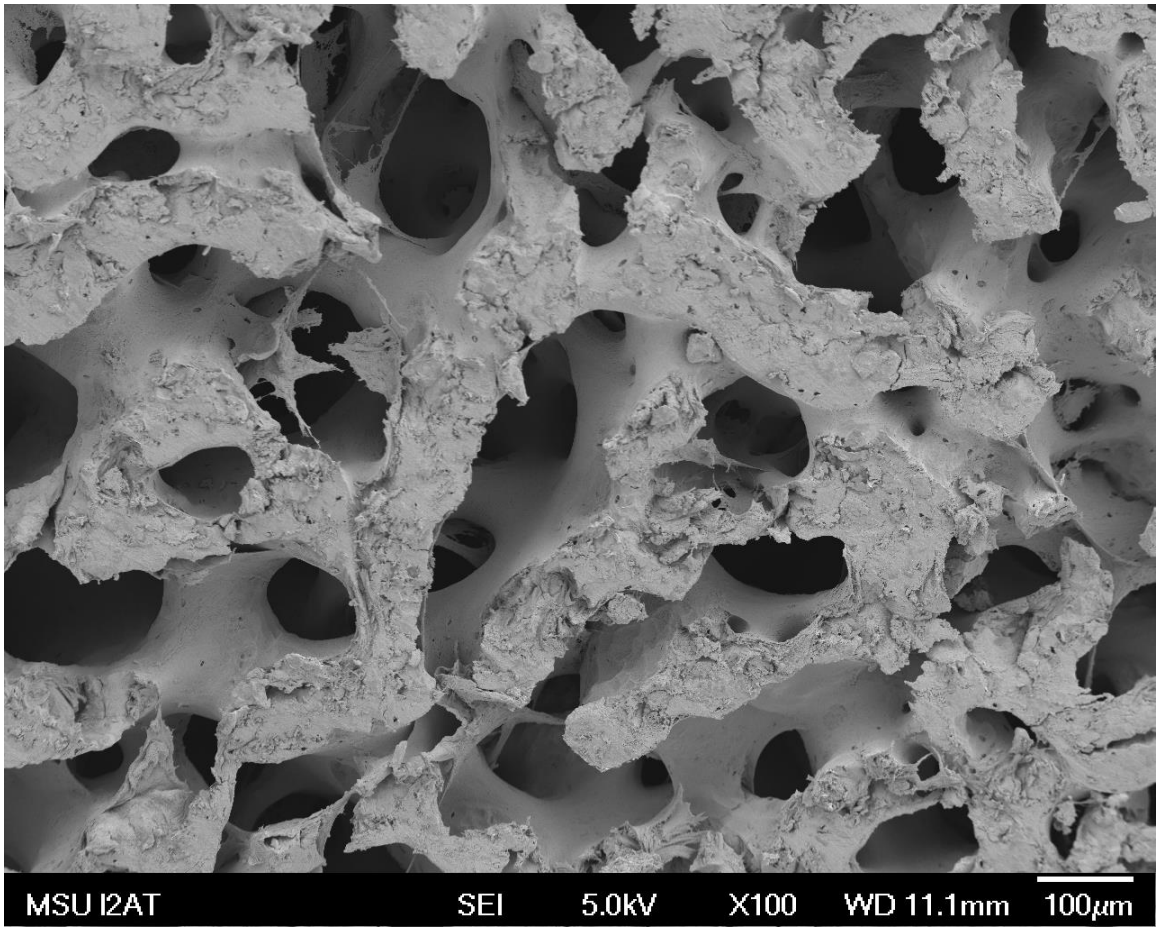

Figure 5.12 SEM image of a native clean bone.

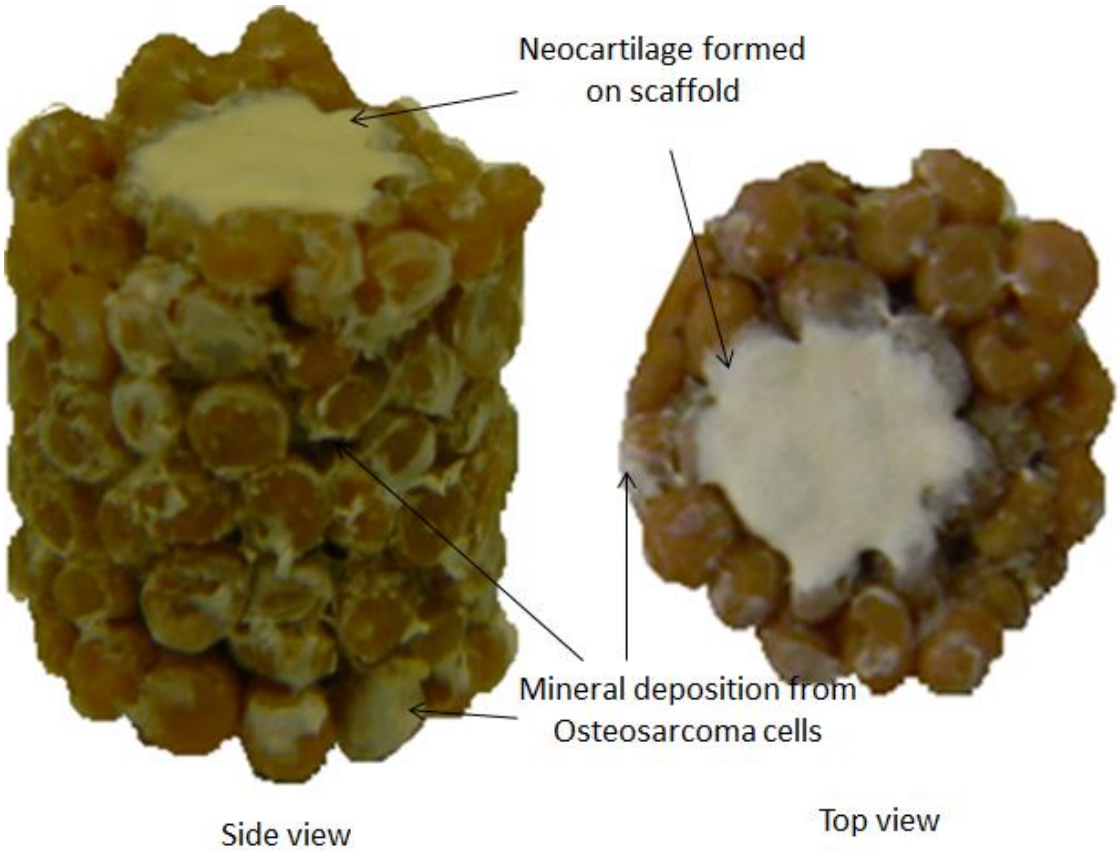

Figure 5.13 Side and top view of the medium bead size biphasic construct showing the mineral deposition and neocartilage formation when dried using hexamethyldisilazane for SEM.

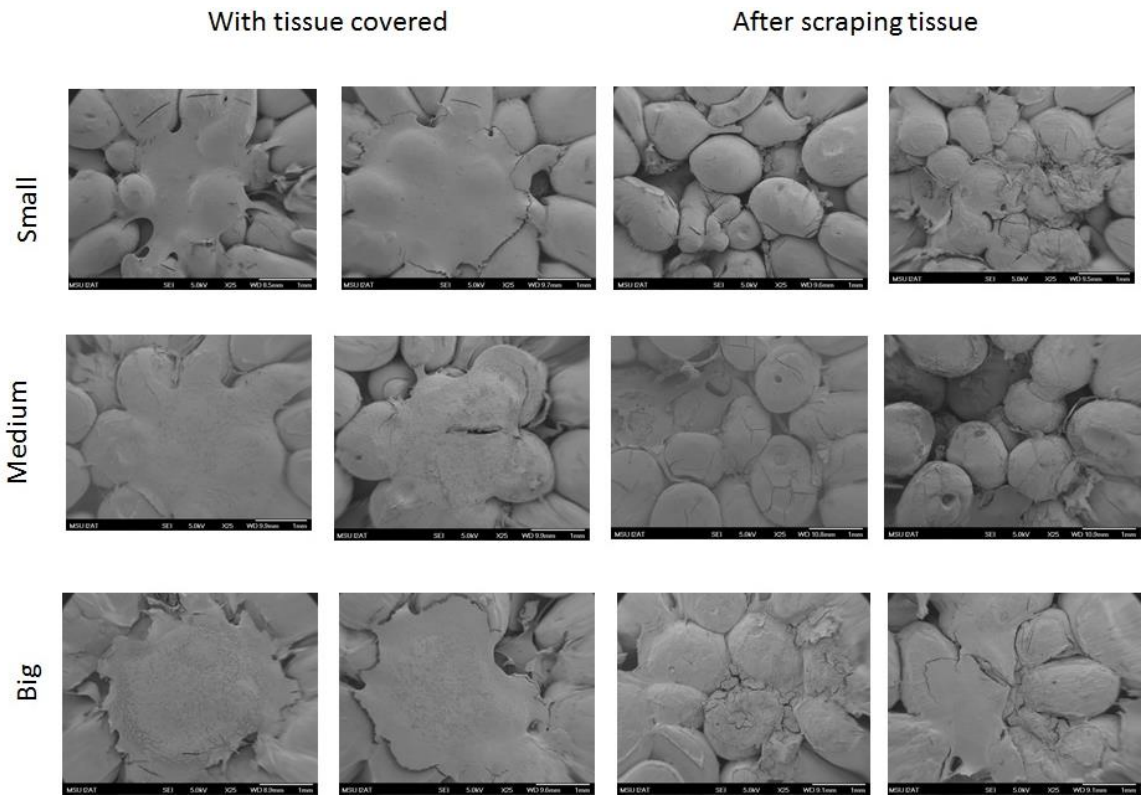

Figure 5.14 Scanning electron micrographs of different bead size collagen coated CHI-CaP scaffolds showing the neotissue formed using porcine chondrocytes and the remnants after scrapping the tissue.

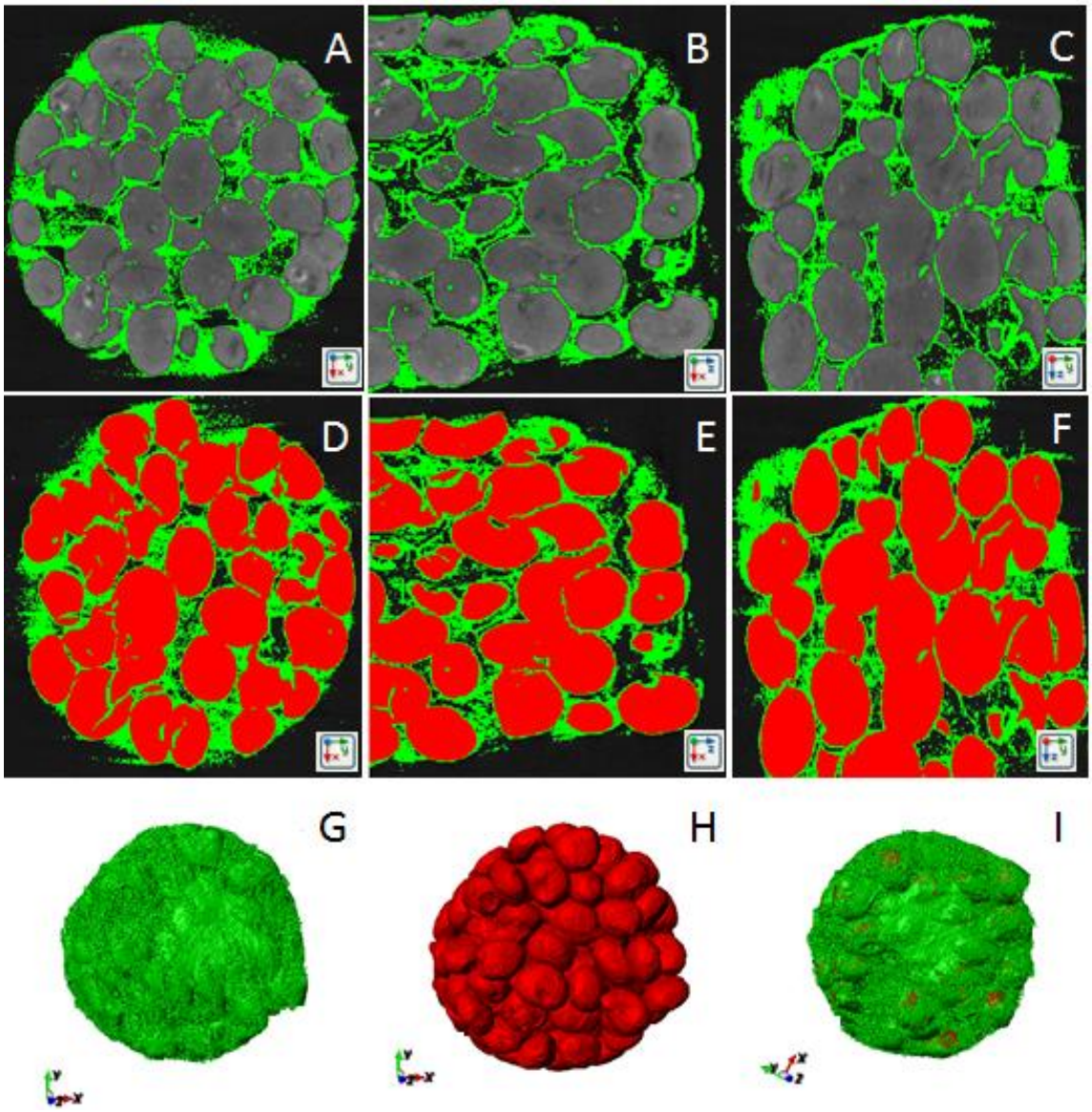

Figure 5.15 microCT images of medium size biphasic constructs

A-C) three different axis with green representing the cellular material, D-F) three different axis with red representing scaffold beads and green as cellular material, G) 3dimensional view only cellular material, H) 3 dimensional view of scaffold without cellular material, I) 3 dimensional view showing cellular material completely covering the scaffold.

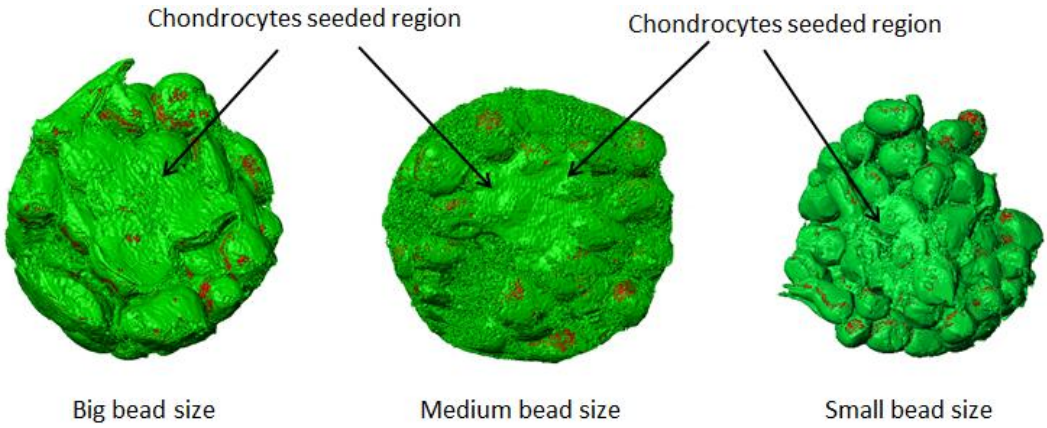

Figure 5.16 Top view microCT images of the bipahsic constructs formed using CHI-CaP scaffolds and osteosarcoma and chondrocytes.

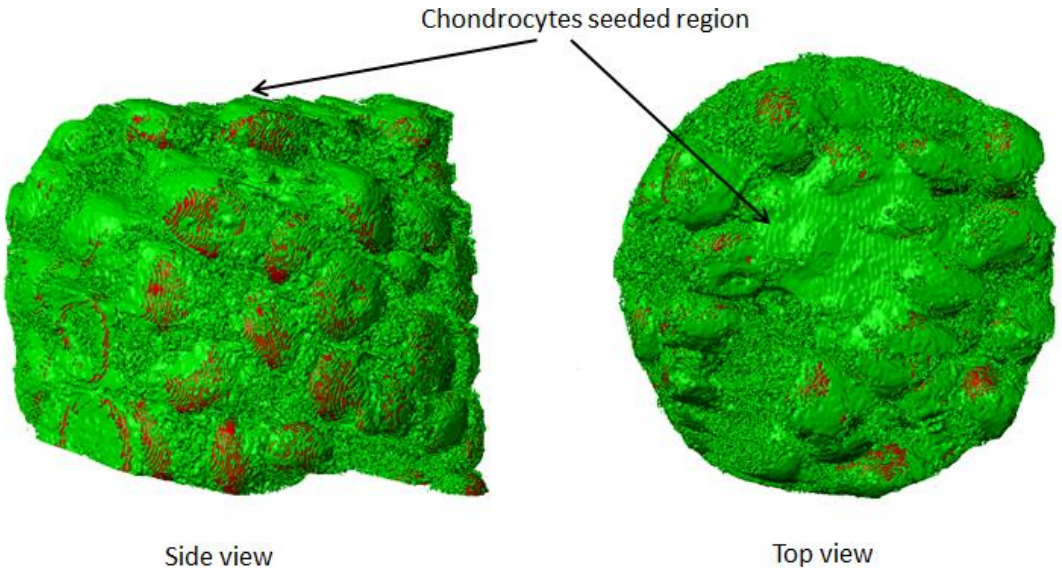

Figure 5.17 Side and top view of the microCT images of medium bead size biphasic constructs,

Biphasic constructs show that the scaffold beads (shown in red) were completely covered by cellular material (green) and clearly distinguishes the chondrocyte seeded area.

5.4 Discussion

In the current study, biphasic constructs were formed using CHI-CaP scaffolds and osteoscarcoma cell line and chondrocytes. In this biphasic approach, scaffold with

osteosarcoma cellular material represents a bony phase, while the neocartilage formed from porcine chondrocytes represents the cartilage phase. Mouse osteosarcoma cells were used for the bone mineral deposition on scaffolds prior to the formation of neocartilage. The porous CHI-CaP scaffolds fabricated in this study were similar to the method proposed by Chesnutt et al. [15] but chitosan with lower DDA was used in this study and our scaffolds faced an extra freeze drying step, which was known to increase the porosity of the scaffolds [6]. In the current study, scaffolds with three different bead sizes were fabricated and scaffold characteristics, and tissue formation were compared among the scaffolds.

CHI-CaP scaffolds of three different bead sizes were fabricated in this study by varying the CHI-CaP droplet size. Porous structure of the scaffolds was made by fusing individual beads using 2% acetic acid. Porosity plays an important role in scaffold design and architecture where it influences the mechanical strength, degradation, and tissue formation on the scaffold. Previous studies have shown that porous structure with highly interconnected pores is necessary for bone growth and vascularization [27,28]. microCT images of all the three bead size scaffolds confirmed interconnected pores, but the pore range for big size beads was more (250-1200 μm). Scaffolds with pore ranging from 100-800 μm are sufficient for tissue growth [29]. The main disadvantage of the large pore size is that the chondrocytes seeded for cartilage regeneration will make their way into the scaffold rather than adhering and forming a tissue on top of the scaffold. A significant difference in the porosity values was observed between big and small size beads. The porosity of small size scaffold was in the lower range of porosity, whereas the porosity of big size beads was more than needed for tissue growth *in vivo* [29,30]. The porosity of

medium size scaffolds was same as shown by Chesnutt et al. [15] and it was also shown that scaffolds of this porosity helps in cartilage tissue formation on CHI-CaP scaffolds [19]. A previous study has shown pore size ranging from 100- 800 μm is sufficient for new tissue formation [29].

The overall compressive modulus was significantly lower in big bead size scaffolds than other groups. Mechanical strength of the scaffolds was affected by porosity which in turn was affected by bead size of the scaffolds. It was shown that the scaffolds with greater porosity have less mechanical strength and the scaffolds with lower porosity have greater mechanical strength [31,32]. CHI-CaP scaffolds will be replacing a bone defect in *in vivo*; therefore, they need to possess mechanical integrity until the new bone formation takes place. The compressive modulus of small size beads at 4 weeks' time period was higher than all the groups, but the porosity of small size beads was smaller which leads to poor tissue growth. The compressive modulus of all the group scaffolds was close and approaching the lower range of human cancellous bone modulus that is in the range of 10-2000 MPa [33].

In the current study, biodegradable CHI-CaP scaffolds, replaces the defected subchondral bone region. Ideally these scaffolds will degrade as the new bone formation takes place. Lysozyme was the enzyme that plays an important role in chitosan degradation [34]. The amount of calcium released is close but smaller than the values reported by Chesnutt but the percentage of weight loss was observed more in big and medium bead size scaffolds than the values reported by Chesnutt [15]. The average weight loss by big bead size scaffolds was greater than other groups, which might be due to large pore size and porosity. The rate of degradation will depend on several factors like

– DDA, crystalline nature, and pore size [15,35,36]. Previous studies have shown that chitosan with higher DDA degrades slower than the chitosan with lower DDA [15,37,38].

SEM images of cell free scaffolds were same for all the three groups except the bead size and pore size. TEM images of similar type of scaffolds showed regular distribution of calcium and phosphate crystals in the scaffold [15]. SEM images of scaffolds with osteosarcoma cells were also same at 3 week and 6 week time periods, with more mineral deposition at 6 weeks. Chondrocytes were cultured for 4 weeks on mineral deposited CHI-CaP scaffolds. The tissue formed from chondrocytes on medium sized scaffolds was more distinctive than the other groups, which was also evidenced in microCT images. The chondrocytes seeded on big size beads might passed through the pores and settled somewhere in the scaffold due to the high porous nature of those scaffolds. On the other hand, the porosity of the small size scaffolds was in the lower range of required porosity, which made the insufficient nutrient and waste material diffusion through the pores.

In this study, the effect of CHI-CaP bead size was clearly studied from porosity, pore sizes, mechanical strength, swelling ratio, degradation, and neocartilage tissue formation. Medium size beads with an average diameter of 0.984±0.11 mm were found to be the best bead size with approximately 34% porosity. Even the mechanical strength of medium size beads was less than the small size beads, but there was no statistical difference. Coating the scaffolds with collagen type I increased cell adhesion which was seen in SEM of biphasic constructs after scrapping the tissue. The main limitation in this study would be the cartilage formation was restricted to 5mm diameter on top of CHI-CaP scaffold. In order to implant these scaffolds, cartilage tissue needs to cover the whole

top surface of the scaffold. More significant values in scaffold characteristics – porosity, degradation, and mechanical strength can be obtained when a larger sample size was used. In the current study we mainly concentrated on identifying the effect of bead sizes but we did not perform many studies to see the phenotype of the cartilage tissue formed. But a previous study has shown that chondrocytes seeded on top on CHI-CaP scaffolds lead to the formation of cartilage like tissue after 4 weeks culture in DCM [16].

5.5 References

[1] Dietmar W. Hutmacher, "Scaffolds in tissue enigneering bone and cartilage," Biomaterials, vol. 21, no. 24, pp. 2529-2543, December 2000.

[2] Franklin T. Moutos and Farshid Guilak, "Composite scaffolds for cartilage tissue engineering," Biorheology, vol. 45, no. 3-4, pp. 501-12, August 2008.

[3] Amaia Cipitria et al., "Porous scaffold architecture guides tissue formation," J of Bone and Mineral Research, vol. 27, no. 6, pp. 1275-88, May 2012.

[4] Sundararajan V. Madihally and Howard W.T. Matthew, "Porous chitosan scaffolds for tissue engineering," Biomaterials, vol. 20, no. 12, pp. 1133-1142, January 1999.

[5] IA Sabree, JE Gough, and B. Deerby, "Mechanical properties of porous ceramic scaffolds: Influence of internal dimensions," Ceramics International, vol. 41, no. 7, pp. 8425-8432, August 2015.

[6] Benjamin T. Reves, Joel D. Bumgardner, Judith A. Cole, Yunzhi Yang, and Warren O. Haggard, "Lyophilization to improve drug delivery for chitosan-calcium phosphate bone scaffold construct: A preliminary investigation," J Biomed Mater Res B Appl Biomater, vol. 90, no. 1, pp. 1-10, February 2009.

[7] Leatrese D. Harris, Byung-Soo Kim, and David J. Mooney, "Open pore biodegradable matrices formed with gas foaming," J Biomed Mater Res, vol. 42, no. 3, pp. 396-402, December 1998.

[8] Hermann Seitz, Wolfgang Rieder, Stephan Irsen, Barbara Leukers, and Carsten Tille, "Three-dimensional printing of porous ceramic scaffolds for bone tissue engineering," J Biomed Mater Res B Appl Biomater, vol. 74, no. 2, pp. 782-2, August 2005.

[9] Jing Zeng et al., "Ultrafine fibers electrospun from biodegradable polymers," J. Appl. Polym. Sci., vol. 89, pp. 1085-1092, September 2002.

[10] Ruiyun Zhang and Peter X. Ma, "Poly(alpha-hydroxyl acids)/hydroxyapatite porous composites for bone-tissue engineering. I. Preparation and morphology," J biomed Mater Res, vol. 44, no. 4, pp. 446-455, March 1999.

[11] Hu Da et al., "The impact of compact layer in biphasic scaffold on osteochondral tissue engineering," PLoS One, vol. 8, no. 1, January 2013.

[12] Pesaramelli Karteek, Sravanthi MAcharla, and Ranjith Anishetty, "Chitosan: A biocompatible polymer for pharmaceutical applications in various dosage forms," International J. Pharmacy & Tech., vol. 2, no. 2, pp. 186-205, June 2010.

[13] GJ Tsai and WH Su, "Antibacterial activity of shrimp chitosan against Escherichia coli," J Food Prot, vol. 62, no. 3, pp. 239-43, MArch 1999.

[14] O Felt, A Carrel, P Baehni, P Buri, and R Gurny, "Chitosan as tear substitute: a wetting agent endowed with antimicrobial efficacy," J Ocul Pharmacol Ther, vol. 16, no. 3, pp. 261-70, June 2000.

[15] B Chesnutt, A Viano, Y Yuan, and et al, "Design and characterization of a novel chitosan/nanocrystalline calcium phosphate composite scaffold for bone regeneration.," J Biomed Mater Res A., vol. 88(2), pp. 491-502, Feb 2009.

[16] Dana L. Nettles, Steven H. Elder, and Jerome A. Gilbert, "Potential use of chitosan as a cell scaffold material for cartilage tissue engineering," Tissue Eng, vol. 8, no. 6, pp. 1009-16, Decemebr 2002.

[17] Hyejin Park, Bogyu Choi, Junli Hu, and Min Lee, "Injectable chitosan hyaluronic acid hydrogels for cartilage tissue engineering," Acto Biomaterialia, vol. 9, no. 1, pp. 4779-4786, january 2013.

[18] R. Jin, L.S. Moreira Teixeira, P.J. Dijkstra, M. Karperien, and C.A. van Blitterswijk, "Injectable chitosan-based hydrogels for cartilage tissue engineering," BIomaterials, vol. 30, no. 13, pp. 2544-2551, May 2009.

[19] Steven Elder, Anuhya Gottipati, Hilary Zelenka, and Joel Bumgardner, "Attachment, proliferation, and chondroinduction of mesenchymal stem cells on porous chitosan-calcium phosphate scaffolds," Open Orthop J, vol. 7, pp. 275-281, July 2013.

[20] Guillaume R. Ragetly, Dominique J. Griffon, Hae-Beom Lee, and Yong Sik Chung, "Effect of collagen II coating on mesenchymal stem cell adhesion on chitosan and on reacetylated chitosan fibrous scaffolds," J Mater Sci Mater Med, vol. 21, no. 8, pp. 2479-90, August 2010.

[21] Jong-pil Seo et al., "Effects of bilayer gelatin/β-tricalcium phosphate sponges loaded with mesenchymal stem cells, chondrocytes, bone morphogenetic protein-2, and platelet rich plasma on osteochondral defects of the talus in horses," Res Vet Sci., vol. 95, no. 3, pp. 1210-6, December 2013.

[22] R Reyes et al., "Comparative, osteochondral defect repair: Stem cells versus chondrocytes versus Bone Morphogenetic Protein-2, solely or in combination," Eur Cell Mater, vol. 25, pp. 351-65, July 2013.

[23] Jiangning Chen et al., "Simultaneous regeneration of articular cartilage and subchondral bone *in vivo* using MSCs induced by a spatially controlled gene delivery system in bilayered integrated scaffolds," Biomaterials, vol. 32, no. 21, pp. 4793-4805, JUly 2011.

[24] Rebecca L. Dahlin et al., "Articular chondrocytes and mesenchymal stem cells seeded on biodegradable scaffolds for the repair of cartilage in a rat osteochondral defect model," Biomaterials, vol. 35, no. 26, pp. 7460-7469, August 2014.

[25] Viorel Marin Rusu et al., "Size-controlled hydroxyapatite nanoparticles as self-organized organic-inorganic composite materials," Biomaterials, vol. 26, no. 26, pp. 5414-5426, September 2005. [26] Steven H. Elder et al., "Production of hyaline-like cartilage by bone marrow mesenchymal stem cells in a self-assembly model," Tissue Eng Part A, vol. 15, no. 10, pp. 3025-36, October 2009.

[27] D. Logeart-Avramoglou, F. Anagnostou, R. Bizios, and H. Petite, "Engineering bone: challenges and obstacles," J Cell. Mol. Med., vol. 9, no. 1, pp. 72-84, January 2005.

[28] Xiaohua Liu and Peter X. Ma, "Polymeric scaffolds for bone tissue engineering," Ann Biomed Eng., vol. 32, no. 3, pp. 477-86, MArch 2004.

[29] Besty M. Chesnutt, Youling Yuan, Karyl Buddington, Warren O. Haggard, and Joel D. Bumgardner, "Composite chitosan/nano-hydroxyapatite scaffolds induce osteocalcin productin by osteoblasts *in vitro* and support bone formation *in vivo*," Tissue Eng Part A, vol. 15, no. 9, pp. 2571-2579, September 2009.

[30] M Borden, M Attawia, Y Khan, SF El-Amin, and CT Laurencin, "Tissue-engineered bone formation *in vivo* using a novel sintered polymeric microsphere matrix," J. Bone Joint Surg Br, vol. 86, no. 8, pp. 1200-8, November 2004.

[31] Zhen Pan and Jiandong Ding, "Poly(lactide-co-glycolide) porous scaffolds for tissue engineering and regenerative medicine," Interface Focus, vol. 2, no. 3, pp. 366-377, June 2012.

[32] I. Sabree, J. E. Gough, and B. Derby, "Mechanical properties of porous ceramic scaffolds: Influence of internal dimensions," Ceramics International, vol. 41, no. 7, pp. 8425-8432, August 2015.

[33] TM Keavney and WC Hayes,. Boca Raton, FL, USA: CRC Press, 1992, p. 285.

[34] Eugene Khor, Chitosan: Fulfilling a Biomaterial's Promise. Oxford, UK: Elsevier, 2001.

[35] Thomas Freier, Hui Shan Koh, Karineh Kazazian, and Molly S. Shoichet, "Controlling cell adhesion and degradation of chitosan films by N-acetylation," Biomaterials, vol. 26, no. 29, pp. 5872-8, October 2005.

[36] Malgorzata Jaworska, Kensuke Sakurai, Pierre Gaudon, and Eric Guibal, "Influence of chitosan characteristics on polymer properties. I: Crystallographic properties," Polymer International, vol. 52, no. 2, pp. 198-295, January 2003.

[37] Hua Zhang and Steven H. Neau, "*In vitro* degradation of chitosan by a commercial enzyme preparation: effect of molecular weight and degree of deacetylation," Biomaterials, vol. 22, no. 12, pp. 1653-1653, June 2001.

[38] Youling Yuan, Betsy M. Chesnutt, Warren O. Haggard, and Joel D. Bumgardner, "Deacetylation of chitosan: Material characterization and *in vitro* evaluation via albumin adsorption and pre-osteoblastic cell cultures," Materials, pp. 1399-1416, August 2011.

CHAPTER VI

SUMMARY

6.1 Summary

The main goal of this dissertation was to form a scaffold-free cartilage tissue on top of biodegradable chitosan calcium phosphate scaffolds for osteochondral defects. Microbeads were made by co-precipitating chitosan with calcium and phosphate. These beads were fused together to form a cylindrical shaped scaffolds with sufficient mechanical strength and porosity for tissue ingrowth. This study exhibited attachment and proliferation of mesenchymal stem cells and chondrocytes. Two different approaches for making biphasic constructs were analyzed and the approach where cells were in direct contact with the nutrients in cell culture media has shown better results.

Cell attachment to these porous CHI-CaP scaffolds has been a major problem. To overcome this, freeze dried scaffolds were coated with type I collagen protein. Coating the scaffolds with an extracellular matrix protein increased cell attachment and proliferation of mesenchymal stem cells. The neocartilage formed on coated scaffolds was similar to native cartilage in collagen architecture. Biphasic cartilage/CHI-CaP constructs were successfully created by high-density seeding of human bone marrow mesenchymal stem cells onto coated scaffolds. The attachment of mesenchymal stem cells to especially type I collagen is mediated by $\alpha 1\beta 2$, $\alpha 2\beta 1$, and $\alpha 11\beta 1$ integrins. This

type of collagen coating would enhance MSC adhesion which improves the performance of chitosan based scaffolds for various applications.

In this study, the bone like cells were initially cultured on scaffold to precondition the scaffold prior to chondrogenic culture. This helps in easy bone formation and vascularization when implanted in the defect site. Individual bead size of these scaffolds plays an important role in porosity, which affects the mechanical strength, degradation, and tissue formation on scaffolds. Scaffolds were fabricated with different bead sizes and a cartilage-like tissue was formed on biphasic constructs using porcine osteosarcoma cells and porcine chondrocytes. The studies showed that sufficient porosity of the scaffolds was needed to support mechanical integrity, rate of degradation, and tissue ingrowth. This study showed that the scaffolds fabricated with medium size beads had ideal porosity, pore size, and with a distinctive cartilage formation compared to other two bead sizes.

All the studies conducted to date have shown the potential of using composite chitosan calcium phosphate scaffolds to support formation of a layer of cartilage through high-density cell seeding for osteochondral defects. But, there were two main limitations of this study using chitosan with approximately 78% DDA. Despite some encouraging mechanical results, the beads do not always stay tightly fused and the scaffolds tend to fall apart with repeated handling and after storage. This was also observed in the in vivo study, where these biphasic constructs formed using rabbit bone marrow derived mesenchymal stem cells and medium bead size scaffolds were tightly fit into surgically created defects in the stifle joints of skeletally matured rabbits. In a study Jana et al. fabricated scaffolds using pristine chitosan dissolved in acetic acid at higher

concentrations, showed increased mechanical properties [1]. Secondly, the rate of degradation, although there was a measurable amount of calcium released and weight loss, but the total scaffold degradation time was too slow. A previous study also showed that chitosan with carboxymethyl groups and using a ratio of high to low molecular weight chitosan for scaffold fabrication would help the scaffolds to degrade faster than using an original chitosan scaffold [2].

6.2 References

[1] Soumen Jana, Stephen J. Florczyk, Matthew Leung, and Migin Zhang, "High-strength pristine porous chitosan scaffolds for tissue engineering,' J Mater Chem, vol. 22, no.13, pp. 6291-6299, January 2012.

[2] Elie Zakhem, and Khalil N. Bitar, "Development of chitosan scaffolds with enhanced mechanical properties for intestinal tissue engineering applications," J Funct Biomater, vol. 6, pp. 999-1011, October 2015.